Study of Caveolae Mechanotransduction Under 3D Compressive Stresses : Comparative Analysis of 2 Models Mimicking Structural and Mechanical Tumor Characteristics

Carlos Ureña Martín

université PARIS-SACLAY

UNIVERSITÉ PARIS SUD
Comprendre le monde, construire l'avenir

Study of caveolae mechanotransduction under 3D compressive stresses: Comparative analysis of two models mimicking structural and mechanical tumor characteristics.

Thèse de doctorat de l'Université Paris-Saclay
préparée à l'université Paris Sud

École doctorale n°568 signalisations et réseaux intégratifs en biologie (Biosigne), aspect moléculaire et cellulaire de la biologie

Thèse présentée et soutenue à Paris le 12 Décembre 2019, par

Carlos Ureña Martín

Composition du Jury :

Karim Benihoud Professeur, Imstitut Gustave Roussy / Université Paris XI	Président
Marie-Pierre Rols Directeur de Recherche, Institut de Pharmacologie et de Biologie Structurale	Rapporteur
Giovanni Cappello Directeur de Recherche, Laboratoire Interdisciplinaire de Physique	Rapporteur
Guillaume Montagnac Directeur de Recherche, Institut Gustave Roussy	Examinateur
Jacky Goetz Directeur de Recherche, Institut d'Hématologie et d'Immunologie	Examinateur
Christophe Lamaze Directeur de Recherche,	Directeur de thèse

NNT: 2019SACLS525

Thèse de doctorat

« Ici on taille pas des bambous»
Christophe Lamaze

«L'homme sait enfin qu'il est seul dans l'immensité indifférente de l'univers d'où il a émergé par hasard. Non plus que son destin, son devoir n'est écrit nulle part. Si vous allez trop loin, vous n'irez nulle part.»

Jacques Monod

Acknowledgements

PhD is a long, full of challenges journey. A journey, nonetheless, filled with rewards. I feel honored and obliged to thank those who helped on my firsts steps as a scientist and shared part of these crucial moments in my path. First I should stress the importance of the role of my supervisor, Christophe: Thanks for the trust and the perseverance, going through my cryptic language usage and always having a contagious will to go forward even when seemed to be hitting a wall.

I would like to warmly thank Dr. Marie-Pierre Rols and Dr. Giovanni Cappello for the precious feedback they gave in the review of my manuscript. I would also like to thank to the members of the jury Dr. Jacky Goetz and Dr. Guillaume Montagnac for kindly accepting my invitation and for the enriching discussion I foresee to come. Not forgetting Pr Karim Benihoud who kindly accepted to preside my thesis jury.

This work, as so many of this kind, would have not been possible without our collaborators. Thanks to Pierre Nassoy and Danijela Vigjnevic for their support, resources and discussion about the encapsulation side of the thesis and for giving me the opportunity of working closely with their teams, Danijela's team is indeed like a second team to me. Thanks to Felipe Court for welcoming at Santiago de Chile and sharing his expertise in the exosomes field. Also thanks to Jean Leon Maitre and Ludmilla for the assistance and the help with the membrane tension measurements
I should also thank Matthieu Piel for being part of my thesis committee, together with Pierre Nassoy and Danijela Vigjnevic, giving precious feedback in early stages of the project.

I could not had done anything of this thesis without the amazing team build on Lamaze's team. First I should thank the two pillars of the team: Cédric giving away all his wisdom, whenever I had scientific doubts; giving away his patience when witnessed my amazing writing skills and my perpetual moving leg. Thanks to Christine, the other pillar of the team, for helping developing my project and being so supportive. Thanks also Nicolas, for being my in lab bromance, sharing his unrefined sense of humor and putting always a smile on my face. Thanks to Melissa, for the uncountable hours in the lab, our amazing gossip sessions and her friendship I know I can count on. Thanks to Satish, for the amazing chicken and this time yes, refined sense of humor (sorry Nico). Also to Chanting, one of the newer faces. Thanks also to our young not so young *cuico culiaó,* Cristian, who welcomed me in Chile and now wish to have an amazing time in the lab. Not forgetting about the postdocs Manon who thinks is from the south, but that's not the real south. Vibha who books "too much" the spinning disk, to Joanna our artisty postdoc

and to Pedro. I should also thanks all the people who is not in the lab anymore, like WeiWei and Daniela.
In addition I should thank to all the Ludger team with who we shared space, lab meetings full of scientifica feedback, and lunch and discussions filled with the most scientific and unscientific topics. Massito the messiah, Estelle, Alena, Thomas, Allison (saving the planet from Curie).and Ewan for his warmth heart and uncountable discussions.

I also I feel the need to thank to my second home during this time. All the people integrating Vignjevic team who faced my constant invasion of benches and lab space. Whit special thanks to Fabien, sharing fatigues in the capsules making and being his work an essential part for the completion of this thesis. Not forgetting Jorgito, the tiny Rastanev, Denis and (welcome) Carlos the smart.

Also I'm happy to thanks all the excellent people I was lucky to meet in the community of institute curie. Building strong friendships and keeping my sanity from falling. Thanks to the international Curie Fam: Ana, Jacopo, Ben, Joseph, Sebastian. Thanks to the microscopic friends I made: Roberta and Sofia. The Spaniard connection building bridges between curie and Pasteur: Julia, Raquel, Juanma, Borja and my friends from Madrid and surroundings (Albacete is considered surroundings, whatever they say). The ITN-Biopol disgusting people, specially to Larisa and the Piel/la montagne team with old, old, auntie Bianca. Also, Dominika and the cooking sprees. Ilya and our monkey business and the first floor Hispanic juebebes.

Finally, I would like to dedicate this last lines to the people outside of my scientific environment. First my caring parents and their essential supply of Spanish charcuterie, my brother and Marta and my super sweet, lovely, evil nieces for whom I could write a chapter apart. To my friends back in town, els breguistes, Alvarito y la chachipandi vicentina with whom I shared so many chapters of my life. For last I would also thank to Orbea for carrying me all this time and bringing me to the places that matter.

Summary

La mécanique et le stress compressif jouent un rôle important dans la progression tumorale. Plusieurs approches ont été développées récemment pour tester le stress en compression dans des modèles 3D *in vitro* (Alessandri, 2013; Montel et al., 2012). Dans le travail présenté ici, nous avons d'abord exploré les effets de contrainte mécanique sur le microenvironnement tumoral et la progression tumorale. Lorsque les fibroblastes, parmi les composants cellulaires principaux du stroma tumoral, présentent un changement phénotypique lié à la tumeur , ils sont appelés fibroblastes associés au cancer (CAF) (Attieh et Vignjevic, 2016). Par rapport aux fibroblastes normaux, les CAF contribuent à la formation d'un stroma plus rigide (Calvo et al., 2013). Néanmoins, il existe une controverse sur le rôle des CAF dans la progression tumorale, car ils ont été signalés à la fois comme suppresseurs et promoteurs, suggérant un rôle antagoniste (Barbazán et Vignjevic, 2019). En outre, les interactions cellule-cellule entre tumeur et stroma, ainsi que leur rôle dans la transmission de force, devraient également être pris en compte (Jang et Beningo, 2019). La compression des tumeurs dans un espace confiné modifie ces paramètres (Alessandri, 2013; Haeger et al., 2014; Helmlinger et al., 1997). En utilisant un modèle de confinement 3D *in vitro* physiologiquement pertinent (Alessandri, 2013), nous montrons que nous pouvons reproduire l'organisation des CAF et leur interaction au stade du carcinome *in situ*. À l'aide de la technologie d'encapsulation, nous avons mis en co-culture des CAF avec des cellules cancéreuses du côlon à l'intérieur de coques élastiques creuses et perméables. Nous montrons qu'en l'absence de contraintes spatiales, les CAF et les cellules cancéreuses ne se mélangent pas mais se séparent en deux agrégats distincts, chacun constitué d’un des deux types de cellules. Cependant, avec la compression générée par le confinement spatial de la capsule, nous observons que les fibroblastes se réorganisent et s’enroulent autour de la sphéroïde des cellules cancéreuses, reproduisant ainsi l’organisation tumeur-CAF observée dans le carcinome *in situ*. Enfin, nous montrons comment la tension de surface des sphéroïdes individuels ne peut expliquer ce comportement à elle seule et comment ces changements semblent dépendre de la réorganisation de la fibronectine, modifiant

vraisemblablement l'équilibre de tension à l'interphase entre les CAF et la capsule d'alginate.

Dans la deuxième partie de ce travail, nous explorons le rôle des cavéoles dans le mechanosignaling des systèmes de compression 3D. La mécanoprotection est l'une des dernières fonctions attribuées aux cavéoles, lorsque notre laboratoire a démontré pour la première fois que les cavéoles peuvent protéger les cellules subissant des contraintes mécaniques des dommages de la membrane en s'aplatissant, limitant ainsi l'augmentation de la tension membranaire (Sinha et al. , 2011b). De plus, sur la base de liens importants existant entre cavéoles et signalisation, notre équipe a proposé l'hypothèse d'un rôle mécano-dépendant des cavéoles sur la signalisation, ces structures se comportant comme un commutateur mécanique dans lequel des composants cavéolaires peuvent interagir avec d'autres effecteurs moléculaires de cascades de signalisation après désassemblage des cavéoles sous contrainte mécanique (Nassoy et Lamaze, 2012). Cette hypothèse a bien été soutenue par plusieurs travaux récents de notre équipe. Tout d'abord, il a été démontré que l'ATPase EHD2, un des composants des cavéoles, faisait la navette entre la membrane plasmique et le noyau dans lequel elle va agir en tant que facteur de transcription. Avec mon projet de doctorat, nous avions pour objectif de traduire ces concepts dans un modèle de cancer physiologiquement pertinent. Pour ce faire, nous avons associé notre expertise des cavéoles à deux études pour étudier les effets du stress compressif sur les cavéoles dans un modèle 3D et pour explorer les événements de signalisation en aval dans cet environnement (Kévin Alessandri et al., 2013; Montel et al., 2011b).

Nous avons démontré que la lignée cellulaire triple négative du cancer du sein (le type de cancer du sein le plus agressif, dépourvu d'expression de HER2, des récepteurs des œstrogènes et de la progestérone) Hs578t est capable de répondre au stress mécanique en 3D en réduisant l'expression protéique de l'ATPase EHD2 et probablement en affectant la dynamique des cavéoles. Nous avons de plus observé que le stress de compression entraînait à court terme des changements dans la distribution et l'architecture

des cavéoles car les cellules présentaient moins de cavéoles à leur surface sous ces contraintes. Il est intéressant de noter que la compression à long terme semble réduire préférentiellement la présence de rosettes cavéolaires (inclusion de plusieurs cavéoles dans la membrane). Nous avons également utilisé notre modèle de cellules 3D pour surveiller l'activation de la voie de signalisation JAK-STAT et nous avons confirmé son inhibition sous une contrainte de compression.

En raison de nos résultats antérieurs établissant le rôle des cavéoles en tant que mécanosenseurs et de la preuve que cette propriété était retrouvée également avec un modèle 3D, nous avons décidé d'effectuer une série de criblages à haut débit. Tout d'abord, nous avons trouvé un profil d'expression génique différentiel sous compression par rapport aux conditions de repos. Fait intéressant, il a été révélé que le profil d’expression génique de chaque méthode de compression (capsule versus système hyper-osmotique) variait de manière significative, notamment pour la régulation de plusieurs voies de signalisation impliquées dans la régulation de la matrice extracellulaire, l’ubiquitinylation, le cytosquelette ou encore les composants exosomes.

Abreviations list

- Extracellular matrix (ECM)
- Atomic force microscopy (AFM)
- Focal adhesions (FA)
- Focal adhesion kinase (FAK)
- Phosphatidylinositol-3 kinase (PI3K)
- Epidermal growth factor (EGF)
- Mesenchymal stem cell (MSCs)
- Epithelial mesenchymal transition (EMT)
- Circulating tumor cells (CTCs)
- Two-dimensional (2D)
- Three dimensional (3D)
- Digital light processing (DLP)
- Electron microscopy (EM)
- Plasma membrane (PM)
- Caveolin1 (Cav1)
- Caveolin 2 (Cav2)
- Caveolin-3 (Cav3)
- Protein kinase c (PKC)
- Interleukin-6/ signal transducer and activator of transcription (IL6/STAT3)
- HR1 and HR2 domains (Helical region 1 and 2)
- Phosphatidylinositol (4,5)-bisphosphate (PIP2)
- Endothelial nitric oxide synthase (eNOS or NOS3)
- Epithelial growth factor receptor (EGFR)
- Transforming growth factor β receptor (TGF-βR)
- Insulin receptor (IR)
- Caveolin scaffolding domain (CSD)
- Caveolin binding motif (CBM)
- Cancer associated fibroblasts (CAFs)
- Janus kinase 1 (JAK1)
- Clathrin heavy chain (CHC)

- Principal component analysis (PCA)
- Gene ontology terms (GO)
- Reverse phase protein assay (RPPA)
- Multivesicular bodies (MSV)

-INTRODUCTION-

Cell mechanics and mechanotransduction

Physiological relevance of cell mechanics in biology

All complex multicellular organisms are composed by cellular units which, scaling up to higher levels of hierarchy, form tissues, organs and, progressively, a whole organism. Cells, as any other object, have physical properties which respond to physical processes.

Not surprisingly a tight connection was found with regard to the importance of macroscopic physical processes paired with biological processes at different levels. One of the first modern science reports on mechanics contributing to the behavior of organs comes back to 1892 with the observations from Julius Wolff, describing the remodeling of human adult bone in response to mechanical stress (Wolff, 1892). It was then followed by the pioneering mathematical modeling work on biological patterning from Thompson (Thompson, 1917). But the close relationship between cell biology and mechanics was not really explored until relatively recent times. It was made possible by the arising of new tools that permit to mimic the stresses that cells stand inside the organism, to image and to measure them. Some good examples are the initial works on traction force from Harris and colleagues. They developed a substrate suitable to observe the deformation that cells exerted on the surface they adhered to. This set up gave knowledge on how cells can pull on the substrata by their own inner machinery (Harris et al., 1980) In addition, the development of magnetic beads coated with fibronectin mimicking peptide Arg-Gly-Asp (RGD), the known ligand of integrin α5β1, allowed to define the binding force of integrin molecules to the substrate (Wang et al., 1993). Through the introduction of microfabrication in cell biology, Ingber and colleagues managed to define the importance of geometry in cell growth and death, showing how cells die on 10 μm squares but survive on 10 μm diameter circle, independently from how cells are attached to the substrate: different extracellular matrix (ECM) molecules or antibodies against integrins (Chen et al., 1997). At the molecular level, the measurement of the folding force and response against force of some proteins such as the globular spring-like domains of titin was made possible by the introduction of atomic force microscopy (AFM) (Rief et al., 1997). At least, tuning the stiffness of a

collagen coated polyacrylamide substrate modulates cell spreading, motility and lamellipodia formation with highly dynamic focal adhesions (Pelham and Wang, 1997). These observations show the importance of substrate physical properties on cell behavior, and give a sight of how traditional cell culture is away from physiological conditions.

Mechanotransduction

Tensegrity model

All the described advances in probing and describing physical reactions and adaptations of the cells gave birth to field of cell mechanics which cover cell biophysics, soft matter physics and rheology, mechanobiology and cell biology. At the crossing between mechanical properties and cell biology one can find mechanotransduction.

Mechanotransduction is the process through which cells convert mechanical stimuli into chemical signals in order to regulate cell behavior and function (Iskratsch et al., 2014). Cells are usually embedded in a complex polymeric structure, the ECM, with whose interactions can be defined both biochemically and mechanically.

Cells are living in a dynamic environment with frequent changes on the physical parameters. Thus, facing both external and internal stimuli from which they have to adapt. One of this adaptations is the re-structuration of its morphology, implying changes either on the mesh of different polymers composing the cytoskeleton, their water content residing on the cytosol and/or the lipid barrier composing the cell membrane **(Figure 1 a)** (Wang et al., 1993).

From all the mechanical strains affecting the cell, we can distinguish endogenous and external mechanical stimuli.
Among the endogenous stimuli, the cytoskeletal assembly itself plays a major role:

- pulling and tensing induced by cytoskeletal filaments formation,
- bonding with the generation of a flexible meshwork that pre-stresses the system to resist deforming forces **(Figure 1 b,c)**.

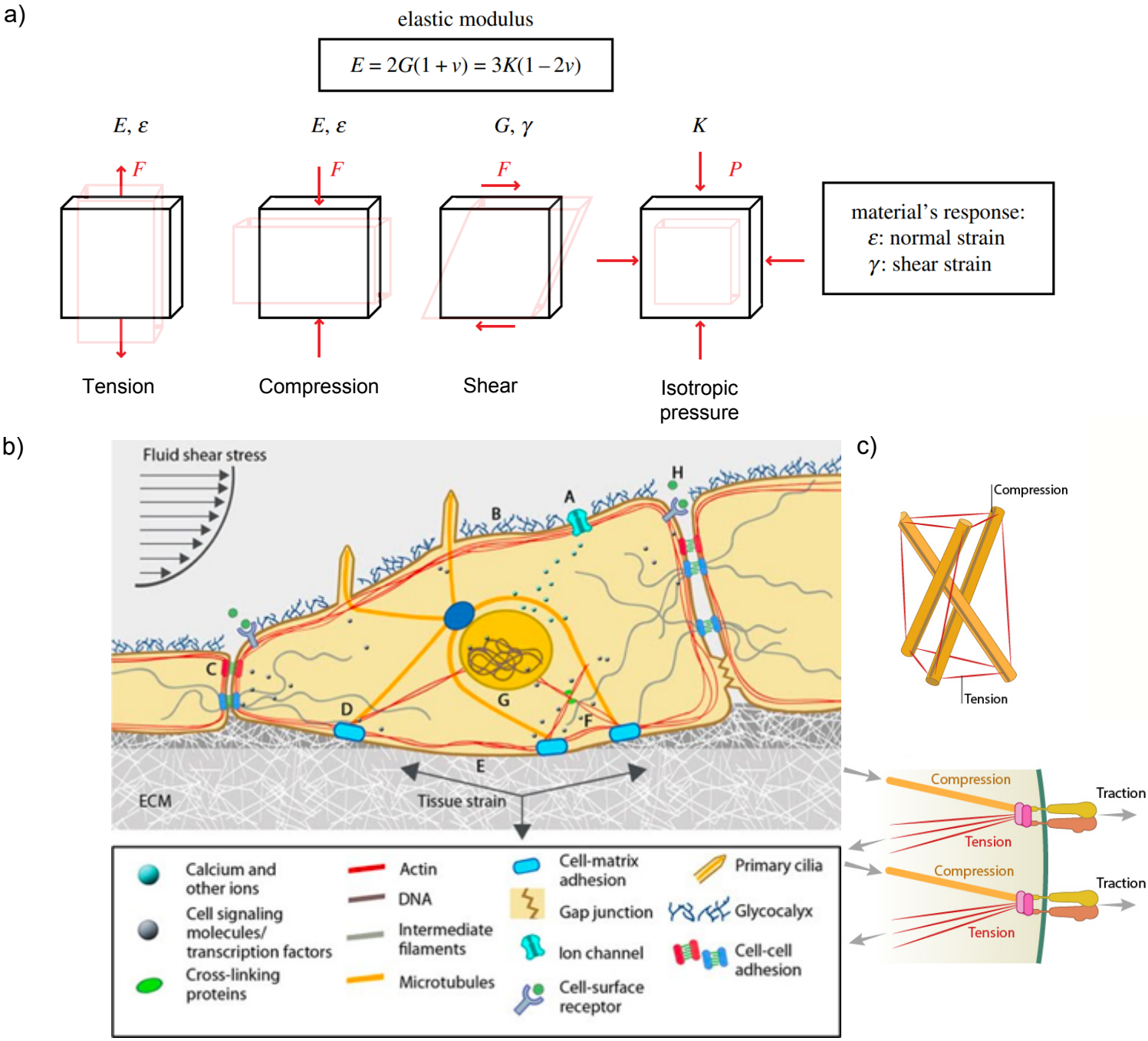

Figure 1. Mechanical forces experienced by the cell

(a) Types of mechanical stresses a cell can experience: When tension is applied to the cell it will result in a deformation of the cell towards the pulling force. When a cell is compressed the response of the material will be a compaction in the direction of the compressive force. Upon shear stress the deformation will be in parallel sense to the applied force. Upon isometric compression the hydrostatic pressure will be translated in a general compaction of the cell. A material resistance to elastic deformation to force (F) or stress (s) is the elastic modulus. E is Young's modulus, a response to tensile or compressive stress, G is the shear modulus, a response to shear stress, and K is the bulk modulus, a response to isotropic pressure.(based on Ayad et al. 2019). **(b)** Schematic representation of different mechanical stresses a cell can face on an epithelia and the components which can participate in the adaptation and response. With cytoskeleton components forming an structural template for the cell which will respond to the previously mentioned stresses and also connect the cell with another cells and with extracellular matrix. **(c)** Schematic of tensegrity model:compression struts and tensed cables exemplifying that stress levels regulate cytoskeletal rigidity. Microtubules (gold rod) support compression on cell-matrix adhesions (represented by actin linking modules in pink and integrin dimers) while the actin filaments (red) experience the cellular tension and stiffen accordingly (**b,c** adapted from mechanical How are forces transduced in a cellular environment? from mechanobio.info).

This preloading adaptable architecture is known as tensegrity (Chen and Ingber, 1999; Ingber et al., 2014) The forces applied by this contractile preloading architecture are mostly generated by the actomyosin machinery. Moreover, the actomyosin complex creates also traction forces on cell-cell contacts and focal adhesions. The tensegrity model should integrate other contributors to the general mechanical landscape of the cell. It should include the nucleus, as the stiffest organelle of the cell, that is able to respond to mechanical cues (Navarro et al., 2016), and caveolae, small mechanoresponsive plasma membrane organelles (Sinha et al., 2011a).

On the other hand, the external forces experienced by cells come either from tension, compression, shear, swelling or the curvature of the cellular membrane. The internal machinery, then, should respond to all the variations at micro and nanometric scales in order to keep cell homeostasis (Chen and Ingber, 1999; Ingber et al., 2014; Iskratsch et al., 2014).

Mechanotransduction and mechanosignaling

In order to respond properly to external forces, cells need molecules capable of feeling these changes and transmit this mechanoresponse. We refer here as mechanotransduction for the process that translates mechanical stimuli into biochemical changes on molecules. Mechanosignaling is part of mechanotranduction but restricted towards the activation or inhibition of signaling pathways.

For signaling pathways, there is usually a need for a receptor to trigger the signaling events after the initial stimulus, but in case of mechanics, what could be this receptor at the cellular level? One needs a mechanosensor, in other words, a biologically active molecule able to respond to mechanical forces by modifying its activity depending on this stimulus. Most common reported cases of mechanoresponse by proteins are based on intramolecular changes with modified folding, which expose new functional domains **(Figure 2 a,b)**. Among the known examples of mechanosignaling, the cell contact with the ECM via integrins is one of the most studied. Integrins switch to an activated conformation in conjugation with inside out mechanisms such as increased extracelullar Mg^{2+} (inside) and forces (out) from the

a)

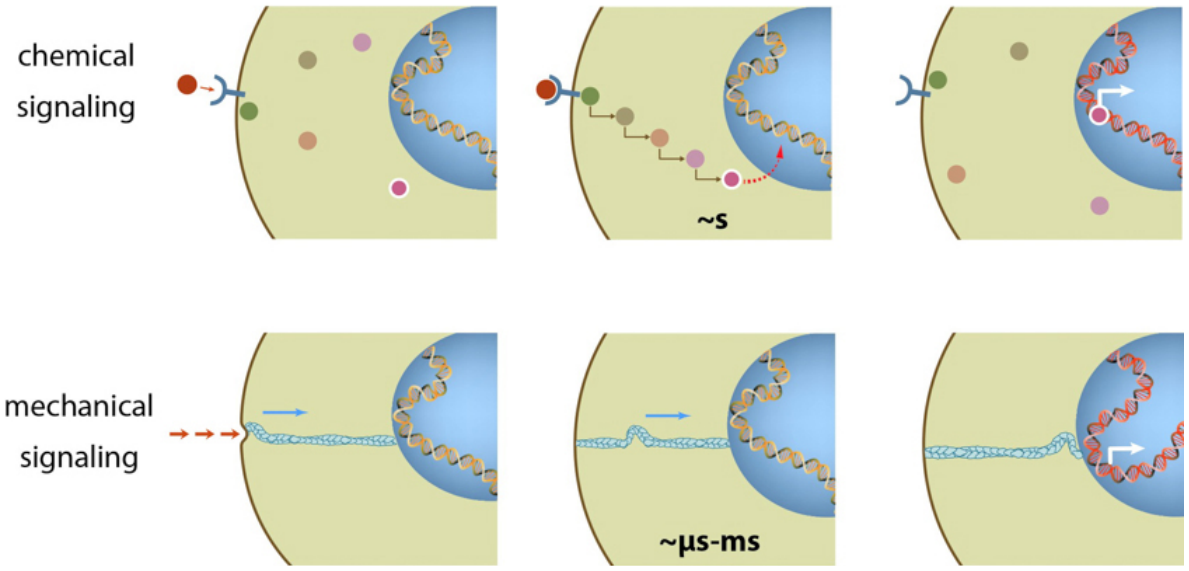
chemical
signaling
~s
mechanical
signaling
~µs-ms

b)

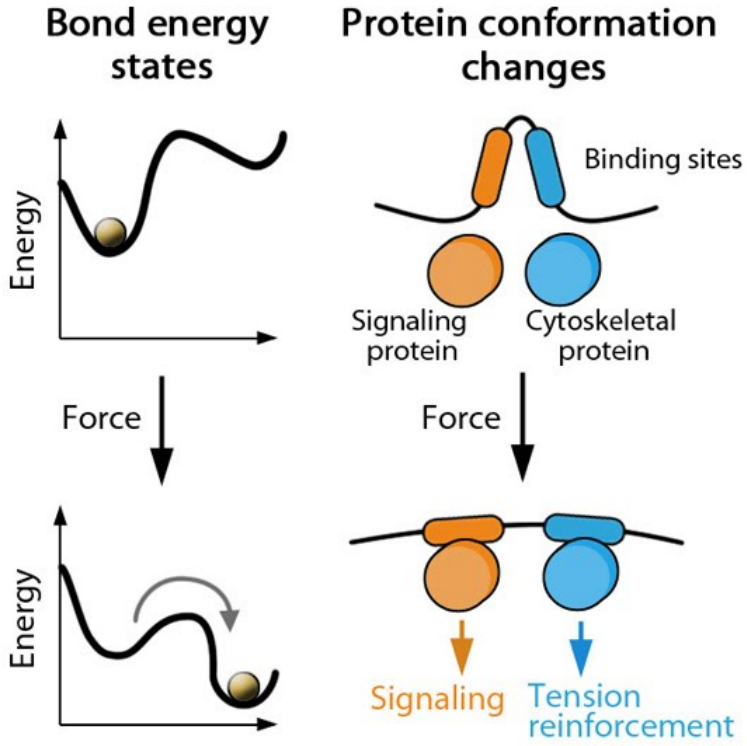
Bond energy states
Protein conformation changes
Energy
Force
Energy
Binding sites
Signaling protein
Cytoskeletal protein
Force
Signaling
Tension reinforcement

c)

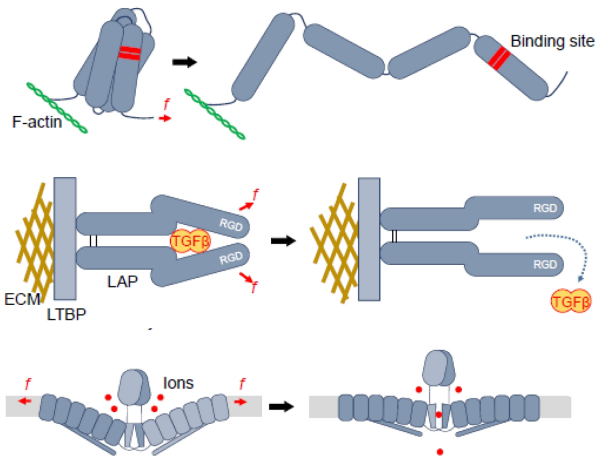
F-actin
Binding site
RGD
TGFβ
RGD
LAP
ECM
LTBP
RGD
RGD
TGFβ
Ions

e)

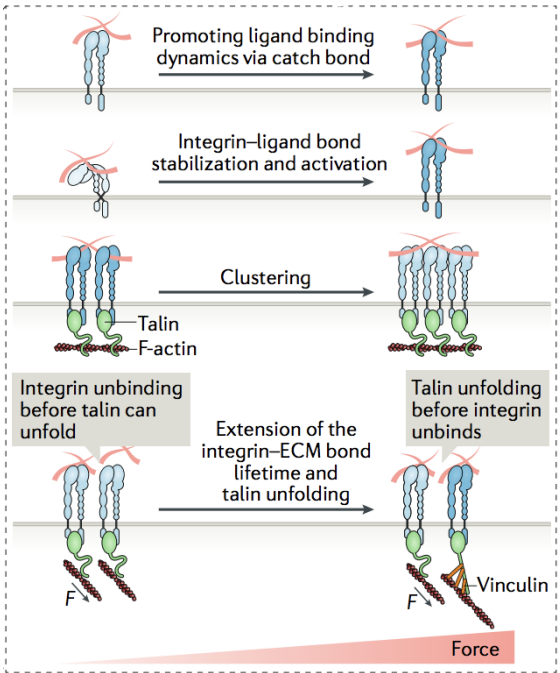
Promoting ligand binding dynamics via catch bond
Integrin–ligand bond stabilization and activation
Clustering
Talin
F-actin
Integrin unbinding before talin can unfold
Extension of the integrin–ECM bond lifetime and talin unfolding
Talin unfolding before integrin unbinds
F
F
Vinculin
Force

Figure 2. Mechanotransduction

(a) Comparison between mechanical versus chemical signal propagation. In the top part, chemical signal originated at the membrane take tens of seconds to travel through the pathways cascades and imply a change on the nucleus. In the bottom part, artistical view on how mechanical stress can propagate (either by stress applied to cytoskeleton or by cytoskeleton contraction) and reach the nucleus in less than 5 microseconds (adapted from mechanical How are forces transduced in a cellular environment? from mechanobio.info). **(b)** Changes in conformation of proteins upon applied force. Applied force lowers energy requirement making stable new conformations which can expose catalytic sites and pass this signal further(adapted from mechanobio.info). **(c)** Model of mechanosensing mechanisms from different mechanosensor. Top, cytoskeletal proteins linked to actin can undergo structural changes upon mechanical forces. This can expose binding sites and promote biochemical signaling. Middle, integrin- tethered latency-associated proteins (LAP) can experience conformational change and release transforming growth factor (TGF). Bottom, Piezo1 schematic with two subunits shown. Each of the subunits have a curved conformation in the lipid bilayer which flatten upon stress on the membrane (adapted from Lim et al. 2018) **(e)** Model depicting activation of integrins response to extracelular matrix signals, suchs as the stabilization of the inegrin-ligand bond, allowing talin unfolding before the unbinding of integrin (adapted from Kechagia et al., 2019)

ECM. This activation permits the separation of the intracellular tails of α and β integrins, which will increase β integrin affinity towards talin **(Figure 2 e)**. The force related mechanism for the formation of the focal adhesions (FA) is initiated by integrins binding to ECM, which slows down their diffusion and promotes their clustering. Integrins are coupled to the actin cytoskeleton via talin and vinculin. At the same time, actin will pull on integrins through talin and vinculin, while talin needs to be stretched to be able to interact with vinculin (del Rio et al., 2009; Kechagia et al., 2019). Later after the initial formation of FA, several signaling molecules are recruited as a response to this force generation/sensing, such as focal adhesion kinase (FAK), Src and phosphatidylinositol-3 kinase (PI3K). They will in turn trigger the activation of growth factor receptors and G-protein coupled receptors at FA (Kai et al., 2016; Kechagia et al., 2019) **(Figure 2 d).**

Regarding signaling, this unfolding mechanism can be compared to phosphorylation since both mechanisms will change the energy landscape of a protein tertiary and quaternary structure thereby modifying protein folding. However, this mechanical response can be faster than the purely chemical way of activation. At the plasma membrane, it has been observed that Src could be remotely activated in only 0,3 s by magnetic tweezers through integrins whereas 12 s are needed for ligand i.e. epidermal growth factor (EGF) mediated activation. This remote rapid activation cannot be fully explained as a local stress would only generate a local deformation, thus the proposed model of distant mechanotransduction assumes that a tensile pre-stress is needed through cytoskeleton and focal adhesion assembly (Na et al., 2008) **(Figure 2 b)**.

Another example are mechanosensitive channels such as the piezo receptors. This family of ion channels responds to an increase of membrane tension by changing their conformation. Under mechanical constraint, these ion channels occupy a greater space in the stretched lipid bilayer, increasing the permeability of the channel to ions. The open conformation allows a subsequent Ca^{2+} influx and the activation of calcium sensitive pathways mainly driven by calmodulin **(Figure 2 c)** (Coste et al., 2010; Volkers et al., 2015).

One striking example of the importance of mechanics in cell biology is its influence on stem cells fate. In a set of experiments performed by Engler, mesenchymal stem cell (MSCs) differentiation was monitored depending on the stiffness of the ECM. Surprisingly, 1 kPa substrate gave rise to neural progenitors, 10 kPa substrate triggers differentiation into myoblast, and cells grown on 100 kPa substrate showed an osteogenic phenotype. Still the effects of three different levels of stiffness dependend on myosin II function, and the priming induced by stiffness was sufficient to reduce the effect of chemical induction towards other lineages (Engler et al., 2006) **(Figure 3 a).**

Role of cell mechanics in cancer

As emphasized by the close interaction between signaling pathways and cell mechanics, it is not surprising that cell mechanics are involved in many physiological and pathological processes including but not limited to cancer

Studies on cancer provide important examples about the relevance of mechanical properties in biology, and the most relevant for this thesis. From a simplistic point of view, tumoral tissue is composed of tumoral cells surrounded by ECM. It is interesting thus that tumors tend to be stiffer than healthy neighboring tissue (Samani et al., 2003; Voutouri et al., 2014) **(Figure 3 b)**. The cancerogenic transformation of a healthy tissue comes along not only with changes in biochemical signaling or genetic expression, but the physical context is also dramatically perturbed, changing at each step of tumor progression: hyperplasia, invasion, dissemination and metastasis (Kumar and Weaver, 2009) **(Figure 3 b)**. This change though has been known for long time since palpation has been common technique for diagnosis in different cancers such as breast cancer since 1982 (Mahoney and Csima, 1982), and the incremented density detected by the imaging techniques (X-ray, ultrasounds) has been used extensively in tumor diagnostic. A 20-fold increase of stiffness has been observed in breast tumors and similar tendencies have been reported in pancreatic and colorectal cancers (Brauchle et al., 2018; Butcher et al., 2009; Levental et al., 2009). The drastic changes of the tumor microenvironment mechanical properties are due to several factors: the increase of cell contractility, the permanent growth of cells

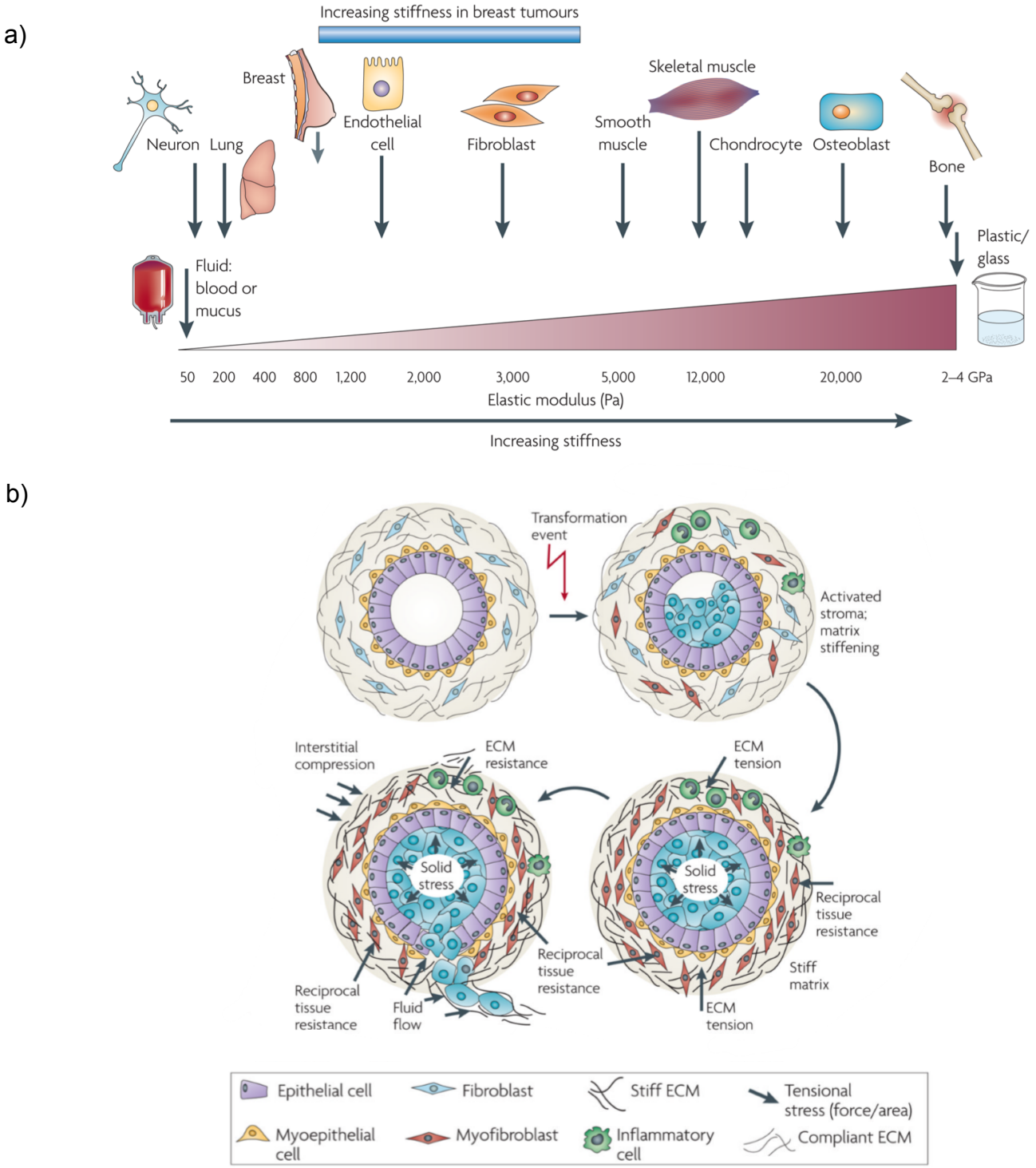

Figure 3. Tissue mechanics and cancer promotion

(a) Mechanical properties of the tissue where cell thrive are of utmost importance for the definition of the cellular identity. Having a big correlation between cell types and the stiffness of the tissue in which specific types reside. In cancer, and specifically in breast tumors, a progressive stiffening of the tissue is appreciated. **(b)** After a transformation event, cells accumulate in the lumen, compromising the structure of the breast duct. This uncontrolled growth will fill the duct and generate compressive stimuli both to the adjacent myoepithelium and basement membrane, which will generate a compressive stress back to the pre-neoplastic cellular mass. This will promote stiffening and remodelling of the ECM which generates a loop on the compression forces experienced by tumoral cells and parenchyma until the tissue structure is compromised and tumor cells can invade outside the ductal area (adapted from Butcher et al. 2009).

in a confined space and the aberrant deposition of ECM. As a consequence, the cancer cells thrive in stiffer substratum, either with increased integrin signaling through the reinforcement of clustering (Elosegui-Artola et al., 2014; Levental et al., 2009), enhanced resistance towards breast cancer cells drugs (Joyce et al., 2018), or facilitated tumor cell invasion and metastasis (Kai et al., 2016).

Therefore, the stiffness modifications present in tumors have important consequences on pathophysiological processes. It is also worth noting that most of the known mechanotransduction pathways are themselves products from oncogenes or tumor suppressor genes. These drastic changes experienced by cells in this altered mechanical environments can produce changes in cells in the same level as a mutation. (Yu et al., 2011). Perturbations of the system can affect the structure of the cytoskeleton, cellular shape, differentiation, cell survival, proliferation, adhesion and migration, which can all, promote cellular invasion **(Figure 3 b).**

Besides the contribution of stiffness from tissue and ECM, tumors can also face other physical stresses such as solid stress, shear stress and interstitial fluid pressure. As tumoral cells keep growing, they are trapped in limited space, the stroma will compress them on the opposite direction to cell growth. In addition, the surrounding tissue will show resistance to this deformation, a phenomenon called “solid stress” **(Figure 3 b)**. In response to the built up stress, at first, cancer cell proliferation decreases as reported in compressive cancer models both *in vitro* and *in vivo* (K. Alessandri et al., 2013; Delarue et al., 2014; Helmlinger et al., 1997). Recently, Mascheroni has modeled how compressive stress in cancer cells populations could increase drug resistance as compared to uncompressed populations, which are less proliferative (Mascheroni et al., 2017). Alterations of mechanical homeostasis have been shown to stimulate colon tumorigenicity with the compression of colon crypts that leads to nuclear translocation of β-catenin, activation of its target genes and hyperplasia in the affected crypts (Fernández-Sánchez et al., 2015). The increase of tumoral solid stress causes also squeezing of the blood vessels present in this tissue, which will temporary hint the tumor progression and generate a necrotic core by lack of nutrient perfusion and hypoxia (Padera et al., 2004; Stylianopoulos et al., 2013). Although hypoxia will briefly stop tumor cell growth, it could increase the risk of metastasis by promoting epithelial mesenchymal transition (EMT) and stemness in

cancer cells (Muz et al., 2015). Moreover, the solid stress that is generated can induce constriction of the lymphatic vasculature, which reduces drainage of the interstitial fluid, further increasing the compression of the tumoral compartment (Jain et al., 2014).

In the body, tumor cells can also face shear stress, when metastatic cells escape the confinement of the primary tumor and intravasate in the vasculature. To survive their transit through the circulatory system, cancer cells with high expression of lamin A/C seems more likely to survive when bloodstream levels of shear stress are applied (Mitchell et al., 2015). In addition, the survival of cancer cells depends on the time spent in circulation and the blood flow pattern. Resting levels of shear stress (0,5-3 Pa) inhibit proliferation but increase the chances of adhesion and extravasation of circulating tumor cells (CTCs) (Ma et al., 2017). On the other hand, using a microfluidics setup in or to apply shear stresses similar to the levels recorded on blood vessels during physical exercise conditions; 6 (Pa) will promote apoptosis on circulating tumor cells (Regmi et al., 2017). Thus, showing how circulating cancer cells need to adapt to the changing conditions in the blood vessels, where high shear stress also increase the chance of contact but reduces the ability to form stable adhesions. This is why in a high number of occasions, tumor cells tend to extravasate on branch points or are clogged in small capillaries **(Figure 4)** (Wirtz et al., 2011). But at the same time, when a stable adhesion is made, increased shear stress stimulates the extravasation. As a consequence, the ideal flow for CTCs to allow both stable adhesion and extravasation is 400–600 μm/s (Follain et al., 2018).

A leap in complexity: 3D cell organization models

Adding a third dimension

In order to have a more comprehensive model of the role of cell mechanics in tumor progression, the architecture of tumors should be taken into account. Most of the experimental knowledge generated in cell biology has been limited in two-dimensional (2D) plastic, glass or silicon substrates, although what we find in vivo are

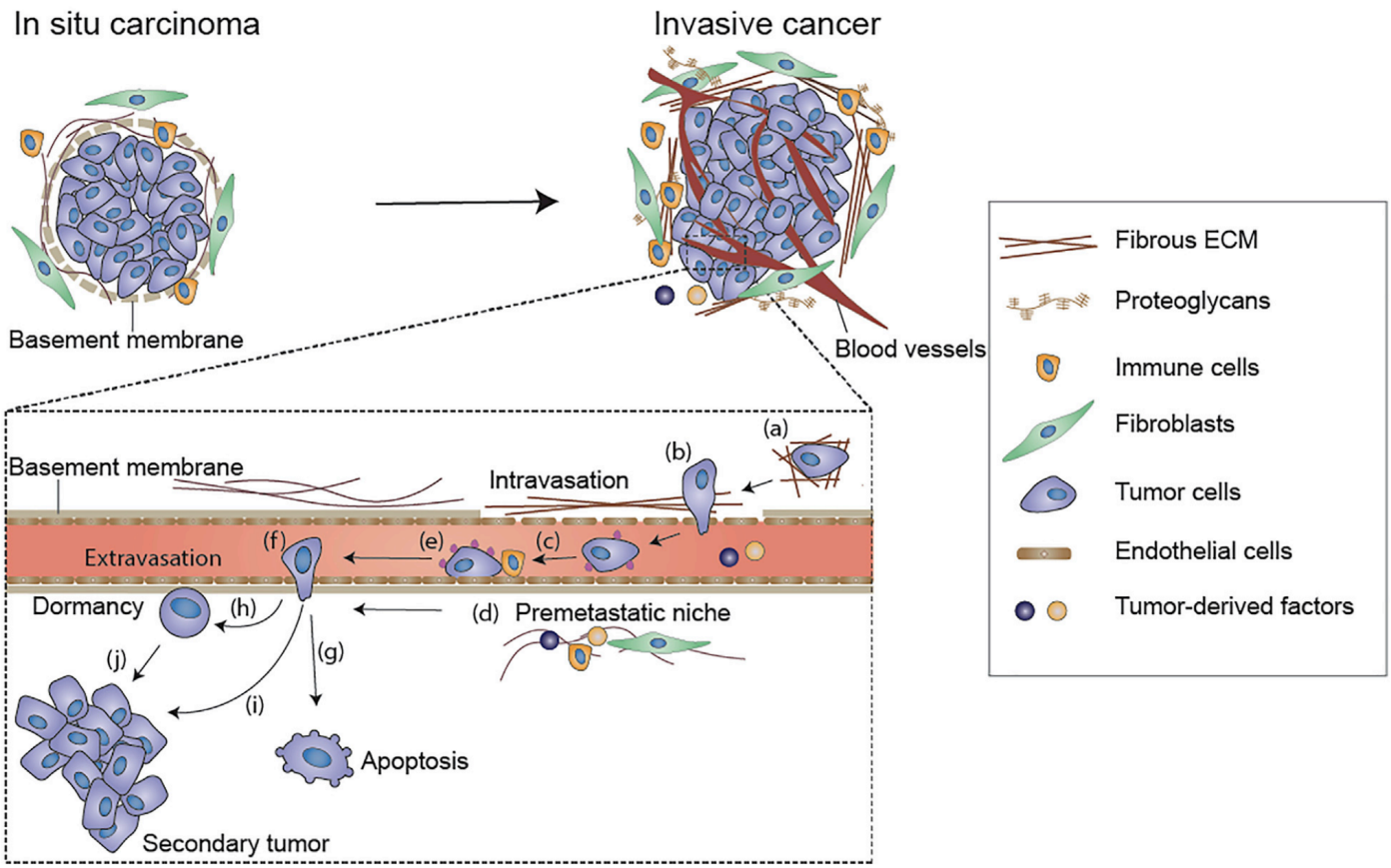

Figure 4. Mechanical perspective on metastasis steps

(a) Mechanical stresses faced by pre-neoplastic cells stimulate migration through parenchyma towards the vasculature. (b) ECM stiffness will further facilitate cancer cell intravasation and epithelial to mesenchymal transition. (c) When cell inside the vasculature this circulating tumor cells (CTCs) will face hemodynamic shear stress, in order to survive CTC can use platelet reaction to shield themselves and integrin- dependent adhesion signaling activation. (d) Primary tumor cells can secrete soluble factors, ECM proteins and exosomes which fosters proper conditions to create a secondary tumor niche. (e) Tumor cells upon an extravasation favorable site. (f) CTCs adhere to the endothelium and migrate between it. (g,h,i) Extravasated CTCs can undergo apoptosis, stay in a dormant state or proliferate into a metastatic tumor (Adapted from (Kai et al. 2019).

cells embedded in ECM with mixed populations of interacting cells with a complex architecture. If on one hand, a simpler 2D system allows to reduce complexity and help to address individual problems on isolated cells, on the other hand, it means that we lose the reality of these processes as compared to a more physiological environment (Baker and Chen, 2012).

It has long been reported that when cells, isolated from tissues, are seeded in 2D culture systems, they lose their differentiated phenotype (Mark et al., 1977) but some of them can easily re-adapt to their physiological phenotype when placed in a three dimensional (3D) culture environment. For instance, mammary epithelial cells, placed in a 3D environment, regain acinar distribution, form a new basal membrane and stop uncontrolled division (Emerman and Pitelka, 1977; Petersen et al., 1992).
These early observations established the importance of adding an additional axis to cell culture techniques for the determination of cell fate. Indeed, when cells were cultured to follow a 3D organization, it led to phenotypes closer to the ones observed during physiological conditions.

But we need to consider that this difference isn't just a difference of adding the third dimension in terms of space for the cells to grow. When the cellular architecture is switched from 2D distribution towards 3D, the changes in several important parameters for the biology of the cell are significantly altered, as reviewed in the next chapter.

ECM in 3D

The main source of significant changes between 2D cell behavior as compared to 3D environments is the important increase of cell-cell adhesions and cell morphology changes from an epithelial-like type (monolayer) to a more mesenchymal architecture. Cells growing in 2D are flat and can grow, spread and migrate horizontally, forcing an apico-basal polarity that in most of cell types is far from physiological situation **(Figure 5 b).**
Indeed, changes in cell architecture can influence cell behavior, as it has been proven by tuning the 2D geometry of cells by ECM protein micropatterning

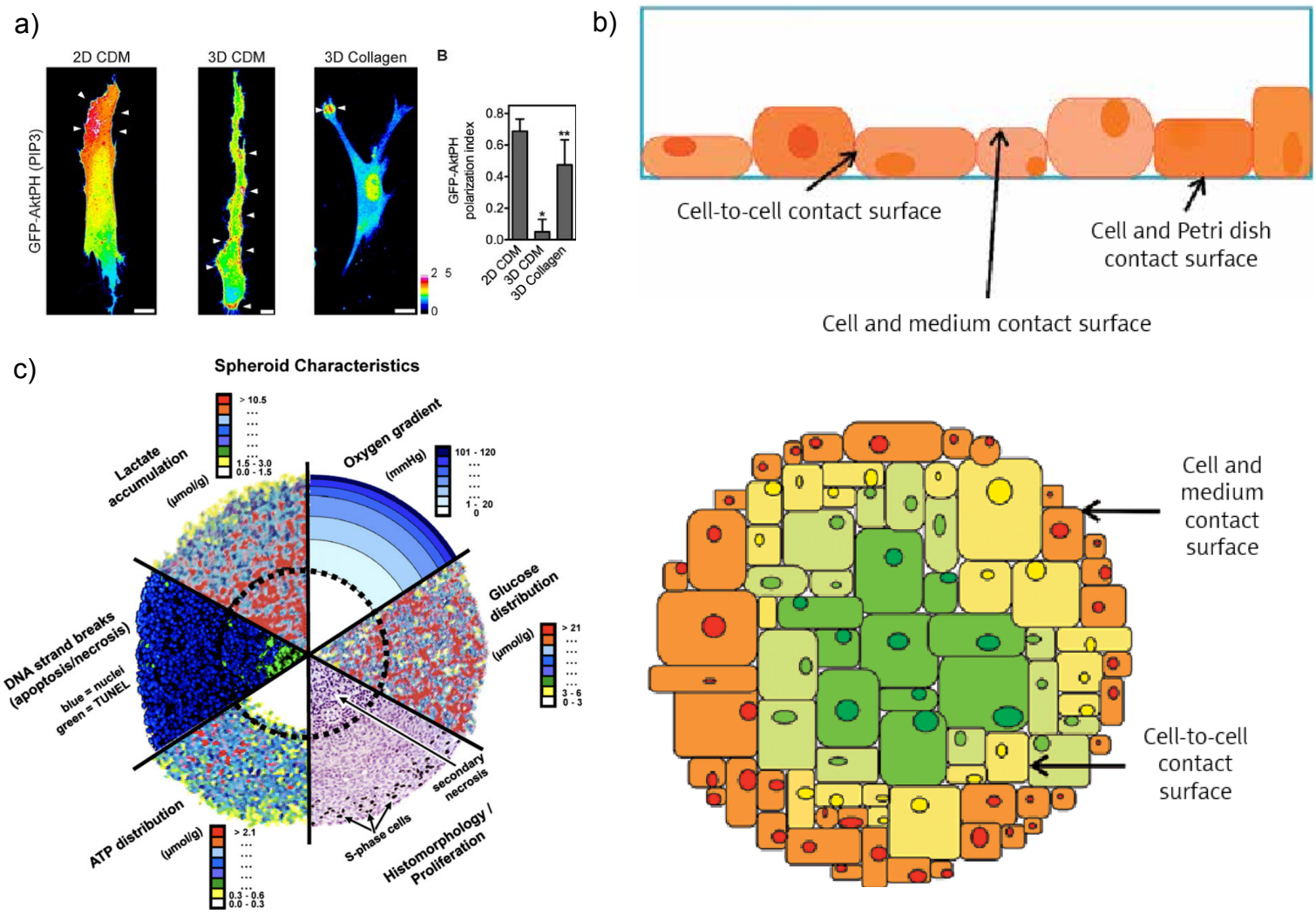

Figure 5. Importance of 3D architecture in cell biology

(a) Effect of 3D matrices on type of migration. Phosphatidylinositol (3,4,5)-trisphosphate (PIP3) localization on cells migrating on 2D and 3D cell derived matrix or embedded on collagen. Where they show a more star-shaped mode of migration (based on Petrie et al. 2012). **(b)** Schematic comparing 2D cell culture with 3D, depicting the low amount of cell-cell contacts of 2D compared with 3D and the reduced ratio between total volume of cells in contact with media, creating different domains depending on their location inside an spheroid (from Kapałczyńska et al. 2016).**(c)** Combination of analytical images of spheroid median sections studied with different technologies (autoradiography, the tunnel assay, bioluminescence imaging, and probing with oxygen microelectrodes) exhibiting the main characteristics of the MCS. (From Hirschhaeuser et al. 2010).

techniques. Specific geometrical shapes can trigger actin and microtubule cytoskeleton remodeling which impacts cell polarity, migration, growth and differentiation (Théry, 2010).
We can find considerable differences in the process of cell spreading in a 3D matrix in comparison with a 2D surface. In a 2D surface, integrin-mediated adhesions promote lamellipodia formation and the actomyosin tension reinforcement of focal adhesions within a few minutes. On the contrary, spreading in a 3D matrix often requires ECM deformation or proteolysis for the cells to migrate. In this context, cell spreading is way slower and takes hours or even days (Khetan and Burdick, 2010).

Cellular morphology and polarization present striking differences when we add the third dimension to the experimental set up. In 2004, Beningo et al. sandwiched fibroblasts between two polyacrylamide gels coated with ECM protein to establish integrin contact sites on two planes **(Figure 5 a).** With this approach, they showed that lamellipodium switch to a more stellated morphology, closer to the membrane morphology observed in fibroblasts *in vivo* (Beningo et al., 2004; Langevin et al., 2005). However, a more complete understanding of how cells organize in tissue and tumors the impact of 3D culture in cell signaling is still needed.

Besides morphological changes, 2D and 3D microenvironments induce differences at the molecular level with divergences in the nature and amount of adhesion proteins (Cukierman et al., 2001). Regarding mechanotransduction, evidence show that stiffness sensing might differ in 3D. For instance, the Mooney team showed that cultured mesenchymal stem cells embedded in 3D RGD-modified alginate gels, exhibit a bimodal response where osteogenesis is occurring maximally at an intermediate stiffness. In contrast, in 2D, the response reached a plateau. This mechanism depends on integrin clustering induced by exerted traction forces, a process which is not observed for cells grown on 2D substrates (Huebsch et al., 2010).

In many mechanotransduction studies using 2D experiments, the tensile forces are investigated by stretching adherent cells on a flat ECM-coated silicone surface, giving homogeneous predictable strains. On the other hand, most of the 3D tissues are highly heterogeneous and anisotropic and how the force is transmitted to the

individual cells depends mainly on the ECM fiber organization. The respective position of each considered cell within the tissue influences how they are constrained by those fibers. For example, in fibrocartilaginous tissue, the extent of stretch could differ dramatically depending on the distance from the attached collagen fibers (Pathak and Kumar, 2011; Upton et al., 2008). Furthermore, cell morphology, its orientation towards the forces and matrix architecture can affect cellular response to these forces. When strains (stretching) are applied to mesenchymal stem cells sitting on aligned or unaligned collagen fibers, the aligned ones exhibit further differentiation into muscle with increased activation of the corresponding signaling effectors as compared to unaligned cells (Heo et al., 2011; Kurpinski et al., 2006).

Besides the differences on how the fibrilar components of the ECM inside the spheroid behave such as increasing the presence of heterogeneous, anisotropic fibrous materials, 3D culture itself can display important differences in the purely mechanical response. While on one hand in 2D environment, the cells can deform out of plane upon a mechanical constraint. On the other hand, when grown in 3D in a spheroid, some cells could feel by a stretch in a point of the spheroid than would be perceived as a compressive stress for other cells in a tangential position. The application of stresses will travel through the body of cells in a spheroid. How cells and adhesions are able to transduce these forces in a 3D environment still needs to be further investigated (Baker and Chen, 2012).

Diffusion in spheroids

Cells grown in 3D will stand differences in terms of accessibility to nutrients and soluble factors as compared to 2D culture. The ECM, either within a spheroid or in gelated artificial matrices, slows down diffusion of molecules and generates sustained gradients. This phenomenon has been shown to play a role in drug resistance and the production of tumorigenic cell fates (Grimshaw et al., 2008; Shield et al., 2009). Cells, located between the proliferative outer layer and the central necrotic core, slow down their proliferation and start to express hypoxia inducible factors, which protects them against different antitumoral approaches like

radiotherapy and chemotherapy **(Figure 5 c)** (Hirschhaeuser et al., 2010; Mascheroni et al., 2017; Mueller-Klieser, 1997). Nevertheless, the transport and availability of soluble factors in a tridimensional ECM is not only depending on diffusion. For instance, pressure domains within the spheroid or tissue induced by deformation can redistribute the interstitial fluid and establish a convective transport of the soluble factors. Furthermore, some coupling between mechanical forces and solute transport have been reported, as discussed by Griffith: the rearrangement of cells in a tissue can change concentration of factors and the pore size, shape and morphology of the ECM (Griffith and Swartz, 2006).

In this subject the main parameters to take into account are: How 3D spatial distribution of the ECM proteins alter cell distribution and sensing of their environment; How this impacts structure and composition; and how different kinds of mechanical forces and their transduction have emerged in 3D setups (Baker and Chen, 2012).

3D culture technologies

For years, many laboratories have attempted to analyze the specific features of cell mechanics in tumors by characterizing the influence of solid stress in 3D environment rather than in cell monolayers cultured in a dish.

22 years ago, the important role of solid stress was reported in multicellular spheroids. To mimic the solid stress experienced by cells in tumors, Helmlinger and colleagues did a simple yet really informative experiment. Tumoral cells were cultured as multicellular spheroids, embedded in increasing concentrations of agarose matrix and let for growth for 30-50 days (Helmlinger et al., 1997). Then, they were able to characterize the equilibrium between the growing tumor cells and the opposite elastic constraint of agarose chains. By checking the proliferation and apoptosis rates, these assays gave precious insights about how a tumor reacts to its own mechanical cues. It revealed that the solid stress reduced spheroid growth, but counter-intuitively it decreased the apoptotic rate as well. This correlates with an increase of cellular packing, which seems to explain partly with the development of

drug resistance in tumors (Helmlinger et al., 1997; Joyce et al., 2018; Mascheroni et al., 2017).

More recently, two novel approaches for 3D cell culture compression have been developed that will be of utmost importance for this thesis, as we used them to investigate the cell machinery in the 3D mechanical response.

Hyperosmotic induced compression

In 2011, the Cappello team and collaborators introduced a new model based on multicellular spheroids that mimic an isotropic external stress by first growing colon cancer cellular spheroids over an agarose cushion and by applying a constant stress with dextran (100kDa) addition, a high molecular weight sugar that is neutral for mammalian cell metabolism. By tuning stress with dextran concentration with a maximum effect observed around 10 KPa, they were able to diminish the level of osmotic stress one-hundred fold less than the hyperosmotic experiments performed until date (1 MPa) **(Figure 6 a).** The portion of dextran that penetrates the spheroid is negligible and the osmotic stress is only applied to the first row of cells, which acts a dialysis membrane. Thus, the compressive stress is transmitted to the rest of the spheroid resulting in an average growth lowered by half at 0,5 kPa and by about 4 times after 5 kPa. The same system was further use to characterize the compression effect on cell volume. They showed a decreased organoid volume, cell jamming, and the overexpression of p27Kip1, a cell cycle inhibitor, few hours after compression thus inhibiting cell proliferation inside the spheroid **(Figure 6 b)** (Delarue et al., 2014; Montel et al., 2011a, 2012). Later, the same team investigated the degree of compression and the anisotropy of the spheroid in various zones. They observed a decreased pressure profile as the distance from the spheroid center increases. Cells are more compressed towards the core relative to the radial direction whereas they are stretched orthogonally to the radius. These deformations are probably a way to dissipate the stress generated by the isotropic compression **(Figure 6 c)** (Dolega et al., 2017).

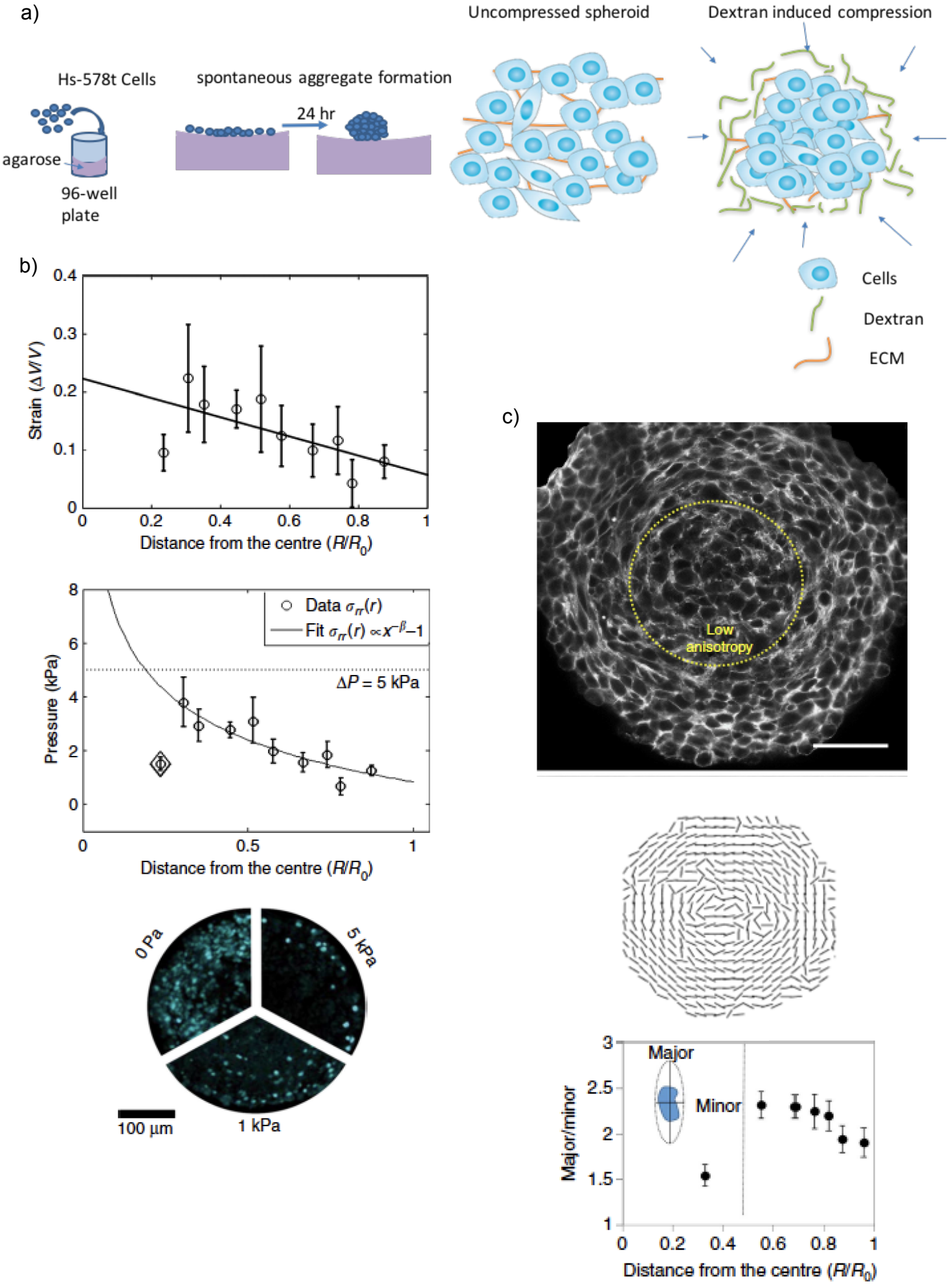
a)
Hs-578t Cells
spontaneous aggregate formation
24 hr
agarose
96-well plate
Uncompressed spheroid
Dextran induced compression
Cells
Dextran
ECM
b)
Strain (ΔV/V)
Distance from the centre (R/R0)
Data σrr(r)
Fit σrr(r) ∝x−β−1
ΔP = 5 kPa
Pressure (kPa)
Distance from the centre (R/R0)
0 Pa
5 kPa
1 kPa
100 µm
c)
Low anisotropy
Major
Minor
Major/minor
Distance from the centre (R/R0)

Figure 6. Hyperosmotic induced compression.

(a) Scheme of the preparation of 3D aggregates through the traditional agar cushion approach (non-adherent surface) and the application of compressive stress through the addition of high molecular weight dextran hyperosmotic solution (no penetration of dextran inside the spheroid. (b) Pressure distribution in CT26 spheroids upon 5 kPa compressive stress. First, pressure profile obtained with an stress/strain calibration curve of polyacrylamide microbeads. Second cellular proliferation in control spheroids and on spheroids with 1 and 5 kPa pressure applied. It shows immunostaining for Ki-67. (c) Organization of cells within CT26 spheroids. firs confocal image of Phalloidin staining at the equatorial plane, with a domain with low anisotropy marked (in high anisotropy zone major axis is perpendicular to radius). Under, scheme of the orientation of the major axis of cells at the equatorial plane. at the bottom anisotropy estimated with ratio of major axis of the cell with the minor and displayed average points along with the distance from center of spheroid (Adapted from Dolega et al. 2017)

Alginate encapsulation technology

The other approach for 3D cell culture we have used here is an innovative microfluidic-based high-throughput method, developed with our collaborators from Pierre Nassoy laboratory, that produces multicellular spheroids. This methodology has the originality to encapsulate cells inside a shell of alginate, a permeable and, in principle, not interacting polysaccharide from algae **(Figure 7 a).**

The system consists of a microfluidics device composed by three aligned co-extrusion channels: a cell solution in the inner capillary, an outer channel where alginate flows and an intermediate solution of sorbitol in physiological osmolarity (300 Osm) in between. The flow of each channel is controlled by syringe pumps and the average total flow is 100 µl/s. The chip containing the three channels produces a jet that decomposes into small regular pearls due to the intrinsic Rayleigh jet instability **(Figure 7 b).** This parameter can be further increased by the application of an electric field to increase the mono-dispersity of the sample and reduce pearl size. Then, the obtained cells/alginate solution droplets immediately gelate at the surface when in contact with calcium **(Figure 7 c)** (Alessandri et al., 2013)

Since the alginate shell is a visco-elastic material, one of the major advantages of this technology is to create a passive compression when cells reach confluence. Indeed, under these conditions, the alginate shell deforms and can be used as a read-out for compressive forces **(Figure 7 d).** An additional advantage from previous setups is the substitution of a bulk hydrogel for a hollow shell to test the compression component (Helmlinger et al., 1997). Using this technology with cancer cells, the initial results are on the same line as the ones obtained by Giovanni Cappello's team with the hyperosmotic induced compression. Indeed, once they reach confluency, cells embedded in the alginate capsule sustain a compressive stress of around 2 kPa, that induces decreased cellular proliferation, increased cell jamming and the presence of a necrotic core under the diffusion limit **(Figure 7e)** (K. Alessandri et al., 2013; Delarue et al., 2014; Montel et al., 2011a, 2012).

More recently, in an effort to scale up and simplify the set-up, the Nassoy laboratory used digital light processing (DLP) 3D printer in order to improve the handcrafted

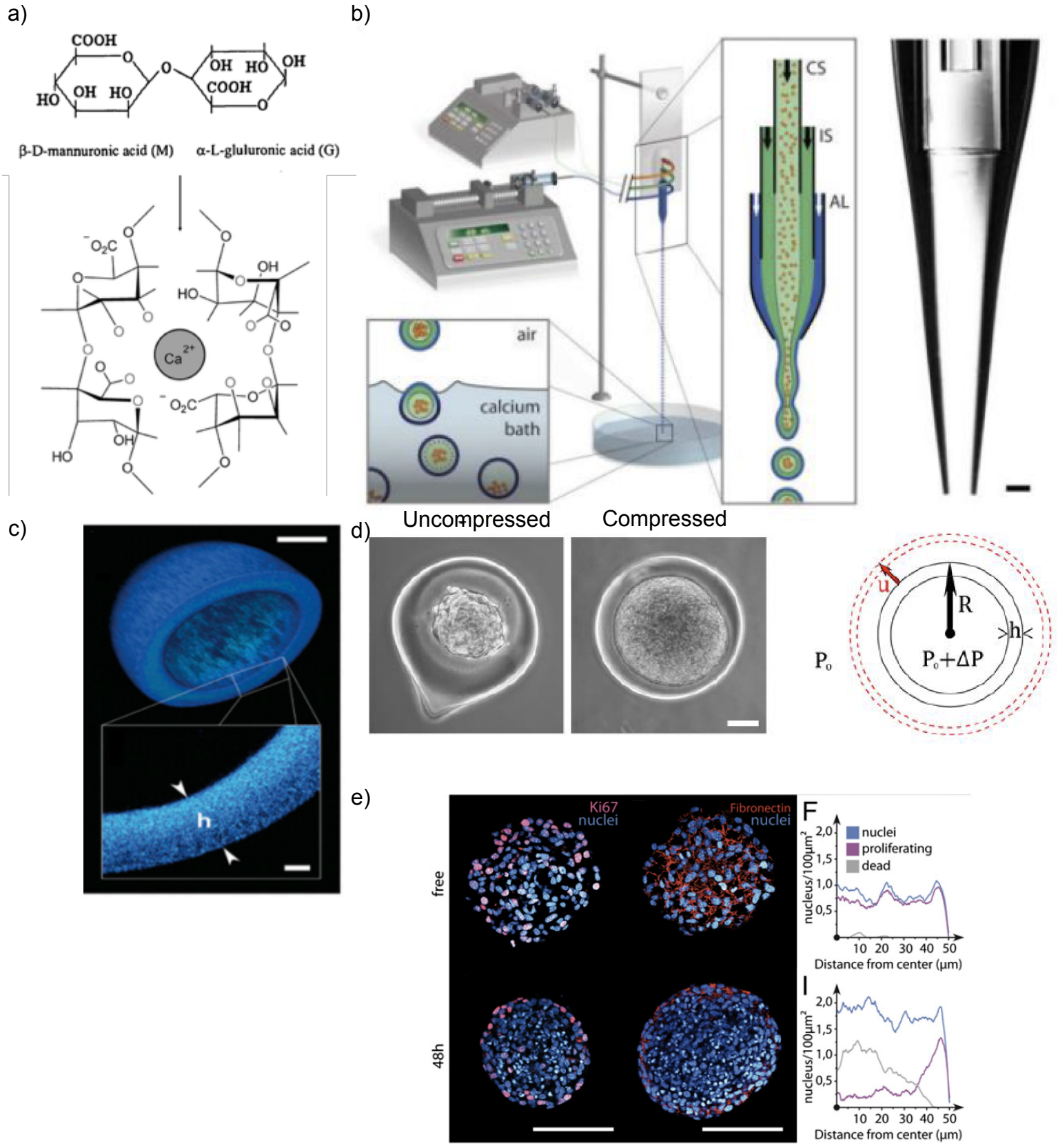

Figure 7. Alginate multicellular spheroids encapsulation for compressive stress

(a) Scheme of alginate monomers: D-mannuronic acid and L- glucuronic acid and how the cationic linkage with calcium promote the gelation. **(b)** scheme of the microfluidic device used for encapsulation. Constituted by 3 channels: inner channel (cs) where the cell solution is inserted, intermediate channels (IS) where and intermediate isosmotic (300 mOsm) sorbitol solution is inserted and an outer channel (AL) where the alginate solution is inserted. The solution will jet and fall onto a calcium bath where the alginate will gelate covering the other two solutions.All the channels are individually controlled by a pump. Right picture of the tip of the microfluidic device. **(c)** Confocal image of an alginate capsule stained with high molecular weight fluorescent dextran. **(d)** Phase contrast image of spheroids growing inside of capsules, depicting uncompressed and compressed states. On the right compressive behaviour of the alginate capsule where the thickness of the shell (h) diminish and it suffers an expansion or radial displacement (u). **(e)** Confocal images of free and 48h compressed spheroids. with cryosections stained for DAPI (blue), KI67 (magenta and fibronectin (red). on the right profiling of nucleus compared with death and proliferating cells (based on Alessandri et al. 2013)

microfluidics co-extrusion device used so far in our laboratories, mainly to overcome the delicate step of manually assembling the three capillaries in the extrusion chip. During my thesis I worked with Kevin Alessandri at Pierre Nassoy's laboratory in Bordeaux in order to implement the 3D printed chip in our team. The current model we are using differs from the previous one published as it has a coextrusion concentrical ring which needs to be completed by adding a 120-140 µm glass capillary pulled tip with its corresponding hydrophobic functionalization in order to have the correct size of capsules between 100 and 200 micrometers diameter (Alessandri et al., 2016)

Concerning the measurable degree of constraint in this system, capsules act, as mentioned above, as a confinement chamber where their deformation can be taken as readout of the degree of constraint or confinement. When the spheroid starts to fill completely the inner space of the capsule, the growth of the cell mass starts to deform the shell of the alginate. Because its viscoelastic nature, there is a restoring force exerted by the bulk material that its translated as a compressing force towards the spheroid. This compressive force can be estimated assuming that the alginate in the shell follows a linear elastic behavior the following formula relating pressure and deformation, knowing the mechanical properties of the alginate:

$$P = \frac{2E}{1-\vartheta} \cdot \frac{h}{R} \cdot \frac{u(R)}{R}$$

with ϑ being the Poisson modulus (ϑ=1/2 for incompressible material), h the thickness of the capsule, and u(R) the displacement. (already analyzed in our system) **(Figure 7 d)** (K. Alessandri et al., 2013).

Cell motility and cell sorting

One of the first questions that I addressed in my thesis work, was, following Fabien Bertillot thesis work; to reproduce and investigate the interactions between cancer associated fibroblasts and cancer cells in a compressive environment. I focused more particularly on how the physical properties of tissues will define their spatial distribution and its role on invasion and metastasis.

It has been known for a long time that distinct cells can segregate by tissue or lineage based on differences on the strength from cell-cell contacts and their affinity between different tissues (the following section its based mainly in Steinberg's classical publication from 1963). It has been long studied how tissues can behave as a fluid, an important parameter in the mathematical modeling of cell and tissue behavior. If we consider multicellular spheroids as liquid droplets and distinct cell types as two immiscible fluids, we can model the interaction of two distinct multicellular spheroids as the coalescence of two liquid droplets. Following this analogy, liquids are also composed by highly mobile subunits (thermal agitation of molecules), and tissues are a coherent mass composed by motile cells.

One important physical property of liquids is surface tension, which defines their natural tendency to minimize the surface area. As liquids are composed of molecules with a polar moment and are attracted to each other in the landscape of minimal free energy, forming a spherical droplet, so do the cells. The surface free energy is part of this minimal free energy landscape, and is also composed by the same molecules but with a non-neutralized polar momentum **(Figure 8 a)**. As free energy will always tend to spontaneously decrease, the molecules will always tend to expose the least of these free ends and, thus minimize the interface **(Figure 8 b)**. Having this principle on mind, mechanical work burden or any other change on this energy equilibrium needs to be applied in order to increase the surface exposure to the interphase (spreading the liquid droplet).

Briefly, the mechanical work $\delta \mathrm{W}$ needed to increase the interface area dA is $\delta \mathrm{W} = \gamma \, \mathrm{dA}$ where γ is the surface tension. If we have two immiscible liquids (two distinct cells populations), then the surface energy can be defined as the interfacial tension and noted γAB so that the mechanical work needed to separate a unit of area of the AB interface between two elements A and B is: $WAB = \gamma A + \gamma B - \gamma AB$

WAB can also be termed as adhesive work. In order to separate two elements of the same type, the mechanical work is defined as $WAA = 2\gamma A$, which is defined as cohesive work **(Figure 8 c)**.

From these equations, we can write:

$$\boldsymbol{WWAB} = \frac{WAA+WBB}{2} - \frac{\gamma AB}{2}$$

Figure 8

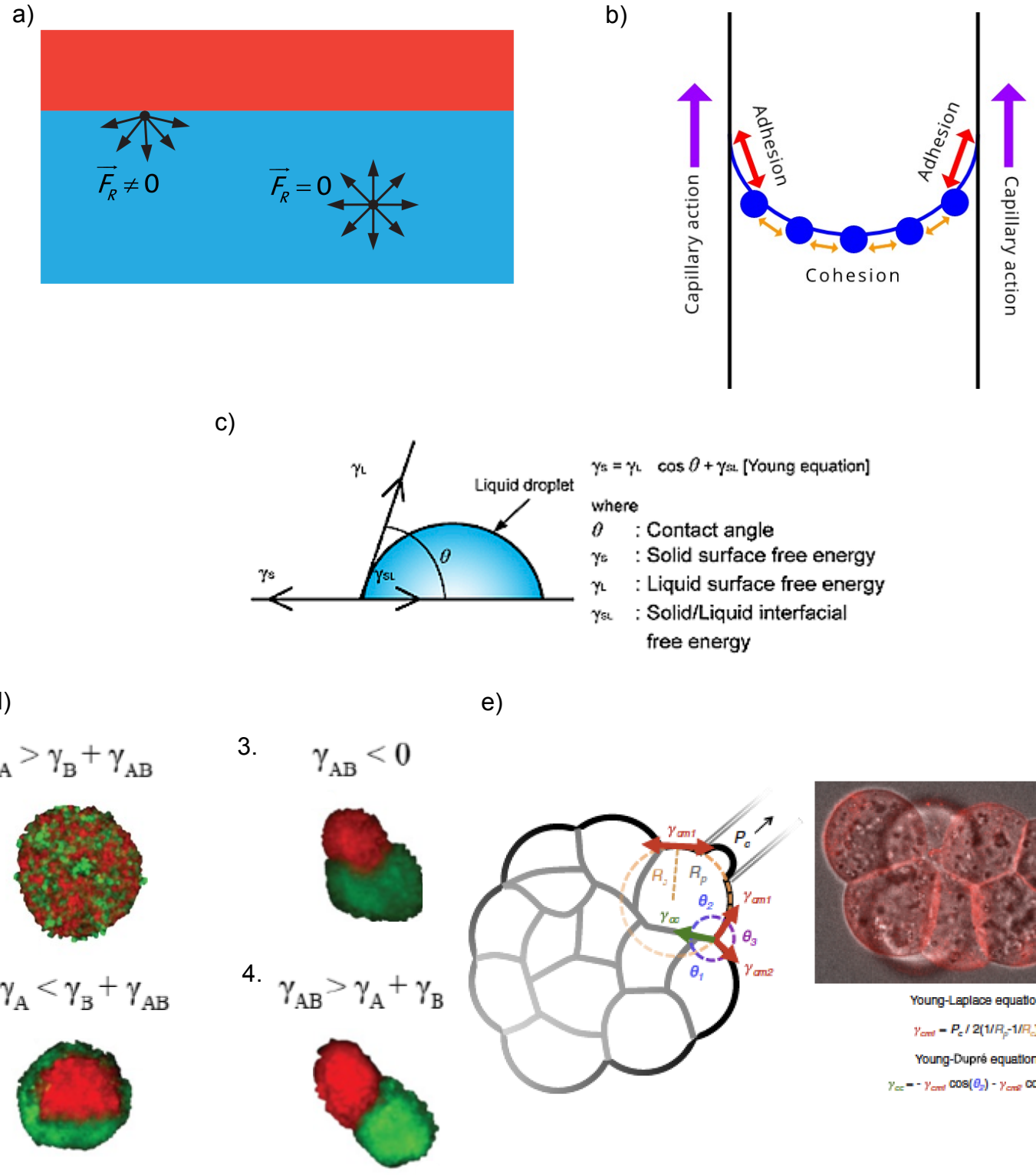

Figure 8. Surface tension and cell sorting

(a) The physical origin of surface tension. Where molecules of a fluid on its surface have an unbalance of forces (from "understanding interphases" at https://www.dataphysics-instruments.com). **(b)** Scheme depicting the adhesive work (different type of particles) versus the cohesive work (between same type) (from Chemistry, water" at https://www.visionlearning.com). Capillary forces are an example of adhesive work of a fluid. **(c)** Scheme of the contact angle from a droplet, defining the degree of wetting by Young-Dupré relationship where it depends on the equilibrium between the superficial tensions with substrata, the liquid and the surrounding media (from "wetting test methods" at http://www.adhesionbonding.com). **(d)** Possible arrangements when we have a mixture of two cell types. 1. both cell types are mixed resulting in a "checkerboard" pattern. 2. Cells with stronger cohesion aggregate in the center while weaker cohesion cells envelope the other type. 3. Partial envelopment of the cells presenting less cohesive forces. 4. No affinity (adhesive force) between both cell types, resulting in two isolated spheres (from Foty and Steinberg 2013). **(e)** Schematic diagram of the surface tension mapping technique. Using a micropipette of radius Rp, the surface of cell of radius Rc is bent to a deformation of size Rp at the critical pressure Pc. The Young-Laplace equation gives the surface tension at the celle medium interface gcm . Pc/2(1/Rp 1/Rc). After measuring two contacting cells of the aggregate, the tension at their cell-cell contact can be calculated following the Young Dupre equation. Right micropipette aspiration at Pc during a surface tension mapping experiment (based on Guevorkian and Maître 2017)

With this equilibrium, the distribution of these two types of units is a function of the cohesive work of each phase, and of the work of adhesion between them. This leads to three types of distribution depending on the equilibrium within the work forces stated before (graphically represented in figure 8 d):

1. a-b adhesions whose strength is higher than the average of a-a adhesions plus b-b adhesions. $WAB \geq \frac{WAA+WBB}{2}$ then $\gamma AB < 0$. This would result in a mixed kind of pattern with patches of each cell type.
2. a-b adhesions whose strength is weaker than a-a adhesions or b-b adhesions. $WAB < \frac{WAA+WBB}{2}$ then $\gamma AB > 0$. Cells types will segregate:
    a. If $WB \leq WAB$ we have $\gamma A > \gamma B + \gamma AB$. This should allow the formation of a sphere with the more cohesive cell type in the center and the less cohesive at the periphery.
    b. If $WAB < WBB$ we have $\gamma A < \gamma B + \gamma AB$. This should allow the formation of a sphere partially engulfed by the less cohesive cell type.
    c. At last, if $WAB = 0$, the lack of adhesive forces will generate two separate aggregates.

To measure the kind of adhesions that take part in this phenomenon, several different approaches have been available since the 90s to measure surface tension from tissues, and to test Steinberg's differential adhesion hypothesis (Foty and Steinberg, 2005; Steinberg, 1963). Among these methodologies that measure cell adhesive and cohesive forces, we can use AFM (Krieg et al., 2008), compression between two parallel plates (Foty et al., 1994), and micropipette pulling (Evans and Yeung, 1989). All these methodologies allow to measure the absolute values of mechanical properties in live tissue or, as done in the current study, spheroids. At the tissue level, the use of micro-aspiration allows to measure macroscopic mechanical properties like viscoelasticity and the tissue surface tension, which depends on the dynamics of tissue deformations.

In order to measure these deformations, we need to deform the material (strain) with a known force (stress). We can look back to 1954 when Mitchison and Swann first used a micro-aspiration device to measure the mechanical properties of sea urchin embryo from fertilization to first cleavage, improving our knowledge on the forces driving cytokinesis (Mitchison and Swann, 2005). Several other examples have followed in different tissues and for different ranges of forces with cell surface

tensions in the pN/µm range for granulocytes (Evans and Yeung, 1989) to tens to hundreds of Pa in the developing heart and brain tissues of chicken (Majkut et al., 2013). In order to measure the surface tension of the spheroids used in this study, we collaborated with Jean-Leon Maître's team. The surface tension of the cell medium interface γcm was determined with the following force balance equation (Young-Laplace equation) $cm = Pc/2(1/Rp\ 1/Rc)$, where Rc is the resting radius of curvature of the interface in contact with the micropipette, Pc is the critical pressure at which cell deformation reaches Rp, the micropipette radius **(figure 8 e)** (Biro and Maître, 2015; Maître et al., 2015).

How the surface tension and the viscoelastic properties of an aggregate relate to the mechanical and biological aspects of cells is still to be fully understood. In previous studies, a link between surface tension of multicellular spheroids with the amount of cadherins in the cell-cell adhesion has been proposed (Foty and Steinberg, 2005). Also, reconstituted aggregates from gastrulating zebrafish embryos led to the conclusion that the differential intercellular adhesions encountered in progenitor cells were not sufficient to explain sorting between them (Krieg et al., 2008). Instead, an additive effect of intercellular adhesion and differences in cell-cortex tension machinery rule this sorting. In addition, the recent work of Maître reports how difference in surface contractility of blastomeres can guide the cell sorting of a developing blastocyst (Maître et al., 2015).

The additive effect of intercellular adhesion and cell-cortex active tension machinery could explain how the tension of a multicellular spheroid is increased at the interface between the cells and the media, and decreased by the tension at the interface between cells. In order for the cell-cortex mediated tension to increase the overall surface tension of the aggregate, it must increase the difference between the tension at cell-media interface and the cell-cell adhesions. Increasing cell-cell adhesions decreases the tension at the interface, thus, increasing the surface tension of the spheroids. The tension at the cell-medium interface is only governed by the cortical tension, while the tension at the cell-cell interface is determined by the cortical tension minus the adhesion at this interface. This is also sustained by a mathematical model predicting the ratio of adhesion to cortical tension dictates tissue surface

tension (Manning et al., 2010). However, differential adhesion hypothesis does not fully explain cell sorting. A plethora of factors influence it, from directed cell migration, proliferation and extracellular matrix deposition could be involved in different degrees depending on the system studied. For example, in mammary glands cell sorting is highly dependent to the interfacial energy of tissue-ECM interaction (Cerchiari et al., 2015).

Caveolae

The main aim of my thesis was to understand how mechanotransduction of compressive stresses is mediated in a 3D cellular model. A seminal study by my laboratory has recently revealed the essential role of caveolae, small plasma membrane (PM) invaginations, in mechanosensing in 2D (Sinha et al., 2011a) (Figure 9 a). Thus, my objective was to test, in a 3D cellular context, the hypothesis that the mechanosensing response of caveolae upon mechanical stress could trigger mechanosignaling events (Nassoy and Lamaze, 2012) **(Figure 10 a)**.

Caveolae, small pits in the PM of around 50-100 nm, were first described in the 50s by electron microscopy (EM) by Palade, in the blood capillaries, and Yamada, on the gallbladder epithelium (Palade, 1953; Yamada, 1955).
Subsequently to their discovery in the gall bladder epithelia, they were found to be highly expressed in tissues that encounter mechanical constrains (like the gall bladder epithelium and vascular endothelium itself), adipocytes, and muscles (Cushman, 1970; Dulhunty and Franzini-Armstrong, 1975) **(Figure 9 b)**.
The main component of caveolae is the Caveolin1 (Cav1) protein that was identified more than 40 years after the discovery of caveolae (Kurzchalia et al., 1992; Rothberg et al., 1992). This was followed shortly by the discovery of the two other known homologues caveolin 2 (Cav2) (Scherer et al., 1996), and the muscle specific caveolin-3 (Cav3), forming the caveolin family (Tang et al., 1996; Way and Parton, 1995).

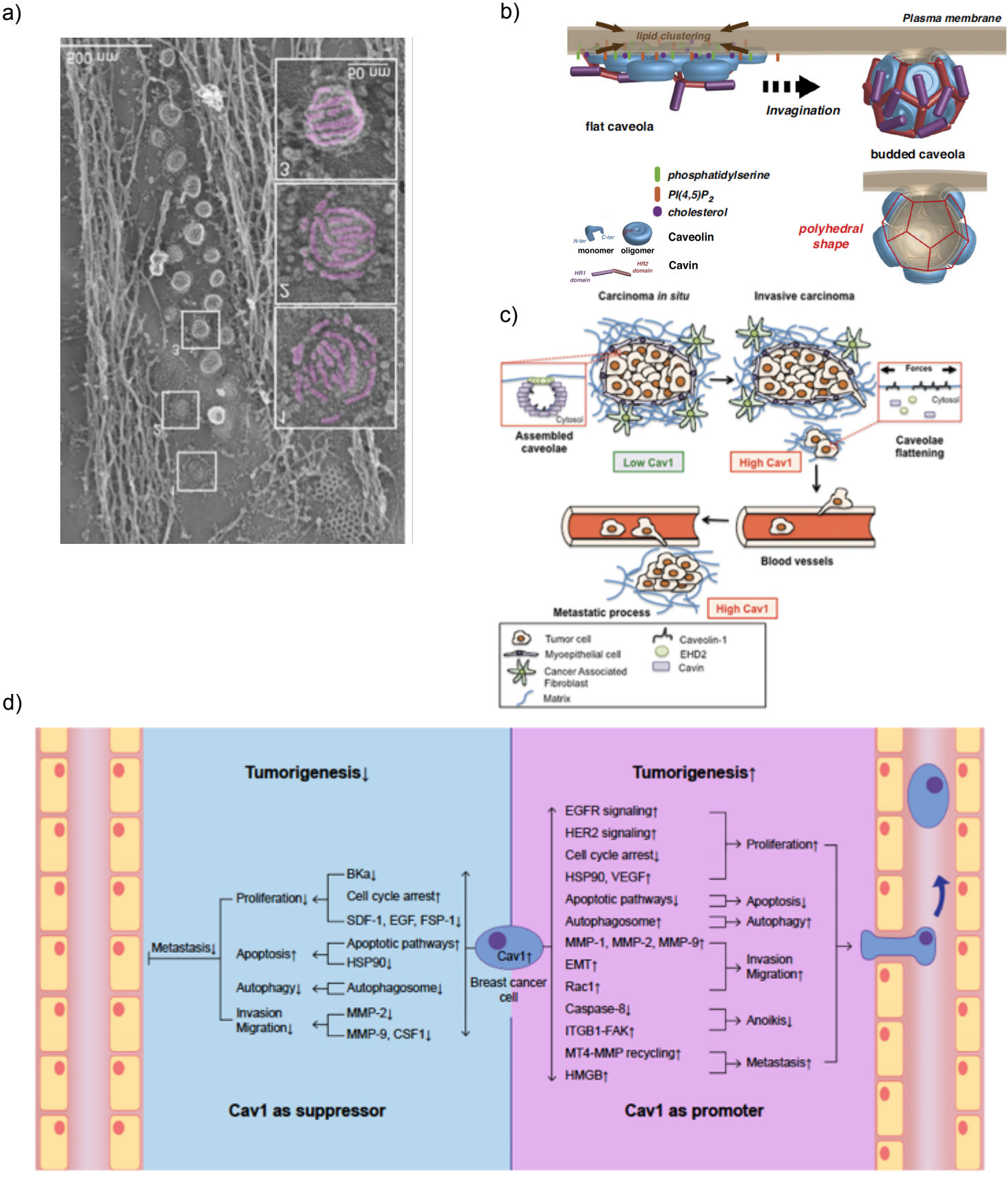

Figure 9. Caveolae morphology and role of caveolae in cancer.

(a) Metal replica EM micrograph of the plasma membrane of myotubes, presenting caveolae at its surface. Different types of caveolar structures could be observed: flat (1), circular (2) and fully budded (3). **(b)** Scheme of caveolae invaginated structure. with the components: caveolin (represented as discs on the membrane) and Cavin (as trimers coating caveolin oligomers) and the clustering of lipids such as cholesterol, PI(4,5)P2 and phosphatidylserine. Representation of flat caveola on left and budded caveolae on the rigth, forming a polyhedric structure where caveolin oligomers position in each pentagonal face and Cavins on the vertices (adapted from Lamaze et al., 2017). **(c)** Potential role of caveolae in tumor progression. Depicting tumor increase of stiffness and Cav1 variable patterns during tumor progression (low during proliferative stages and high on metastatic) and how this caveolar proteins expression pattern could be explained by the mechanical confinement of cells in cancer and the mechanical response of caveolae. **(d)** Dual Cav1 roles as tumor suppressor/oncogene in breast cancer carcinogenic process.

For long, caveolins were thought to be sufficient to form caveolae until the discovery of cavins, a new family of proteins that were required for caveolae morphogenesis (Aboulaich et al., 2004; Hill et al., 2008; Liu et al., 2008; Vinten et al., 2001). Indeed, it has been reported that the prostate cancer PC3 cell line or the nematode *Caenorhabditis elegans* express Cav1 but not cavin-1 and as a consequence lack caveolae structure (Hill et al., 2008; Tang et al., 1996). The cavin protein family is composed of four members. Cavin1 was the first to be identified as highly associated with caveolae enriched membrane fractions from human adipocytes, by mass spectrometry (Aboulaich et al., 2004; Vinten et al., 2005, 2001). It was followed by the identification of Cavin 2 which is also involved in membrane curvature induction and acts as a substrate for protein kinase c (PKC) (Hansen et al., 2009; Mineo et al., 1998). Cavin-3 also interacts with PKC and seems to play a role in the internalization and trafficking of caveolae (Izumi et al., 1997; McMahon et al., 2009, p. 3). And the last discovered member, Cavin 4, which is the muscle specific isoform (Bastiani et al., 2009; Ogata et al., 2008). One of the important features of Cavins is the presence of the HR1 and HR2 domains (Helical region 1 and 2), which allow their oligomerization **(Figure 9 b)** (Kovtun et al., 2014). Cavins, by interacting through the HR1 domain can form trimers were Cavin-1 can be associated to either Cavin-2 or -3 at a ratio of 2-3 to 1 (Gambin et al., 2013; Ludwig et al., 2013). Meanwhile the ratio of Cavin-1 to Cav1 association was estimated to be 1 to 4, and independent from other cavins. Altogether, a bona fide caveolae would be composed of approximately 150-200 caveolin subunits and 50 cavins for the whole complex (Gambin et al., 2013; Kovtun et al., 2015; Lamaze et al., 2017).

Several non-essential proteins have also been identified as playing a role in caveolae biogenesis. Pacsin-2, a F-BAR protein which senses membrane curvature, so far the only one of the F-BAR family to be identified in caveolae, seems to be involved in the regulation of caveolae morphology (Hansen et al., 2011; Senju et al., 2011). Moreover, the dynamin-2 GTPase and, of utmost importance for this study, the dynamin-like ATPase EHD2 have been both localized at the neck of caveolae (Ludwig et al., 2013; Oh et al., 1998). Among the roles of EHD2 in caveolae, my host team has recently published the first example of direct mechanotransduction mediated by caveolae, through the shuttling of EHD2 to the nucleus upon the stretching of the PM. In consequence of this nuclear shuttling, EHD2 is able to modify

Figure 10

a)

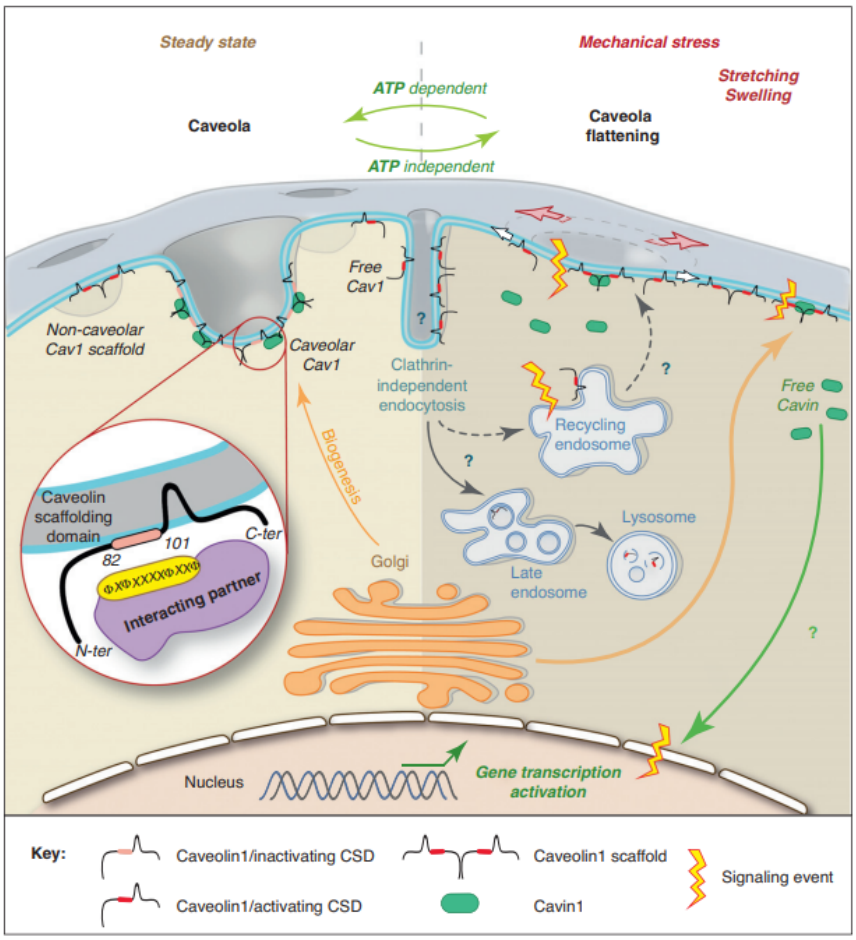

b)

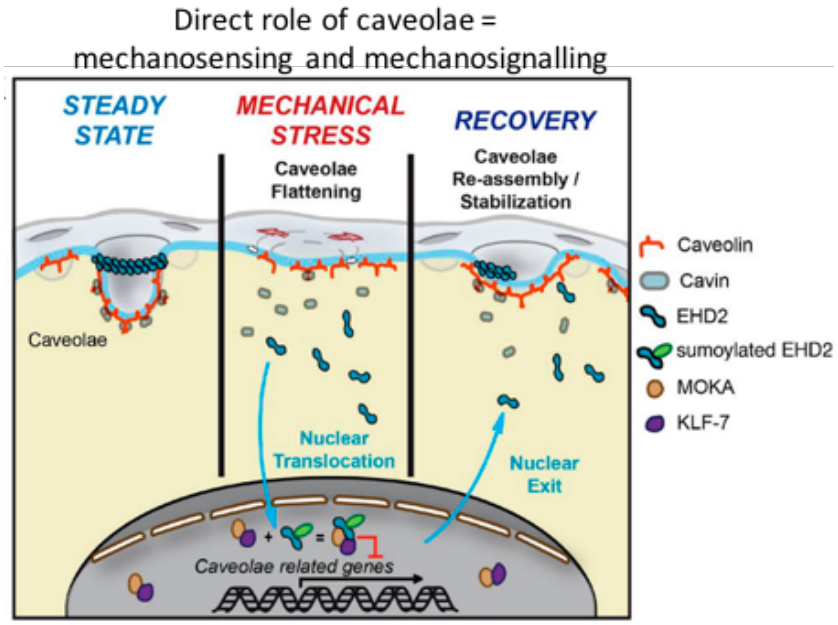

Figure 10. Caveolae mechanosensing role

(a) Working hypothesis on caveolae mechanosignaling for this project: Most of the caveolae is in its budded conformation in resting conditions. On response to mechanical stress, caveolae flatten out in the plasma membrane, providing additional membrane and buffering membrane tension. After this flattening event, caveolar structural components (Cav1 and Cavin1) are able to freely diffuse at the plasma membrane and the citosol. If the stress is retrieved the reformation of caveolae would fastly happen in an ATP-dependent manner. Caveolar components could be interacting with different signaling pathways. Specially Cav1, inhibiting different kinases through its caveolin scaffolding domain (from Nassoy and Lamaze 2012). **(b)** Caveolae remains invaginated at steady state and the integrity of the caveolar coat is intact. But it immediately disassembles upon a membrane tension increase. Then, caveolins, cavins and EHD2 are released, allowing EHD2 to shuttle to the nucleus, thus, forming a complex with the cofactors KLF-7 and MOKA, inducing transcriptional activity. Upon some resting time without the mechanical stress source there is a recovery of the caveolar complex, reducing EHD2 levels at the nucleus (from Torrino et al. 2018).

cell gene expression **(Figure 10 b)** (Torrino et al., 2018). Furthermore, EHD2 was reported to stabilize caveolae at the PM, through binding to the actin cytoskeleton (Stoeber et al., 2012). This may explain why, as shown in the case of the breast cancer cell line MDA-MB-436, which presents low EHD2 and high Cav1 expression levels, caveolae are absent, a possible consequence of the lack of EHD2 to stabilize these organelles (Torrino et al., 2018). Interestingly, the other proteins from EHD family (1,2 and 4) are also functionally involved in stabilizing the neck of caveolae. Indeed, the depletion of all three EHDs cause defects on the caveolar neck structure and a loss of caveolae after mechanical stress (Yeow et al., 2017).

Importantly, the caveolae structure is not exclusively composed of proteins. Lipids have an important role in caveolae formation and, presumably, functions. What we know so far about caveolae formation is that lipids, particularly cholesterol, are essential for caveolin oligomerization at the Golgi apparatus and caveolae invagination at the plasma membrane (Hayer et al., 2010a; Kurzchalia et al., 1992). Cav1 is known to bind cholesterol with a 1 to 1 stoichiometry (Murata et al., 1995). Once at the PM, caveolin oligomers promote the clustering of specific lipids, forming nanodomains (Sonnino and Prinetti, 2009). Among the lipids clustered, one can find sphingolipids, phosphatidylserine, involved in the clustering of caveolin and thus, caveolae (Hirama et al., 2017) and phosphatidylinositol (4,5)-bisphosphate (PIP2) which initiate caveolae formation via electrostatic force interaction with the HR1 and HR2 domains of cavins (Kovtun et al., 2014; Lanzafame et al., 2006). Additionally, an study on rat adipocytes measured the lipidic content of caveolin where the average adipocyte caveolae contained about $22*10^3$ molecules of cholesterol, $7.5*^3$ of sphingomyelin and $23*10^3$ of glycerophospholipid, also showing high levels of ganglioside GM3 (Örtegren et al., 2004)

Another unresolved question is whether caveolae assemble as a flat structure that will bend and bud inward to form the characteristic cup-shaped invagination or whether its preformed at the trans-Golgi and then fused to PM.
Recent structural studies propose, on one hand, a dodecahedron model for caveolar architecture, composed by discs of cavin complexes covering the caveolin oligomers

forming each pentagon of the coat **(Figure 9 b)** (Ludwig et al., 2013; Stoeber et al., 2016). On the other hand this disc proposed stoichiometry do not explain the striated coat observed on metal replica of the plasma membrane with deep etch EM and atomic force microscopy techniques **(Figure 9 a)** (Lamaze et al., 2017; Torrino et al., 2018; Usukura et al., 2016)

Caveolae are involved in a different range of cellular functions, which will be briefly reviewed here.

Caveolae in cell trafficking

Caveolae were first thought to be endocytic carriers due to their localization at the PM and their morphological similarity to clathrin coated pits. For instance, they were described to be involved in receptor-mediated transcytosis of albumin and low-density lipoprotein in endothelial cells (Ghitescu et al. 1986; Schubert et al. 2001). Moreover, some cargos can trigger caveolae mediated endocytosis like SV40 virus or Cholera toxin because these cargoes bind to GM1, a glycosphingolipid highly enriched in caveolae (Anderson et al., 1996; Pang et al., 2004; Tran et al., 1987). Once endocytosed, caveolae can be found fused with early endosomes (Shvets et al. 2015). Extracellular glycosphingolipids, lactosylceramide and cholesterol, with Src kinase activation, can also trigger the internalization of caveolae (Le Lay et al., 2006; Morén et al., 2019; Sharma et al., 2003; Singh et al., 2003). A consensus was recently reached in the field, which agreed that caveolae primary function is not endocytosis (Parton et al., 2019).

Caveolae in signaling

Since caveolins are Src-kinase substrate and caveolae host G-protein-coupled receptors, it was early proposed by Michael Lisanti that caveolae might play a major role in cell signaling (Lisanti et al., 1994). Later on, several additional signaling pathways have been linked to caveolae, with the apparent paradox that most effectors could not be localized into caveolae whether it is endothelial nitric oxide synthase (eNOS or NOS3), H-Ras, epithelial growth factor receptor (EGFR),

transforming growth factor β receptor (TGF-βR) or insulin receptor (IR) (Lamaze et al., 2017).

Moreover, several pieces of evidence suggest that Cav1 can directly interact with signaling molecules (transmembrane receptors, kinases, enzymes…), resulting in most cases in inhibition of the signaling effector (Czarny et al., 2000; Ju et al., 1997; Volonte and Galbiati, 2009). This interaction could occur through a specific region of caveolin (aa 82-101 in Cav1), known as the caveolin scaffolding domain (CSD), initially shown to be sufficient to inhibit eNOS activity (Gratton et al., 2000). In addition, a phage display assay has identified a high number of proteins with some degree of interaction with Cav1, which resulted in the discovery of a common sequence known as the caveolin binding motif (CBM), that would potentially interact with the Cav1 CSD (Couet et al., 1997; García-Cardeña et al., 1997). This assumption has however been challenged by an *in silico* structural study suggesting that most CBM domains should be "hidden" CBM in the quaternary structure of the Cav1 interacting partners (Collins et al., 2012). Likewise, the Cav1 CSD would be embedded in the PM, and therefore poorly accessible. These studies however were performed *in silico* and it is possible therefore, that the CSD-CBM interaction may be differently regulated *in vivo*. Indeed, it was proposed that caveolins could undergo conformation changes after phosphorylation on Tyr14 or Ser80 residues, or other modification of caveolae structure, exposing the CSD to potential interactors (Jung et al., 2018; Lamaze et al., 2017; Shajahan et al., 2012).

The role of caveolae in signaling may not exclusively be related to caveolins and direct interactions with its signaling effectors. The lipid composition of caveolae is likely to impact on the possible clustering of signaling molecules into caveolae. There are examples reported, such as the effect of caveolae disassembly on Cav1 and sphingolipids redistribution and also c-Src activation (Gervásio et al., 2011), calcium pumps localized in caveolae (Fujimoto, 1993), or impact on calcium signaling through phospholipase Gα in association with IP3 which need the environment that caveolae offers to function properly (Fecchi et al., 2006; Guo et al., 2015, 2011). Finally, recent data in my laboratory indicate that caveolae mechanosensing is tightly associated with the regulation of mechanosignaling (Dewulf et al., 2019; Tardif, 2018; Torrino et al., 2018).

Role of caveolae in mechanoprotection and mechanotransduction.

As mentioned before, cells experiencing high level of mechanical stresses have in common their enrichment in caveolae structures at the PM. Such examples are illustrated by adipocytes, endothelial cells, muscle cells, bladder cells, lung cells… Already in 1975, changes in caveolae architecture could be observed in skeletal muscle from frog upon muscle elongation and also in smooth muscle from the sea slug *Aplysia californica*, after freeze fracture treatment for EM (Prescott and Brightman 1976; Dulhunty and Franzini-Armstrong 1975). It was not known however if these changes could have been artefactually induced by muscle mechanical rupture. In 2011, in a collaborative effort from our laboratory with physicists, my laboratory established, for the first time, the role of caveolae as mechanosensors that flatten upon increase of PM tension, and thereby buffer membrane tension increase. PM tension buffering through caveolae flattening occurs in an actin- and ATP-independent manner (whereas the reformation of caveolae depends on ATP) (Sinha et al. 2011).

Since this seminal work, the importance of the mechanoprotective role of caveolae has been confirmed in many other cell types *in vitro* (Dewulf et al., 2019; Yeow, 2018) but also *in vivo* in different animal models such as zebrafish for skeletal muscle and notochord integrity (Garcia et al., 2017; Lim et al., 2017; Lo et al., 2015), and mouse for cardiac endothelium viability and function (Cheng et al., 2015).

Caveolae flattening leads to the release of caveolins and caveolar glycosphingolipids into the PM, and cavins in the cytosol (Gervásio et al., 2011; Sinha et al., 2011a). It is therefore possible to propose that the cycle of caveolae disassembly/reassembly will probably affect several of the functions that have been classically assigned to caveolae, in particular cell signaling (Nassoy and Lamaze, 2012) **(Figure 10 a)**. A first example was provided by H-Ras whose localization was affected under mechanical stress, most likely by the perturbation generated by caveolae flattening on caveolar lipid organization (Ariotti et al., 2014). More recently, my laboratory has shown that EHD2 is translocated to the nucleus upon mechanical stress and caveolae flattening to modify gene expression (Torrino et al., 2018), endowing caveolae with a mechanotransducing function organelle. Furthermore, our team has revealed that under mechanical stress the regulation of mechanoprotection by

caveolae is directly coupled with the regulation of interleukin-6/ signal transducer and activator of transcription (IL6/STAT3) signaling in muscle cells and that this regulation is absent in Cav3-mutated dystrophic patients (Dewulf et al., 2019).

Role of caveolae in cancer

Having in mind the roles of caveolae in signaling, it is not surprising to find a close relation of caveolae and its components in cancer and tumor progression. This leads us to the next questions, which is the role of the mechanical response of caveolae on cancer? And how cancer cells can interpret this mechanical signaling in the complex environment of the 3D architecture present in tumors (Lamaze and Torrino, 2015a).
(Having in mind the previously introduced links between cancer and mechanics and the prominent roles of caveolae in both signaling and mechanics)
Caveolae have been related to several cancer-associated mechanisms: cell transformation, proliferation, migration, invasion, drug resistance, and angiogenesis (Goetz et al., 2008). Although caveolae and more precisely Cav1 have been extensively studied, the roles of caveolae in cancer remain poorly understood. Furthermore, the role of caveolae is debated as two contradictory functions have emerged in studies on cancer. Indeed, Cav1 can act as an oncogene or as a tumor suppressor, which most likely will depend on the context and stage of cancer but this remains pure speculation at this stage.
For example, the inhibition of Cav1 in some signaling pathways, especially MAP kinases, is partly responsible for its tumor suppressor role (Engelman et al., 1997; Galbiati et al., 1998). On the other hand, many oncogenes such as Src, K-Ras and Bcr-Abl can down-regulate the transcriptional level of Cav1 mRNA. In addition, the knockdown of *CAV1* in the murine fibroblast cell line NIH-3T3 causes cell transformation, promoting tumor formation once injected into nude mice (Galbiati et al., 1998). This transforming role of Cav1 was further confirmed with the generation of *CAV1* KO mice, which were more prone to develop skin tumors after additions of carcinogenic stimuli (Le Lay and Kurzchalia, 2005).

Whereas it seems to have protective role at early stages, by inhibiting cell cycle progression and proliferation, Cav1 appears to favor metastasis in more advanced

tumor contexts and during invasion (Gould et al., 2010; Riwaldt et al., 2015; Trimmer et al., 2011) **(Figure 9 c, d).** Indeed, Cav1 protein expression could promote migration and invasion by increasing Rac1 activation through PI3 Kinase subunit p85α and RhoA/Rho associated protein kinase pathway, via Src-dependent Cav1 phosphorylation (Díaz et al., 2014; Joshi et al., 2008). Moreover, clinical data revealed a correlation between the upregulation of Cav1 and decreased survival for patients of pancreas, esophageal, breast, renal, brain and prostate cancers (Goetz et al., 2008)

But, we can see more clearly the, at first sight contradictory, dual tumor suppressor/oncogenic roles of Cav1 expression in cancer when we look into its pattern with more detail: Comparing prostate cancer cells Cav1 expression in metastatic sites overexpressed Cav1 in comparison to original tumor (Yang et al., 1998). Meanwhile different mutations on caveolin1 had been identified on around 35% ER-alpha positive breast cancers, thus correlating Cav1 functional inactivation to tumorigenesis. (Li et al., 2006)

Changes in Cav1 expression also affect its interaction with the tumor environment, a major factor for invasion and migration processes. For example, the loss of Cav1 expression in tumor associated fibroblasts has been reported to correlate with more deposition of ECM components in the tumor microenvironment along with a poor prognosis for breast cancer patients (Trimmer et al., 2011; Witkiewicz et al., 2009). Furthermore, the expression of Cav1 influences the remodeling and reorganization of ECM, facilitating invasion and metastasis (Goetz et al., 2011).

Cav1 is not the only caveolar component affected during tumor progression. A loss of Cavin-1 expression has been found in prostate cancer, in relation with a higher degree of migration and metastasis, which can be hypothesized to be linked with the reduction found in protein secretion in prostate cancer cell line PC3 secretory pathways (Gould et al., 2010; Inder et al., 2012). Others isoforms of Cavins such as Cavin-2 is downregulated in breast, kidney and prostate tumors (Altintas et al., 2013; Li et al., 2008) and Cavin-3 is associated with chemoresistance acquisition in colorectal cancer (Moutinho et al., 2014). EHD2 expression is diminished as well in several studies in melanoma (Welinder et al., 2017), esophageal squamous cell

carcinoma (Li et al., 2013), breast cancer (Shi et al., 2015; Yang et al., 2015) and hepatocellular carcinoma (Liu et al., 2016). Therefore, it is now considered as marker for poor prognosis in patients and correlates with higher invasion and metastasis. On the contrary, higher expression of EHD2 in papillary thyroid carcinoma had been correlated with poorest prognosis and higher risk of recurrence (Kim et al., 2017).

At the moment, there is no consensus on the role in cancer progression of caveolae and the interaction of caveolae components outside of the caveolae structure. Thus, we need to integrate the roles of caveolae in signaling and mechanics with the different stages of cancer. In order to achieve this goal. We need a model mimicking the pathophysiological context of cancer more faithfully than the 2D standard cell culture.

-OBJECTIVES

The major aims in this thesis are:

First, to investigate the interactions between cancer associated fibroblasts and cancer cells in a compressive environment, focusing on how the physical properties of tissues will define their spatial distribution and its role on invasion and metastasis.

Second, to understand how mechanotransduction induced by compressive stress is mediated in a 3D cellular model. I have therefore tested in a 3D cellular context, the hypothesis that the mechanosensing response of caveolae upon mechanical stress could trigger mechanosignaling events.

-RESULTS-

Role of mechanical stress in tumor-fibroblast interactions within 3D culture models

Objectives and summary

In the following section, we explored the effects of mechanics on tumor microenvironment and tumor progression. When fibroblasts, one of the main cellular components of the tumor stroma, become phenotypically modified together with the tumor, they are termed cancer associated fibroblasts (CAFs) (Attieh and Vignjevic, 2016). In comparison with normal fibroblasts, CAFs contribute to a stiffer stroma through increased contractility and ECM deposition (Calvo et al., 2013). Still, there is controversy about the role of CAFs in tumor progression as they have been reported to be both suppressors and promotors, suggesting an antagonistic role (Barbazán and Vignjevic, 2019). Besides, cell-cell interactions between tumor and stroma, together with their role in force transmission should be also taken into account (Jang and Beningo, 2019). Compression of tumors in a confined space alters these parameters (Alessandri, 2013; Haeger et al., 2014; Helmlinger et al., 1997). In the present work, using a physically relevant *in vitro* 3D confinement model (Alessandri, 2013), we show that we can recapitulate the organization of CAFs and their interaction at the stage of carcinoma *in situ*. Using the encapsulation technology, we co-cultured CAFs with colon cancer cells inside hollow, permeable elastic shells. We show that in the absence of spatial constraints, CAFs and normal cancer cells do not mix but segregate into two separate aggregates made of the individual cell types. However, upon compression, provided by the capsule spatial confinement, we observe that fibroblasts reorganize and enwrap the cancer cells spheroid, thus recapitulating tumor-CAFs organization observed in carcinoma *in situ*. Finally, we show how the surface tension of individual spheroids cannot explain this behavior alone, and how these changes seem to be dependent on fibronectin reorganization, presumably changing the tension equilibrium at the interphase between CAFs and the alginate capsule.

Pressure induces fibroblasts spreading through fibronectin reorganization

Fabien Bertillot[1,‡], Carlos Urena Martin[2,‡], Kevin Alessandri[1, x], Ludmilla De-Plater[3], Basile Gurchenkov[1,y], Florian Fage[4], Atef Asnacios[4], Christophe Lamaze[2], Jean-Leon Maitre[3], Pierre Nassoy[5,6,*], Danijela Matic Vignjevic[1,*]

[1] Institut Curie, PSL Research University, CNRS UMR 144, F-75005 Paris, France
[2] Institut Curie, PSL Research University, U934/UMR3215, F-75005 Paris, France
[3] Institut Curie, PSL Research University, UMR3666/U1143, F-75005 Paris, France
[4] Laboratoriess Matieres et Systems Complexes, F-75013, France
[5]LP2N, Laboratoire Photonique Numérique et Nanosciences, Univ. Bordeaux, F-33400 Talence, France
[6]Institut d'Optique Graduate School & CNRS UMR 5298, F-33400 Talence, France
[‡] These authors contributed equally to this work.
[x] current address: TreeFrog Therapeutics, ENSTB, 33076 Bordeaux, France
[y] current address: ICM, Brain and Spine Institut, F-75013, France

[‡]Equal contribution, * co-corresponding authors: Danijela Matic Vignjevic and Pierre Nassoy, e-mail: danijela.vignjevic@curie.fr; pierre.nassoy@u-bordeaux.fr

Abstract

The tumor microenvironment plays a key role in tumor progression. An important component of the tumor microenvironment is cancer-associated fibroblasts (CAFs). At the late tumor stages, CAFs stimulate tumor invasion by remodeling the extracellular matrix and leading cancer cell migration. However, at the early stage of tumor progression, before the onset of invasion, cancer cells and CAFs are segregated. CAFs are found at the tumor periphery, forming a continuous and cohesive layer surrounding the tumor. It is not clear how this peculiar organization of early-stage tumors is achieved. Current in vitro model systems based on the co-culture of cancer cells and fibroblasts fail to recapitulate this organization.

In this work, we have developed a physiologically relevant 3D in vitro model that recapitulates CAFs organization, as seen in carcinoma in situ. Using the cellular capsules technology, we co-cultured CAFs and cancer cells inside hollow, permeable, and elastic shells. We found that in the absence of spatial constraint, fibroblasts and cancer cells do not mix but rather segregate in two aggregates made of individual cell types. However, upon confinement (provided by the capsule), fibroblasts enwrap cancer cell spheroid, recapitulating the tumor-CAFs organization observed in carcinoma in situ. Using a combination of biophysical methods, live imaging, and immunostaining assays, we found that buildup of compressive stress and reorganization of the fibronectin network are necessary to induce fibroblasts spreading over the aggregates of tumor cells. We propose that the compressive stress generated by the tumor growth may represent a mechanism by which fibroblasts enwrap the tumor. This novel 3D in vitro model system could be used not only as a better mimic of the carcinoma in situ stage but also to study the impact of the presence of stromal cells on the radio- or chemo-therapy resistance.

Introduction

Cancer progression is multistep process that involves tumor growth and dissemination of cancer cells through the body. But on their journey, cancer cells are not alone. Their microenvironment, the extracellular matrix (ECM) and different cell types such as immune cells, blood vessels, and cancer-associated fibroblasts (CAFs) play an important role in cancer progression. By secreting growth factors and cytokines, CAFs stimulate proliferation of cancer cells and induce stem cell properties[1, 2]. CAFs also stimulate invasion[3] of cancer cells by remodeling the ECM[4-6], pulling cancer cells out of the tumor[7] and leading their invasion[8].

However, at the early stage of tumor progression, before the onset of invasion, cancer cells and CAFs are segregated. CAFs accumulate at the tumor periphery, forming continuous and cohesive layer surrounding the tumor[6]. It is not clear how this peculiar organization of early-stage tumors is achieved. The use of in vitro 3D cell co-culture models is expected to be the first strategy to explore. However, while multicellular spheroids are now widely used, and prepared using a variety of methods, studies based on co-culture multicellular tumor-stroma spheroids are still rare, and, to the best of our knowledge, aim to investigate the impact of the presence of stromal cells on radio- or chemo-therapy resistance of these more realistic tumor models.

Here we have generated an in vitro model for carcinoma in situ, and we asked if cancer cells and fibroblasts have the capacity to self-organize or if external cues are required. We observed that fibroblasts do not spontaneously envelop cancer cells. Instead, using a combination of biophysical methods, live imaging and immunostaining assays, we found that confinement, buildup of compressive stress and reorganization of fibronectin network are necessary to induce fibroblasts spreading over the aggregates of tumor cells. We propose that the compressive stress generated by the tumor growth may represent a mechanism by which CAFs enwrap the tumor as observed in vivo.

Results

Spatial confinement is required to induce and maintain fibroblasts organization around cancer cells

In order to generate a 3D model that recapitulates early tumor stages, we encapsulated non-invasive colon cancer cell line HT29 and NIH3T3 fibroblasts in hollow permeable elastic shell made of alginate using Cellular Capsule technology[9]. We anticipated different scenarios after encapsulation: i) the two cells types mix randomly resulting in a unique spheroid with checkerboard pattern; ii) cells completely segregate making two separate spheroids; iii) cells partially segregate with one cell type enwrapping the other (Fig. 1A). Then we monitored the dynamics of co-cultures over 15 days using time-lapse bright-field and fluorescence microscopy (Fig. 1B; Suppl. Movie 1). During the first 5 days of co-culture, when cells occupied only part of the total volume of the capsule, cancer cells and fibroblasts self-sorted forming two spheroids composed exclusively of one cell type. Segregation of cells could be explained by differential adhesion properties of these cells. Indeed, fibroblasts mainly express N-cadherins, while HT29 cancer cells mainly express E-cadherins. Similar cell sorting depending on the nature of cadherins has already been reported and was the first evidence for the Differential Adhesion Hypothesis (DAH)[10]. The length of interface between spheroids started increasing after about 7 days of co-culture, spheroids deformed and filled the unoccupied space. After about 9 days, 3D confluence was reached as spheroids completely filled up the capsule. Continuing growth of spheroids after this stage caused dilatation of the capsules as previously reported for encapsulated monocultures[9], and even more importantly, a drastic cellular reorganization (Fig. 1B, t=11 days, Fig. 1C). Fibroblasts started squeezing between alginate shell and cancer cells, and by day 13, they completely enwrapped cancer cell spheroid as seen in the epifluorescence snapshots (Fig. 1B) and revealed more strikingly by immunostaining and in toto confocal microscopy (Fig. 1D).

To validate the physiological relevance of this model for tumor progression, we also used untransformed CAFs isolated from the tumors of the colon cancer patients and co-cultured them with cancer cells. Due to much slower proliferation of CAFs in comparison with cancer cells, CAFs were scarcer in the capsules. Nevertheless, after

confluence, similarly as NIH3T3 fibroblasts, CAFs spread over cancer cells and adopted a needle-like shape resembling CAFs observed *in vivo* (Suppl. Fig. 1).

To further test if confinement is required for the specific organization of cells as seen in carcinoma in situ, we co-cultured fibroblasts and cancer cells using the more classical spheroid preparation method of the non-adhesive agarose wells, i.e., in the absence of confinement. As in the capsule, cells segregated and formed individual spheroids. By keeping both types of spheroids in close proximity, we never observed fibroblasts enveloping cancer cells spheroids even after more than 15 days of co-culture (data not shown). This shows that spatial confinement is necessary to induce the reorganization of the fibroblasts around cancer cells.

To test whether confinement is also required to maintain this cellular organization once the fibroblasts have enwrapped the cancer cell spheroid, we dissolved the capsule. Surprisingly, upon release of the confinement, fibroblasts started regrouping and reformed a spheroid attached to the cancer cell spheroid, similar to the initial stage, within less than 10h (Fig. 1E, Supp. Movie 2).

Altogether, these data show that co-cultured cancer cells and fibroblasts exhibit a self-organization transition into structures resembling carcinoma in situ, with fibroblasts enwrapping aggregates of cancer cells. This transition is triggered and maintained by spatial confinement.

Build-up of compressive stress is required to induce fibroblasts reorganization

Next, we assessed whether confinement alone (i.e. spatial constraints or cell crowding in a closed volume) was sufficient to drive fibroblasts reorganization or if this process originates from a mechanical stress (e.g. a threshold in the compressive force applied to the spheroids). As previously done[9], the pressure exerted by the growing aggregate of cells onto the elastic capsule, or conversely the restoring pressure exerted by the capsule onto the aggregate (according to action-reaction law), can be derived from capsule inflation according to a variant of the Hooke's law for a spherical hollow spring: $P = \frac{2E}{1-\nu} \cdot \frac{h}{R} \cdot \frac{u(R)}{R}$ where *u(R)* is the radial displacement at a distance $R_{in} \leq R \leq R_{out}$ from the center of the capsule, E the elastic modulus of the alginate gel (E=68 kPa), *n* the Poisson's ratio (*n*=1/2). We thus monitored the pressure exerted onto the capsule as a function of time (Fig. 2A). By comparison with

previously studied mono-cultures of mesenchymal-like cancer cells[9], the magnitude of the pressure is here about 2-fold larger, but the overall evolution is similar. Indeed, we found that pressure rapidly increased within the first ~ 30h at a rate of 0.55 kPa/h, followed by an abrupt decrease in the rate of pressure build-up (~0.22 kPa/h). Then we correlated these pressure measurements with the onset of fibroblast spreading (Fig. 2B). We observed that, in average, fibroblast enwrapping is triggered at P_{th}= 5±3 kPa. Despite the large variability, it remains noteworthy that less than 12% of the capsules, fibroblasts start to spread below 2kPa (Fig. 2B). This indicates that confinement alone is not sufficient to induce fibroblasts spreading, which only occurs over a pressure threshold, suggesting a mechanosensitive mechanism.

Because cells keep on dividing when confined, we cannot rule out that, instead of a pressure threshold, the rate of pressure buildup is the major determinant for fibroblasts spreading. To critically test the presence of a given pressure threshold, we blocked the growth of spheroids, and compared the outcome with continuously growing spheroids. We incubated the capsules with an anti-proliferative drug, mitomycin-C, at time t=0 corresponding to confluence (Fig. 2C). The impact of mitomycin C on growth inhibition was actually delayed by about 15-20h. Spheroids went on increasing in size, but at a slower rate compared to control capsules. They completely arrested about 15 hours after confluence (Fig. 2C). In controls, the number of capsules in which fibroblasts spread on cancer cells were increasing over time, as pressure builds up, reaching ~90% of capsules with spread fibroblasts at 35h (Fig. 2F). In mitomycin C-treated co-cultures, at a given time point, the percentage of capsules with spread fibroblasts was always lower than in the control capsules, which is consistent with the fact that volume, hence pressure, is reduced. Remarkably, in the time window over which growth is fully inhibited (typically 15-35 h), the percentage of capsules with fibroblast spreading remained roughly constant at about 25%. After 100h, the number of capsules in which fibroblasts spread did not evolve any longer remaining constant (34%). Of note, the value of the mean threshold in pressure P_{th} derived above means that, for a spheroid population, about 50% of spheroids exhibit a fibroblast-spreading pattern. The observed fraction of mitomycin-treated capsules with fibroblast spreading is thus qualitatively consistent with the value of P_{th}.

Together these data show that pressure, and not simply confinement, is necessary to induce fibroblasts spreading over cancer cells.

To gain more insight into how fibroblasts envelop cancer cells we performed two-photon live imaging at the onset of confluence (Fig. 2D, Supp. Movies 2 and 3). We observed that fibroblasts are dynamic even before the onset of spreading. The spreading started with fibroblasts stepping out as loosely cohesive chains of cells exhibiting dynamic cycles of protrusive activity. In few occasions, fibroblasts also detached from the chain and migrated as individual cells. This phenotype is reminiscent of moving cell network of neural crest cells [11] and other mesenchymal cells [12]. We then asked whether confinement could be the trigger of fibroblasts migration as it was shown in previous studies in 2D [13] and 3D [9]. However, we observed that prior to confluence, fibroblasts at the spheroid periphery were already highly motile while fibroblasts at the center were almost immobile (Supp. Movie 4). To quantify fibroblasts migration before and after confluence we tracked trajectories of individual fibroblasts (Fig. 2E) at the spheroid periphery and extracted standard parameters such as instantaneous speed and persistence path. While we did not find any difference in the speed distribution (Fig. 2E), the mean path persistence of fibroblasts increased significantly from 0.20 prior to confluence to 0.47 after confluence (Fig. 2F). Together, those data show that pressure does not affect the speed of fibroblasts but rather increase their persistence.

Surface tension of fibroblast spheroid is higher than cancer cells

The spreading of fibroblasts over cancer cells phenotypically reminds of a developmental process when one tissue envelops the surface of another, e.g. the epiboly in zebrafish. This process is driven by decrease of surface tension of the enveloping tissue [14-16]. In the framework of the Differential Adhesion Hypothesis, which relies on the liquid behavior of multicellular aggregates, two main scenarios can be anticipated i) if the interfacial tension (or adhesion energy) is large compared to the surface tensions of the two spheroids, a side-by-side morphology is expected for the two spheroids, and ii) for moderate interfacial tension, lower tension (or cohesion energy) spheroid will enwrap higher tension one, leading to a core-shell morphology.

To gain insight in the mechanism for the observed morphological transition under compression, we measured the surface tension of fibroblasts and cancer cell

spheroids using the micropipette aspiration assay[17] (Fig. 3B). These experiments (n=4) were performed on mono-cultures of cancer cells and fibroblasts in two conditions, in the absence of external compressive stress (i.e freely growing spheroids in the absence of capsule) and 10 days after confluence, corresponding to the stressed configuration. All surface tension values fall in the 10-30 mN/m range, in line with previous reports[18]. However, quite strikingly, while the surface tension of control fibroblast spheroids γ_f^0 is not significantly altered by compression ($\gamma_f^0 \approx \gamma_f^c$), the effect of confluence on cancer cells spheroids is more drastic: their surface tension in the unstressed state γ_c^0, which is 3-fold lower than γ_f^0, is increased by more than 2-fold upon compression. The difference between γ_f^c and γ_c^c is thus decreased although it remains significant. Altogether, before confluence, the observed side-by-side configuration and the measured surface tensions indicate that the interfacial tension γ_{fc}^0, which is not directly measurable, is high, at least of the order of $\gamma_f^0 - \gamma_c^0$ ≈20 mN/m. Using a simplified surface energy model, we may calculate the surface energies of the initial side-by-side (E_0) and of the compressed core-shell (E_c) morphologies. By further assuming that the volumes of the cancer cell and fibroblast spheroids, r_c and r_f, are equal to r and that growth is negligible between both states, the radius R of the composite spheroid (with fibroblasts surrounding cancer cells) is $R=2^{2/3}r\approx1.6r$. We finally get: and . Since , we obtain for the surface energy difference: . The enwrapping morphology is then energetically favorable if , ie. . From this coarse estimate, we derive that the interfacial tension vanishes (if it does not become negative).

In order to decipher the origin of this vanishing interfacial tension, we perturbed cell cortex tension by inhibiting cell contractility, more specifically the Rho pathway signaling, Rho-associated protein kinase (ROCK) and myosin II by respectively using Y-27632 and blebbistatin. We applied the drugs about 15h before confluence. We then measured the proportion of capsules in which we observed spreading at different time points before and after confluence. None of the drugs triggered spreading of fibroblasts before confluence, neither impeded or significantly increase spreading of fibroblasts after confluence (Fig. 3C). We thus concluded that decrease in cell cortex tension is not the direct cause of fibroblasts spreading.

Fibronectin reorganization is required for fibroblasts spreading

While difference in cell-cortex tension is the major contributor of tissue surface tension in embryos, cell-matrix-cell adhesions have also been shown to have an important contribution in tissue cohesion in cell lines that do not express any cadherins. For example, tissue cohesion and surface tension depend on the ability of cells to both secrete and assemble extracellular matrix. We thus stained the co-culture of fibroblasts and cancer cells for fibronectin prior and after confluence. At the early stage, before confluence, the fibroblast spheroids were enriched in dense fibrillar bundles of fibronectin mostly localized between cells, suggesting that fibronectin mediates cell aggregation, cohesion and compaction in fibroblasts (Fig. 4A). By contrast, in cancer cell spheroids fibronectin was only detected intracellularly, suggesting that cancer cells are able to produce fibronectin but lack the ability to secrete it or assemble it into fibrils (Fig. 4A). At the onset of spreading of fibroblasts over cancer cells, in the core of fibroblast aggregate, thick bundles of fibronectin were still observed in between cells as (Fig. 4B, region 1). However, at the front of spreading cells, fibronectin was detected only bellow the cells at the interface with the capsule (Fig. 4B, region 1). The appearance of the network also changed and consisted in thinner and sparser fibers. We have not detected fibronectin or any other ECM deposition at the cancer cell surface suggesting that the fibroblasts spreading is not due to an increase in the affinity between cancer cells and fibroblasts. At final stages, when fibroblasts completely enwrapped cancer cells, we observed that fibronectin network was mainly localized at the interface with the capsule as a continuous 2D layer (Fig. 4A). Until now, we have treated the inner wall of the capsule as an inert non-adhesive substrate as alginate gels properties do not support cell attachment. However, deposition of fibronectin at the alginate interface suggests that compressive stress and confinement favors fibronectin relocalization and anchorage to alginate despite its low affinity for proteins.

Altogether, decrease in inter-fibroblast fibronectin and the formation of fibronectin layer at the surface of the capsule, could support spreading of fibroblasts. To test this possibility, we have perturbed fibronectin fibrilogenesis by inhibiting b3 integrin using cilengitide[4]. We applied cilengitide at confluence and 3 days later we quontified the proportion of capsules in which fibroblasts enwelopped cancer cells (Fig. 4C). We found that upon cilengitide treatment, in only about 25% of capsules fibroblasts spread oved cancer cells, in comparison to 80% of untrited capsules. We thus

concluded that fibronectin deposition at the capsule wall is necessary to induce fibroblasts spreading over cancer cells.

Conclusions

In this work, we have developed a new 3D *in vitro* model that recapitulates the organization of CAFs around the tumor as it is observed *in vivo*. We used the cellular capsule technology to co-culture cancer cells and fibroblasts. We found that buildup of compressive stress, and not only geometrical confinement, is necessary to induce and maintain the organization of fibroblasts around cancer cells. The spreading of fibroblasts over cancer cells correlates with the reorganization of fibronectin network. At uncompressed stage, fibronectin is located in between fibroblasts possibly acting as a "glue". This could be similar to the recently described stitch adhesions that acts as cell-cell adhesion structures between primary fibroblasts[19]. Under compressive stress, the amount of fibronectin between fibroblasts decreases, with fibronectin being deposited at the interphase with the alginate shell which could stimulate spreading of fibroblasts.

We believe that this novel *in vitro* model would be a beneficial tool to investigate the crosstalk between CAFs, pressure and the tumor at the pre-invasive stage of carcinoma *in situ*. For example, it could be used to study the role of CAFs at the carcinoma *in situ* stage, specifically if CAFs stimulate or restrain[20] tumor progression. By accumulating around the tumor, CAFs can induce stiffening the ECM causing accumulation of compressive stress[21], which was shown to slow down tumor growth *in vitro*[9, 22, 23]. On the other hand, accumulation of compressive stress might also enhance tumor progression. Stiffening of the ECM was shown to promote malignancy and invasiveness of cancer cells[24-26], and compressive stress, independently of stiffness, promotes cancer cell motility and invasion *in vitro*[9, 13]. The model could also be used to test if CAFs, and the associated ECM, by enwrapping cancer cells, could prevent the entry of immune cells and consequently tumor eradication. Similarly, by enveloping cancer cells, CAFs may protect cancer cells from radio or chemotherapy by acting as a "shield" or "buffer". Altogether, we believe that this complex 3D *in vitro* model system could represent a more physiological mimic of tumors.

Material and Methods

Cell lines and primary cell cultures

We used human colon carcinoma HT29 cells (ATCC HTB-38; American Tissue Culture Collection), mouse fibroblasts NIH3T3 stably expressing GFP (AKR-214, Cell biolabs) and human primary non-immortalized fibroblasts isolated from fresh colon cancer samples from patients treated at Lariboisière Hospital, Paris[4]. Written consent from the patients and approval of the local ethics committee was obtained. All cells were maintained in DMEM (Invitrogen) supplemented with 10% (vol/vol) FBS (Invitrogen) in a humidified atmosphere containing 5% CO2 at 37 °C, with medium changed every 2 days.

Encapsulation of cells into alginate hollow spheres

Encapsulation of cells was performed as described in Alessandri et al[9]. Briefly, the outermost phase (AL) was prepared by dissolving 2.5% wt/vol sodium alginate (Protanal LF200S; FMC) in water and by adding 0.5 mM SDS surfactant (VWR International). The solution was filtered at 1 µm using glass filter (Pall Life Science) and stored at 4°C. The intermediate phase (IS) was a 300mM sorbitol (Merck) solution. The innermost phase (CS) was obtained by detaching sub-confluent cells from the culture flask with 0.5% Trypsin-EDTA (Invitrogen). After washing with culture medium, cells were spun (300 g, 3 min, 20°C), and resuspended in 300 mM sorbitol solution at an approximate concentration of 3.10^6 cells per ml.

The three fluid phases (cell suspension (CS), intermediate solution (IS), and (AL) were loaded into syringes (10MDR-LL-GT SGE; Analytical Science) with needles fitted to Teflon tubing (0.5-mm i.d.; Bohlender). The other ends of the tubing were inserted into the appropriate inlets of the co-extrusion device, which is clamped vertically to a post inside a laminar flow hood. The syringes were mounted on syringe pumps (Low Pressure Syringe Pump neMESYS) that control fluid injection at the desired flow rates. We mostly used one set of flow rates q_{CS} = 20 mL·h^{-1}, q_{IS} = 20 mL·h^{-1}, and q_{AL} = 30 mL·h^{-1} to make “thick” capsules, i.e. typically with a shell width of 30 µm for a radius of 150 µm. After initiation of the flows, the compound microdroplets were directed to a gelation bath containing 100 mM calcium chloride (VWR International) and traces of Tween 20 (Sigma), placed at approximately at 0.5 m below the outlet of the device. Capsules were immediately filtered and transferred

to the appropriate culture medium within less than 5 min. Cellular capsules were placed inside an incubator (37°C, 5% CO2). Cells aggregated to form spheroids within few days.

Immunofluorescence

Spheroids were fixed in 4% paraformaldehyde in PBS at RT for 40 min, which was sufficient to dissolve the shell. After washing with 0.01% BSA in PBS, the aggregates were incubated in 0.1% Triton X-100 in PBS (Sigma) for 40min at RT. BSA was used to prevent spheroids from binding to the plastic of bottom dishes and pipette tip. After washing twice with 0.01% BSA in PBS, spheroids were incubated with primary antibodies diluted in PBS containing 0.01% BSA overnight at 4°C. Specifically we used fibronectin and vimentin (1:50, Sigma). After washing twice with 0.01% BSA in PBS, the spheroids were incubated in PBS containing 0.01% BSA and Alexa Fluor-conjugated secondary antibodies, Phalloidin Alexa Fluor 647 and DAPI (Thermofisher) at ratio of 1:200, 1:200 and 1:500 respectively for 2 hours at RT. The cell aggregates were finally washed 4 times in 0.01% BSA in PBS before mounting for imaging.

Imaging of fixed and live spheroids

To prevent displacement or drift of the capsules during imaging, we designed custom-made holders. Holes (diameter of ~2mm) were drilled in 50mm plastic-bottom Petri dish. A 20mm square glass coverslip (0.16mm thick) was glued to the bottom of Petri dish using epoxy resin (Loctite 3430; Radisopares-RS Components). To prevent displacement of capsules, a 0.2% ultra-pure low-melting-point agarose (Sigma) solution made in serum-free culture medium was prepared and cooled down at 37°C. The percentage of agarose was chosen to generate minimal stress on the growing spheroids (~0.2%). Each well was filled with 4-5 spheroids or capsules mixed with 10-20µl of the 0.2% agarose solution. After 10min gelation of the agarose at RT, 10% FBS and 1% Antibiotic-Antimycotic in culture medium (for live imaging) or PBS (for fixed imaging) was added to each dish.

Spheroids growth inside the capsules was monitored by phase contrast microscopy. Around 64 capsules were selected from the whole batch of cellular capsules and individually transferred to each well of home-made holders. Each capsule was imaged every 20 or 30 min up to 3 or 5 days using Nikon Eclipse Ti inverted

microscope (10×/0.3-N.A. dry objective; Nikon Instruments) equipped with a motorized stage (Märzhäuser) and climate control system (The Brick; Life Imaging Systems). The microscope and camera (CoolSNAP HQ2; Photometrics) were driven by Metamorph software (Molecular Devices). The microscope was equipped with fluorescent lamp to capture the dynamics of NIH3T3 expressing GFP spheroid. The culture medium was renewed by one-half every 2 days. Imaged were processed using Fiji.

3D imaging was performed using an inverted Acousto Optical Beam Splitter two-photon, laser-scanning confocal microscope SP8 (Leica) coupled to femtosecond laser Chameleon Vision II (Coherent Inc) equipped with a 40×/0.95-N.A. oil-immersion objective. The microscope is further equipped with three non-descanned HyD (Hybrid) detectors: NDD1 (500-550 nm), NDD2 (≥ 590nm) and NDD3 (450 nm). To monitor cell dynamics of HT29 cells inside the spheroid we incubated the spheroid in FM 4-64 (Thermofisher) at a concentration of 2 µg/mL. Images were collected every 30 min for 42 hours. Imaged were processed using Fiji and Imaris.

Drugs assays

To block cell proliferation, spheroids were incubated in culture medium supplemented with 20 ug/mL Mitomycine-C (Roche) for 4h. Migration of cells was not impacted under this treatment.

To inhibit cell contractility, spheroids were incubated in culture medium using 50µM myosin II inhibitor, blebbistatin (Sigma) or 100 µM ROCK inhibitor, Y-27632 (Sigma). To inhibit fibronectin fibrillogenesis, capsules were treated with 1 µM cilengitide (Selleckchem).

Analysis of Spheroid Growth and Pressure

The average radius of a spheroid at each time point was defined by $\mathrm{R} = \sqrt{\frac{S}{\pi}}$, where S is the equatorial cross-section of the spheroid. The equatorial cross-section of the spheroid was measured using a custom-made macro in Fiji. For each time point, the macro makes binary images of the spheroid from phase-contrast images. The confluence time (t = 0) was determined as the time for which spheroid growth exhibits an inflection point. We verified that this time coincides with the visual determination of confluence. For thick capsule, the pressure may be determined by considering the

capsules as thin-walled pressurized vessels in the framework of isotropic linear elasticity [27]: $P = \frac{2E}{1-\vartheta} . \frac{h}{R} . \frac{u(R)}{R}$, where E is the Young's modulus of alginate shell measured to be E=68 ± 21 kPa, ϑ is the Poisson's modulus ($\vartheta = 0.5$ according to volume conservation of the shell), h is the thickness of the alginate shell, $u(R) = \frac{(R(t)-R_0)}{R_0}$ is the radial displacement at a distance R from the center of the capsule. To determine u(R) we monitored the evolution of R(t) following the protocol described above.

Decapsulation assay

Using capsules in which NIH3T3 were spread around HT29 (11 days after confluence) alginate shells were dissolved by incubation in PBS for 5 min at RT. Bare spheroids were then individually transferred in 96 wells plates coated with agarose cushion (1% in serum-free culture medium) and imaged overnight by phase contrast and epi-fluorescence imaging.

Cells Tracking and Analysis inside Spheroid

NIH3T3 trajectories inside spheroid were tracked manually. The (x,y) position of the centroid of nucleus was manually determined for each time point. For each cell, trajectories were reconstituted concatenating positions of all centroids. Trajectories were stopped when the cell disappeared from the imaging plane or when the cell divided. Using a custom-made MATLAB (MathWorks) program, we computed various parameters of the trajectories: instantaneous speed and persistence.

The instantaneous speed is the speed of a cell at a specific time point t and is defined by $v(t) = \frac{\sqrt{\left(x(t_{i+1})-x(t_i)\right)^2+\left(y(t_{i+1})-y(t_i)\right)^2}}{\Delta t}$.

Micropipette experiments

Capsules containing spheroids made of mix of cancer cells and fibroblasts were decapsulated about 3 days after confluence, once fibroblast started enwrapping cancer cells. Spheroids were placed in suspension in a non-adhesive glass bottom culture dish and incubated at 37°C and 5% CO2 for microaspiration. As controls we use spheroids made of single cell types growing without confinement in the non-adhesive agarose wells. The micro-aspiration setup (28) was built on an inverted

Leica microscope equipped with an Eppendorf Transferman micro-manipulator holding micropipettes connected to a Fluigent MFCS EZ microfluidic pump. Images were acquired with a 40x/0.8NA dry objective. The surface tension at the cell-medium interface (γ_{cm}) of spheroids was measured as previously described [17]. Surface tension was calculated using Laplace's law:

$$\gamma_{cm} = \frac{P_c}{2\left(\frac{1}{R_p} - \frac{1}{R_c}\right)}$$

in which R_c is the resting radius of curvature of the spheroid at the location of the measurement, P_c is the critical pressure at which spheroid deformation reaches R_p, the micropipette radius. Shape analysis was performed using ImageJ [28].

Figure 1

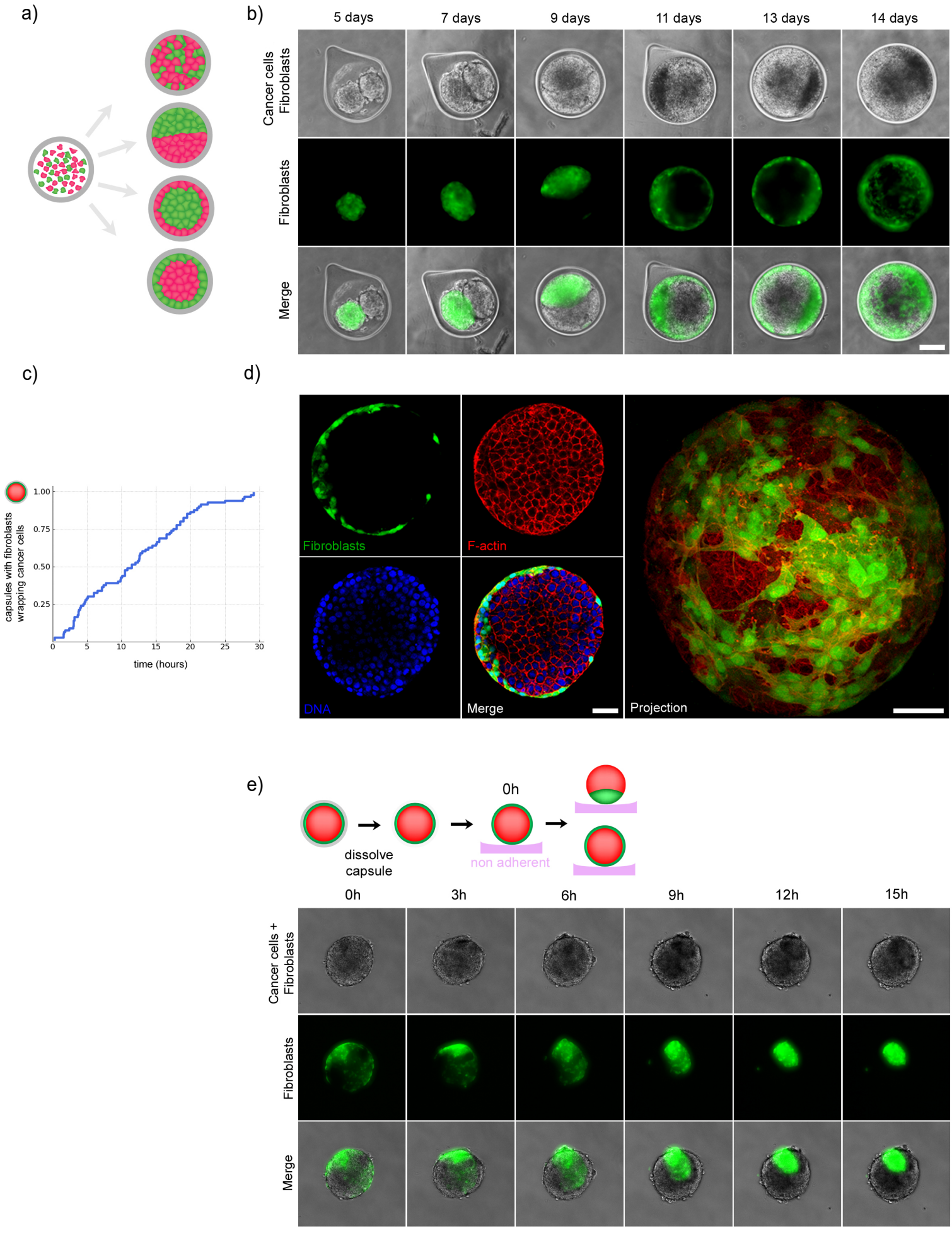
a)
b)
5 days
7 days
9 days
11 days
13 days
14 days
Cancer cells Fibroblasts
Fibroblasts
Merge
c)
capsules with fibroblasts wrapping cancer cells
1.00
0.75
0.50
0.25
0
5
10
15
20
25
30
time (hours)
d)
Fibroblasts
F-actin
DNA
Merge
Projection
e)
dissolve capsule
0h
non adherent
0h
3h
6h
9h
12h
15h
Cancer cells + Fibroblasts
Fibroblasts
Merge

Figure 2

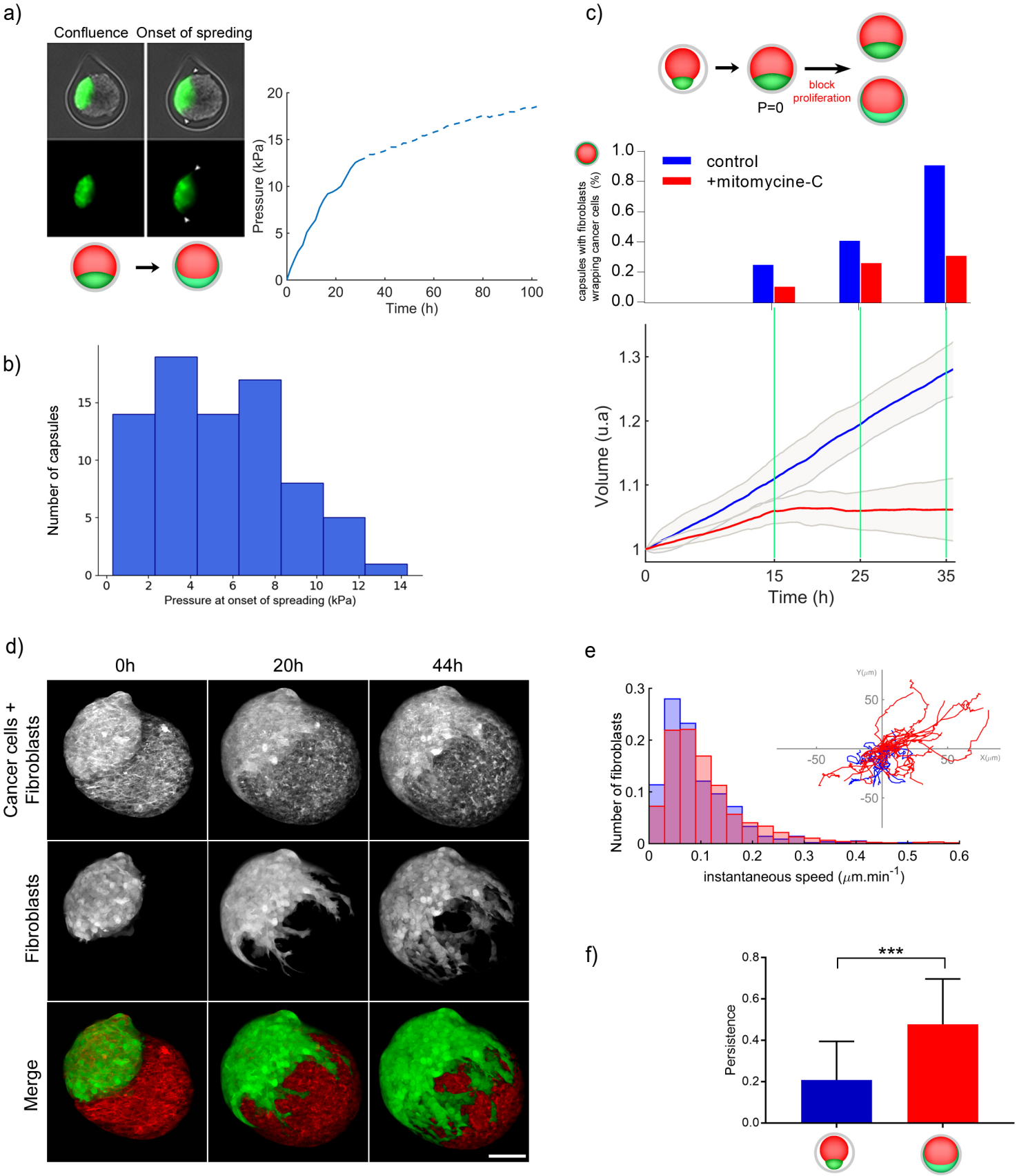
a)
Confluence
Onset of spreding
Pressure (kPa)
Time (h)
b)
Number of capsules
Pressure at onset of spreading (kPa)
c)
P=0
block proliferation
control
+mitomycine-C
capsules with fibroblasts wrapping cancer cells (%)
Volume (u.a)
Time (h)
d)
0h
20h
44h
Cancer cells + Fibroblasts
Fibroblasts
Merge
e)
Number of fibroblasts
instantaneous speed (μm.min-1)
f)
***
Persistence

Figure 3

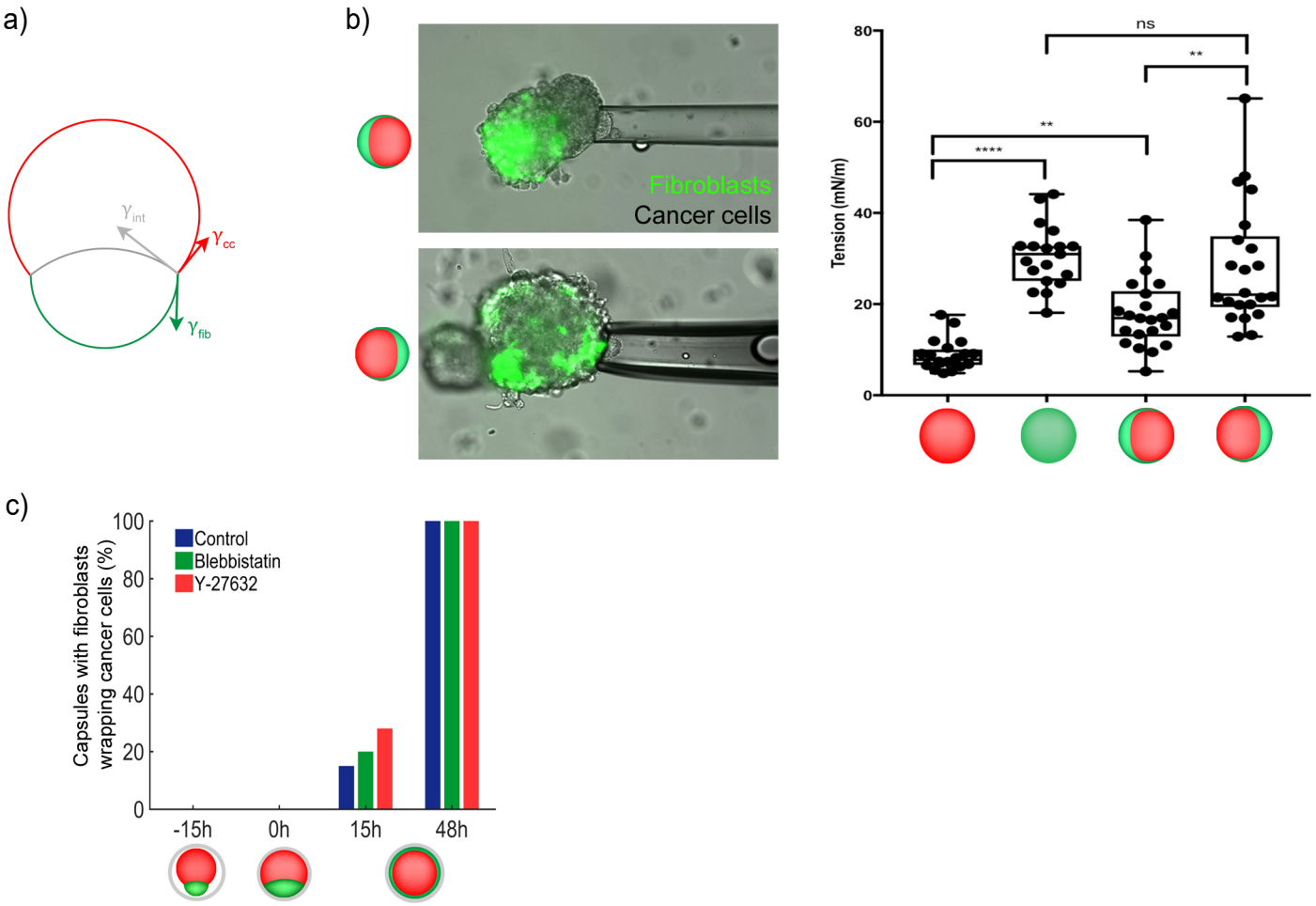
a)
γ_{int}
γ_{cc}
γ_{fib}
b)
Fibroblasts
Cancer cells
ns
**
**
****
Tension (mN/m)
0
20
40
60
80
c)
Capsules with fibroblasts wrapping cancer cells (%)
Control
Blebbistatin
Y-27632
0
20
40
60
80
100
-15h
0h
15h
48h

Figure 4

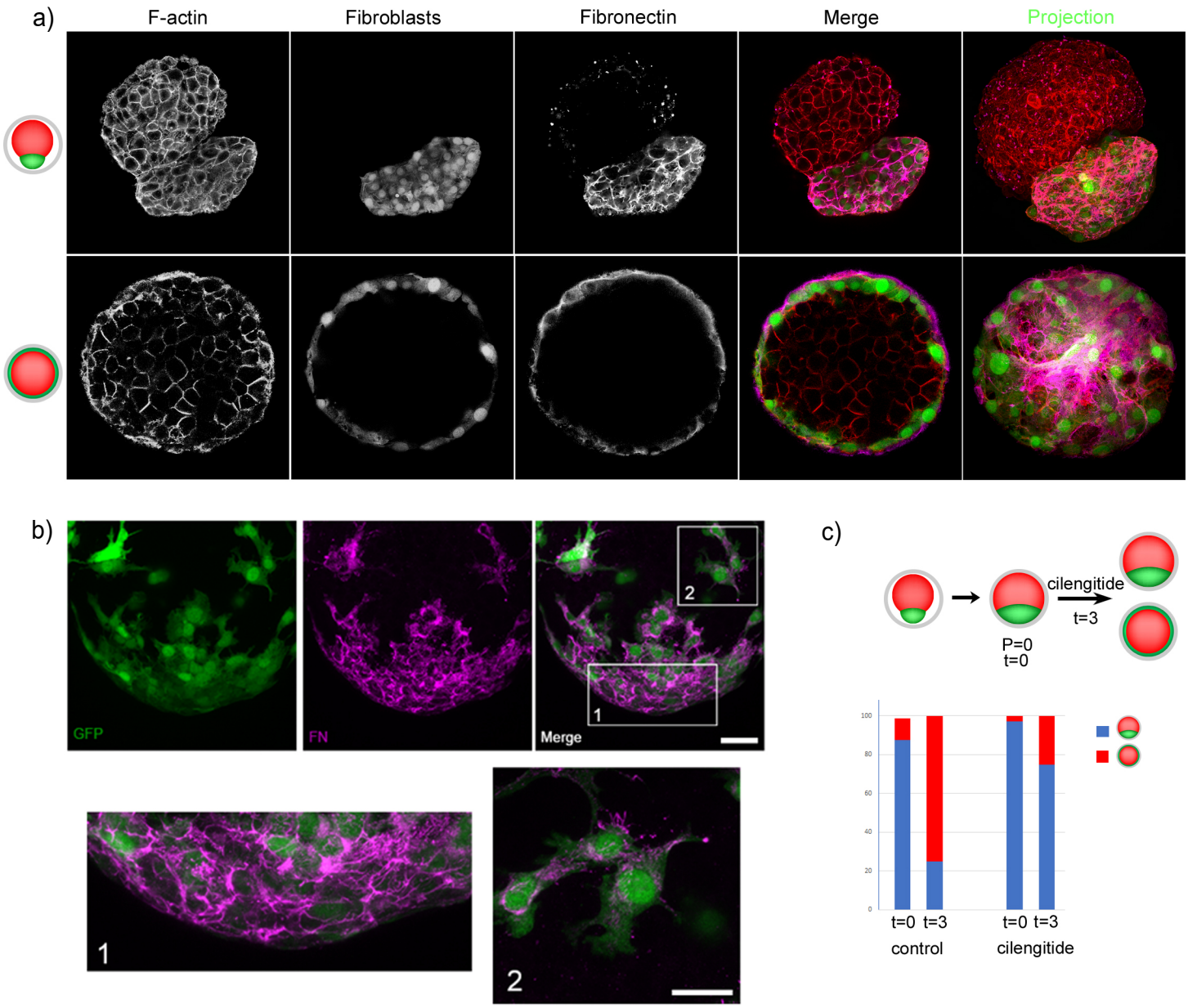
a)
F-actin
Fibroblasts
Fibronectin
Merge
Projection
b)
GFP
FN
Merge
1
2
c)
cilengitide
t=3
P=0
t=0
100
80
60
40
20
0
t=0 t=3
t=0 t=3
control
cilengitide

Supplementary Figure 1

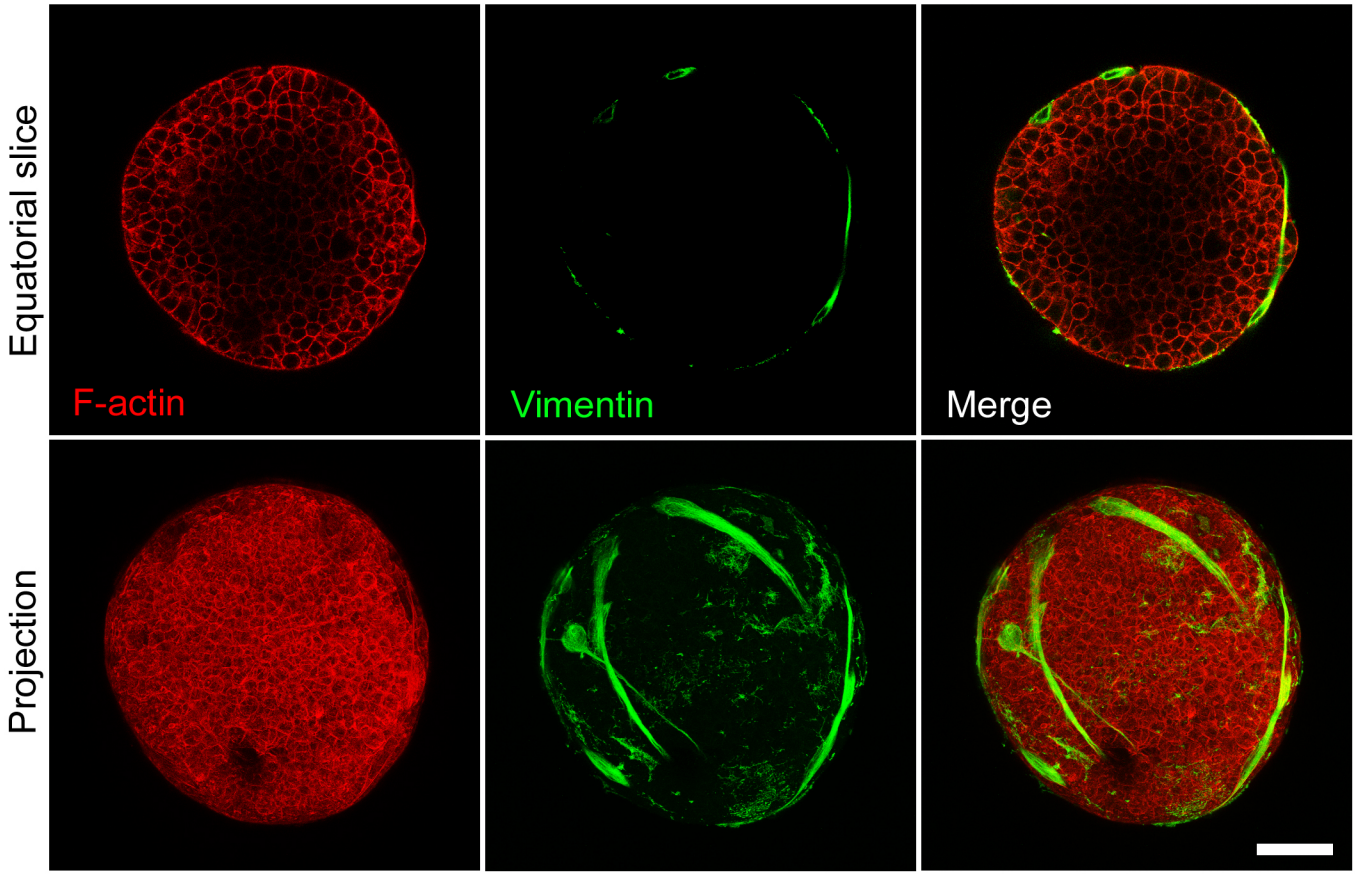

Figure Legends

Figure 1. Fibroblasts envelop cancer cells under confinement

A. Schematic representation of possible outcomes after encapsulation of cancer cells and fibroblasts as single cells into alginate capsules.

B. Evolution of co-culture of HT29 cancer cells and GFP expressing NIH 3T3 fibroblasts over time in alginate capsules. Time t = 0 corresponds to encapsulation of cells. First row: Phase contrast image showing cancer cell and fibroblast spheroids; second row: epifluorescent image of fibroblasts expressing GFP (green); last row: Merge. Scale bar, 100 µm.

C. Percentage of capsules in which fibroblasts envelop spheroids of cancer cells over time. T=0 corresponds to confluent stage.

D. Confocal image of a fixed spheroid. All cells were visualized by staining F-actin (phalloidin, red) and DNA (DAPI, blue). Fibroblasts were discriminated as cells expressing GFP (green). Left, equatorial slices. Right, maximal projection. Scale bar, 50 µm.

E. Evolution of cancer cells spheroids enwrapped with GFP expressing NIH 3T3 fibroblasts over time after removal of alginate capsules. Time t = 0 corresponds to capsule dissolution, thus release of the confinement. Scale bar, 100 µm.

Figure 2. Buildup of pressure drives fibroblasts spreading

A. Micrographs representing onset of confluence and onset of spreading. Pressure evolution over time, starting from confluence (t=0). Way copy to 11 settings

B. Pressure at the onset of fibroblast spreading. n=53 capsules.

C. Lower graph, volume of capsule normalized to the volume at onset of confluence as a function of time for control (blue line) and cells treated with mitomycin C (red line). Gray shadow: standard deviation. Time t = 0 corresponds to confluence. (Upper graph) Frequency of capsules in which fibroblasts started to envelop cancer cells at different time points (T1=15h, T2=25h and T3=34h) for control (blue bars) and mitomycin C -treated co-cultures (red bars).

D. Two-photon live imaging of a co-culture of cancer cells stained by membrane die FM4-64 (red) and fibroblasts expressing GFP (green) at the onset of confluency. Scale bar: 50µm.

E. Distribution of the instantaneous speed prior (blue bars) and after confluence (red bars).
F. Left, ceconstituted fibroblast 2D trajectories prior to confluence (blue line) and after confluence (red line). Time step: 20min. Typical trajectory length: 15 hours. Right, path persistence prior to confluence (blue) and after confluence (red).

Figure 3. Surface tension of fibroblast spheroid is higher than cancer cells

A. Individual (dots) and mean ± SEM (bars) surface tension measurements on cancer cell spheroids (red) and fibroblast spheroids (green) growing without confinement and co-cultures after onset of fibroblast spreading. One way ANOVA test was performed (***$p < 0.001$). Three independent experiments were performed. n = the number of spheroids.
B. Frequency of capsules in which fibroblasts enveloped cancer cells in the presence of different drugs at 15h and 48h after confluence. Time t = 0 corresponds to confluence. Drugs were added 15h before confluence.

Figure 4. Fibronectin reorganization is required for fibroblasts spreading

A. Confocal images of co-culture at 5 days which corresponds to early stage, before confluency (upper row) and 10 days, which corresponds to final stage with fully spread fibroblasts. Both cell types are labeled with phalloidin (F-actin, red), fibroblasts expressed GFP (green), fibronectin is labeled with antibodies (pink). Scale bar: 20 μm.
B. Confocal images of co-culture at the onset of fibroblasts spreading. Fibroblasts expressed GFP (green), cancer cells are unstained; fibronectin is labeled with antibodies (pink). Insets, higher magnification of boxed regions. Scale bars: 20 μm.
C. Frequency of capsules in which fibroblasts enveloped cancer cells in the presence of cilengitide 3 days after confluence. Time t = 0 corresponds to confluence. Drugs were added 15h before confluence.

Supplementary data.

Suppl. Figure 1.

Confocal images of co-culture of primary human untransformed CAFs (vimentin, green) and cancer cells (HT29) after confluency. Scale bar, 25 μm.

References:

1. Kalluri, R. The biology and function of fibroblasts in cancer. *Nat Rev Cancer* **16**, 582-598 (2016).
2. Lenos, K.J. *et al.* Stem cell functionality is microenvironmentally defined during tumour expansion and therapy response in colon cancer. *Nat Cell Biol* **20**, 1193-1202 (2018).
3. Attieh, Y. & Vignjevic, D.M. The hallmarks of CAFs in cancer invasion. *Eur J Cell Biol* **95**, 493-502 (2016).
4. Attieh, Y. *et al.* Cancer-associated fibroblasts lead tumor invasion through integrin-beta3-dependent fibronectin assembly. *J Cell Biol* (2017).
5. Barbazan, J. & Matic Vignjevic, D. Cancer associated fibroblasts: is the force the path to the dark side? *Curr Opin Cell Biol* **56**, 71-79 (2019).
6. Glentis, A. *et al.* Cancer-associated fibroblasts induce metalloprotease-independent cancer cell invasion of the basement membrane. *Nat Commun* **8**, 924 (2017).
7. Labernadie, A. *et al.* A mechanically active heterotypic E-cadherin/N-cadherin adhesion enables fibroblasts to drive cancer cell invasion. *Nat Cell Biol* **19**, 224-237 (2017).
8. Gaggioli, C. *et al.* Fibroblast-led collective invasion of carcinoma cells with differing roles for RhoGTPases in leading and following cells. *Nat Cell Biol* **9**, 1392-1400 (2007).
9. Alessandri, K. *et al.* Cellular capsules as a tool for multicellular spheroid production and for investigating the mechanics of tumor progression in vitro. *Proc Natl Acad Sci U S A* **110**, 14843-14848 (2013).
10. Duguay, D., Foty, R.A. & Steinberg, M.S. Cadherin-mediated cell adhesion and tissue segregation: qualitative and quantitative determinants. *Dev Biol* **253**, 309-323 (2003).

11. Scarpa, E. *et al.* Cadherin Switch during EMT in Neural Crest Cells Leads to Contact Inhibition of Locomotion via Repolarization of Forces. *Dev Cell* **34**, 421-434 (2015).
12. Haeger, A., Krause, M., Wolf, K. & Friedl, P. Cell jamming: collective invasion of mesenchymal tumor cells imposed by tissue confinement. *Biochim Biophys Acta* **1840**, 2386-2395 (2014).
13. Tse, J.M. *et al.* Mechanical compression drives cancer cells toward invasive phenotype. *Proc Natl Acad Sci U S A* **109**, 911-916 (2012).
14. Schotz, E.M. *et al.* Quantitative differences in tissue surface tension influence zebrafish germ layer positioning. *HFSP J* **2**, 42-56 (2008).
15. Morita, H. *et al.* The Physical Basis of Coordinated Tissue Spreading in Zebrafish Gastrulation. *Dev Cell* **40**, 354-366 e354 (2017).
16. Wallmeyer, B., Trinschek, S., Yigit, S., Thiele, U. & Betz, T. Collective Cell Migration in Embryogenesis Follows the Laws of Wetting. *Biophys J* **114**, 213-222 (2018).
17. Guevorkian, K. & Maitre, J.L. Micropipette aspiration: A unique tool for exploring cell and tissue mechanics in vivo. *Methods Cell Biol* **139**, 187-201 (2017).
18. Guevorkian, K., Colbert, M.J., Durth, M., Dufour, S. & Brochard-Wyart, F. Aspiration of biological viscoelastic drops. *Phys Rev Lett* **104**, 218101 (2010).
19. Pankov, R., Momchilova, A., Stefanova, N. & Yamada, K.M. Characterization of stitch adhesions: Fibronectin-containing cell-cell contacts formed by fibroblasts. *Exp Cell Res* **384**, 111616 (2019).
20. Ozdemir, B.C. *et al.* Depletion of carcinoma-associated fibroblasts and fibrosis induces immunosuppression and accelerates pancreas cancer with reduced survival. *Cancer Cell* **25**, 719-734 (2014).
21. Stylianopoulos, T. *et al.* Causes, consequences, and remedies for growth-induced solid stress in murine and human tumors. *Proc Natl Acad Sci U S A* **109**, 15101-15108 (2012).
22. Helmlinger, G., Netti, P.A., Lichtenbeld, H.C., Melder, R.J. & Jain, R.K. Solid stress inhibits the growth of multicellular tumor spheroids. *Nat Biotechnol* **15**, 778-783 (1997).
23. Montel, F. *et al.* Stress clamp experiments on multicellular tumor spheroids. *Phys Rev Lett* **107**, 188102 (2011).

24. Provenzano, P.P. *et al.* Collagen density promotes mammary tumor initiation and progression. *BMC Med* **6**, 11 (2008).
25. Goetz, J.G. *et al.* Biomechanical remodeling of the microenvironment by stromal caveolin-1 favors tumor invasion and metastasis. *Cell* **146**, 148-163 (2011).
26. Levental, K.R. *et al.* Matrix crosslinking forces tumor progression by enhancing integrin signaling. *Cell* **139**, 891-906 (2009).
27. Landau LD, P.L., Lifshitz EM, Kosevich AM Theory of Elasticity Third Edition: Volume 7 (Butterworth-Heinemann). 3rd Ed. (1986).
28. Schindelin, J. *et al.* Fiji: an open-source platform for biological-image analysis. *Nat Methods* **9**, 676-682 (2012).

Study of caveolae response under 3D compressive stress

Objectives and summary

Mechanoprotection has been one of the latest functions assigned to caveolae, when, some years ago, our laboratory demonstrated for the first time that caveolae can protect cells experiencing mechanical stresses from membrane damage by flattening out, thus limiting membrane tension increase (Sinha et al., 2011b). Moreover, based on the important links between caveolae and signaling, my team proposed the hypothesis of a mechano-dependent role of caveolae on signaling, behaving like a mechanical switch in which caveolar components may interact with other molecular effectors of signaling cascades after mechanical disassembly (Nassoy and Lamaze, 2012). More recently, this hypothesis was indeed demonstrated by several works from our team. First, the caveolae neck ATPase EHD2 was shown to shuttle from the PM to the nucleus and regulate transcription(Torrino et al., 2018). Then, my host lab has described how some of the Cav3 human mutations associated with muscle dystrophies, induce a loss of functional caveolae and abolish the normal inhibitory role of Cav3 in IL6-STAT3 mechano-signaling in muscle cells (Dewulf et al., 2019). Furthermore, our unpublished data reveal that when caveolae respond to mechanical stress, one of their major component Cav1 interacts with the tyrosine kinase Janus Kinase1 (JAK1), thus inhibiting JAK-STAT pathway in mouse embryonic fibroblasts and human cancer cells (Tardif, 2018), emphasizing again the importance of caveolae in mediating both mechanoprotection and mechanosignaling. During my PhD project, we aimed to translate these concepts in a more physiologically relevant model for cancer. To do so, we combined our expertise in caveolae together with two assays to investigate the effects of compressive stress on caveolae in 3D and then explore the downstream signaling events in this environment (Kévin Alessandri et al., 2013; Montel et al., 2011b).

In the present work, we revealed that breast cancer triple negative cell line (most aggressive breast cancer cell type, lacking expression of HER2, estrogen receptor and progesterone receptor) Hs578t is able to respond to mechanical stress in 3D by

reducing the protein expression of caveolae ATPase EHD2 and presumably by affecting caveolae dynamics. We further observed that compressive stress leads to changes in the distribution and architecture of caveolae, at short term, as cells exhibit less caveolae at their surface under these constraints. Interestingly, long-term compression appeared to reduce preferentially the presence of caveolar rosettes (inclusion of several caveolae in the membrane). We also used our 3D cell model to monitor the activation of the JAK-STAT signaling pathway and confirmed its inhibition under compressive stress.

Because of our previous results establishing a role of caveolae as mechanosensors and some evidence that this property was also occurring in 3D, we decided to perform a series of high-throughput screenings. First, we found a differential gene expression profile under compression compared to resting conditions. Interestingly, it revealed that the gene expression profile of each compressive methodology (capsule versus hyper-osmotic system) varied significantly as they do not have similar effect on the regulation of several pathways such as extracellular matrix regulation, ubiquitinylation, cytoskeleton, exosome components and secretion…

Finally, we focused our investigations on exosome secretion and biogenesis under mechanical stress conditions, and whether caveolae are component of the observed mechano-response. This way, we demonstrated the importance of Cav1 in exosome release under mechanical stress and how compressive stress could affect release but also uptake of exosomes.

The corresponding data of these results are developed in the following pages.

Investigating the caveolae mechanoresponse in triple negative breast carcinoma

Considering the established albeit controversial relation that exists between caveolae and its components, with cancer, we first wanted to select a suitable cell line for the purposes of our study that aimed at identifying the role of the caveolae response under mechanical stimuli in a 3D environment. Shortly, the requirements were a breast carcinoma cell line able to grow independently from anchorage/adhesion, expressing identifiable relevant levels of caveolar proteins, and negative for estrogen, progesterone, and the HER-2/neu gene since this is the profile of the breast carcinomas with the less survival ratio (Dent et al., 2007). A screening for the protein expression of caveolar components on the different type of breast cancer cell lines, made by members of our laboratory, revealed that Hs578t cell line meets all the chosen criteria **(Figure 11 a)**. Interestingly, among all the breast cancer cell lines tested, several of them expressed amounts of caveolae components similar to non-carcinogenic cell lines, but only Hs578t expressed high levels of EHD2 **(Figure 11 a,b).**

3D Compressive stress decreases the expression of the caveolae ATPase EHD2

In order to test the reaction of these cells under compressive stress, we adapted the hyperosmotic-induced compressive stress designed in the the team of Cappello (Montel et al., 2012, 2011b). For investigating the response of mammary breast cancer cells against compression for long periods of time, we formed spheroids containing approximately 10, 000 cells. The subsequent addition of high molecular weight dextran (~1-2,6 MDa) allows to induce compressive stress for different time periods (12 hours, 3 days, and 5 days). At the end of each experimental condition, spheroids were harvested and lysed. The expression of the main caveolar components was tested by western blotting, revealing an average 60% reduction of EHD2 expression after 5 days of constant compressive stress (p=10 kPa) **(Figure 12 a,b)**. This decrease of protein expression was not observable neither for other caveolar components (Cav1, Cavin-1 and Cav2), nor for the clathrin heavy chain

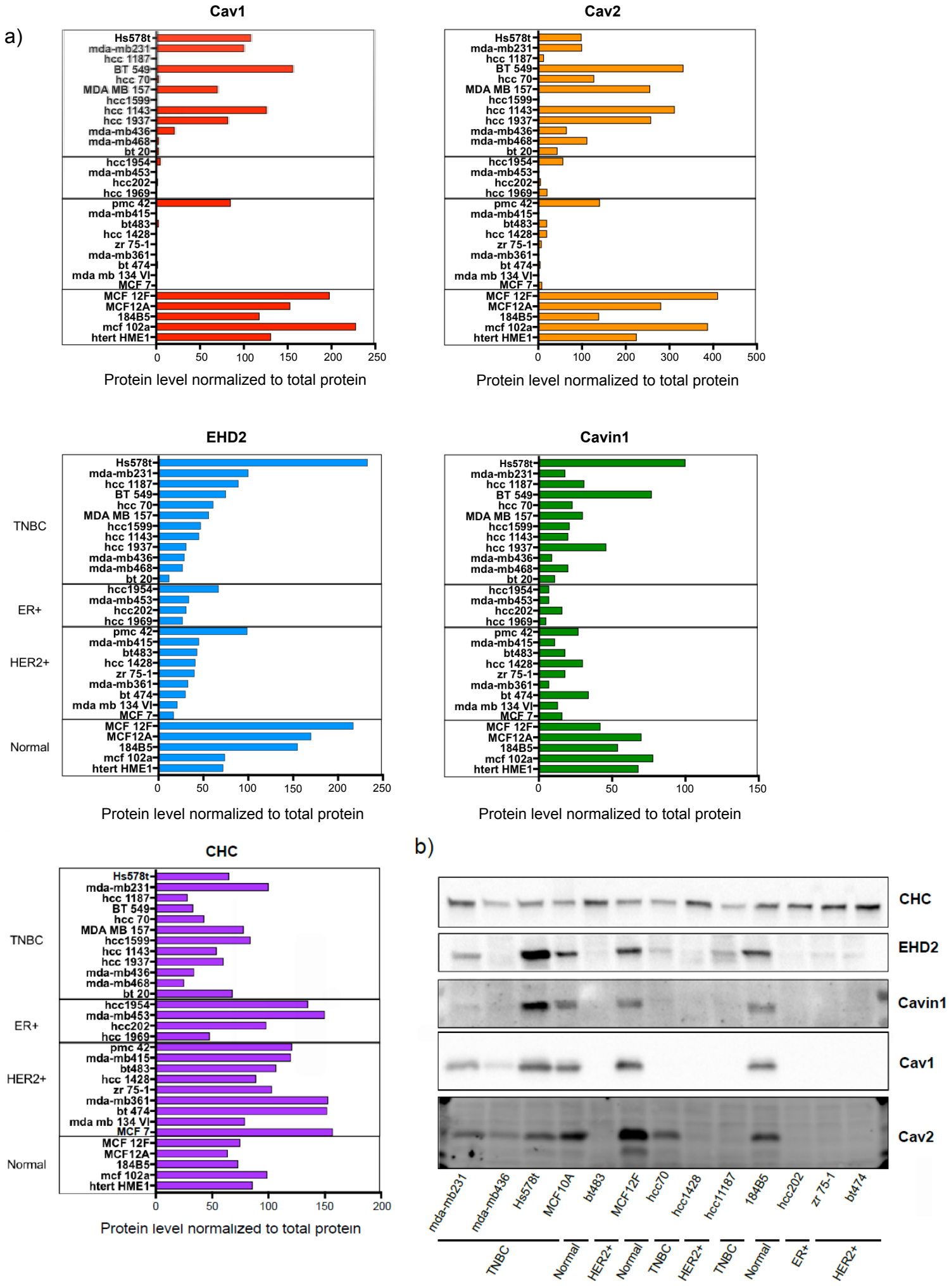

Figure 11. Protein expression levels of caveolar components in breast cancer cell lines.

(a) Protein level quantification for caveolar component proteins in breast cancer cell lines, classified as triple negative breast carcinoma (TNBC), estrogen receptor positive (ER+), HER2 positive (HER2+) and non-carcinogenic breast cancer cell lines (Normal). Protein levels are normalized to the total protein content of the samples, determined by StainFree technology. Data are mean of three independent experiments. **(b)** Representativeinmunoblots for selected cell lines.

(CHC), the main component of clathrin coated pits **(Figure 12 a,b)**. This result could be interpreted as an adaptation of the cells to the constant source of mechanical stress by changing the stability of caveolae since EHD2 is known to anchor caveolae at the plasma membrane, especially under stress (Stoeber et al., 2012; Yeow et al., 2017). It could also reflect a switching-off the EHD2 mechanotransduction mechanism that triggers caveolae-dependent signaling as recently described in our study (Torrino et al., 2018).

The next step was to reproduce these results in another experimental system to confirm the decrease of expression of the caveolae ATPase EHD2 under compression. To do so, we adapted and optimized the co-extrusion device developed by our collaborators in Pierre Nassoy's team (Institut d'Optique d'Aquitaine). Indeed, during my thesis, I contributed to the improvement of the system with our collaborators, by adding a copper ring with current circuit to increase the mono-dispersity during the capsule production, and by optimizing the functionalization protocol with specific hydrophobic tips. After the encapsulation step, detailed in the material and methods chapter, cancer cells were grown until their own growth against the alginate wall would promote a consequent compressive stress, due to the viscoelastic properties of the material. In other words, this time point corresponds to the stage when the cells fill up all the available space inside the capsule and when the capsule shell starts to be deformed **(Figure 13 b)**. To reach this compressive state, we need to wait between two and four weeks from the cell encapsulation time. Then, we left the cells in this compressive state for approximately one week before lysing them and monitoring their protein content. At this last stage, one can observe the appearance of a necrotic core in the center of the cell spheroid. It has been previously reported how this necrotic core appeared only on the last stage under compression, even when the capsule radius is under the critical distance for the diffusion of the nutrients **(Figure 13 b)** (Kévin Alessandri et al., 2013). But in the current experiments the observations of an appearance of a necrotic core happens before the spheroid reaches the compression point. Whether it is the compression forces that generate this necrotic core is still an open question. After one week of compression, cells were analyzed for the protein expression of caveolae components. Again, we found, a striking reduction of EHD2 expression level compared to agar spheroids unlike the other caveolar components tested (Cav1,

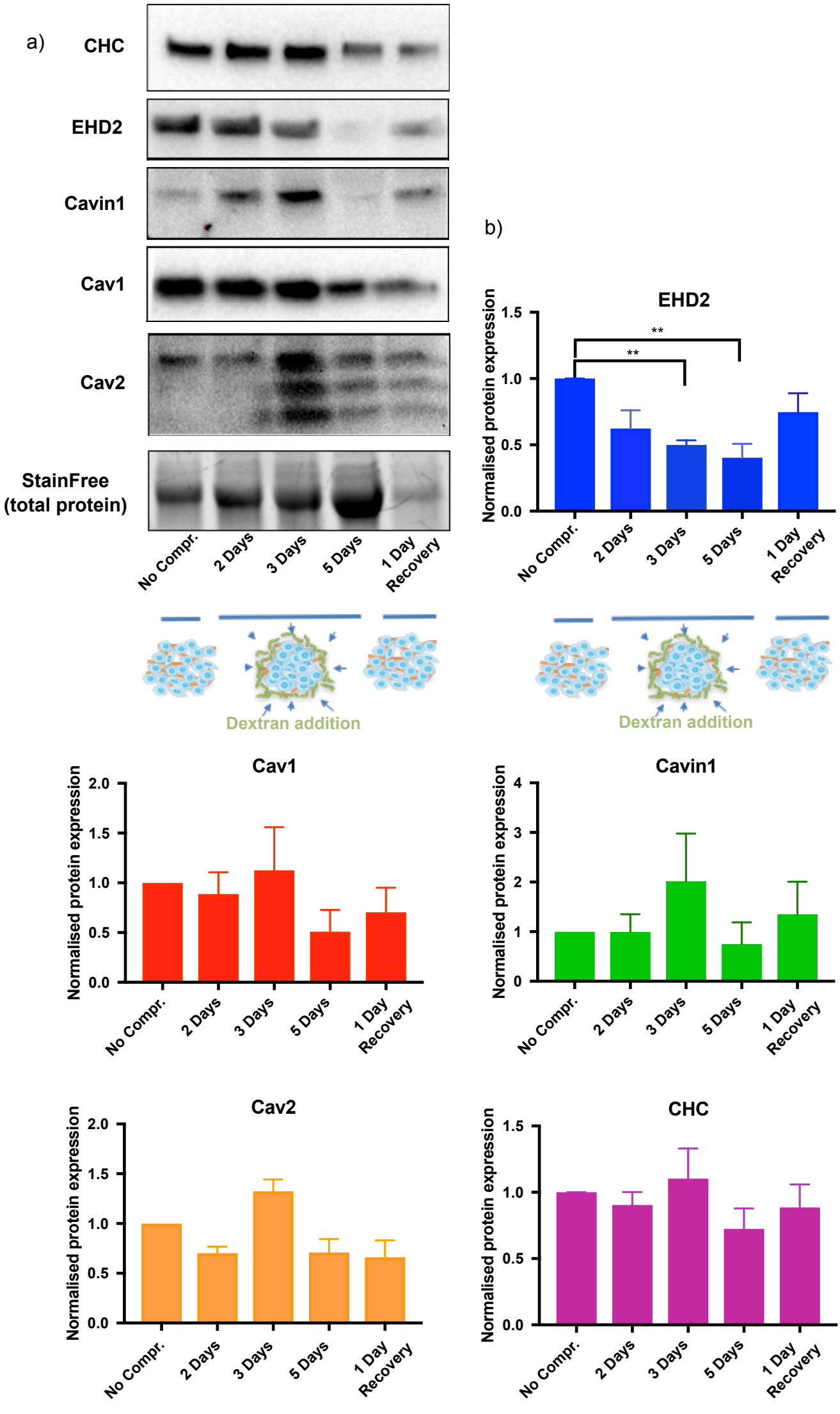
a)
CHC
EHD2
Cavin1
Cav1
Cav2
StainFree
(total protein)
No Compr.
2 Days
3 Days
5 Days
1 Day
Recovery
b)
EHD2
Normalised protein expression
1.5
1.0
0.5
0.0
**
**
No Compr.
2 Days
3 Days
5 Days
1 Day
Recovery
Dextran addition
Dextran addition
Cav1
Normalised protein expression
2.0
1.5
1.0
0.5
0.0
No Compr.
2 Days
3 Days
5 Days
1 Day
Recovery
Cavin1
Normalised protein expression
4
3
2
1
0
No Compr.
2 Days
3 Days
5 Days
1 Day
Recovery
Cav2
Normalised protein expression
2.0
1.5
1.0
0.5
0.0
No Compr.
2 Days
3 Days
5 Days
1 Day
Recovery
CHC
Normalised protein expression
1.5
1.0
0.5
0.0
No Compr.
2 Days
3 Days
5 Days
1 Day
Recovery

Figure 12. Hyperosmotic-induced compression reduces EHD2 protein levels.

(a) Representative inmunoblots of caveolar components in Hs578t cells without compression (No Compr.), or after 2 days, 3 days or 5 days after the addition of dextran to exhert compressive stress, and after 1 day of recovery. **(b)** Expression level of caveolar components normalized to total protein levels in the experimental conditions described in (a). Statistical analysis with one-way ANOVA **P ≤ 0.01.

Cav2 and Cavin-1) or CHC which all exhibit non-significant variations **(Figure 13 a,c)**.

Compressive forces on spheroids lead to loss of caveolae

Our finding that EHD2 expression was lost in two different 3D compressive systems, led us to understand the consequences of EHD2 loss on the formation or maintenance of caveolae structures. As already mentioned, EHD2 has been involved in caveolae stability at the membrane and its reformation during recovery after mechanical stress release (Matthaeus et al., 2019; Morén et al., 2012; Stoeber et al., 2012; Torrino et al., 2018). Since caveolae flatten in response to 2D stretch (Sinha et al., 2011b), we wanted to investigate how mechanical stress in 3D could affect caveolae at short (few minutes) and long (several hours or days) terms. This will help us to answer the question of how this loss or decrease of EHD2 expression would affect caveolae architecture, location and biogenesis.

We processed spheroids after compression induced by hyperosmotic-induced compression for 5 minutes, 1 day or 5 days, and compared them to control spheroids without any compressive stress. Spheroids were fixed and processed for electron microscopy (EM) **(Figure 14 a)**. Subsequently, clathrin coated pits and caveolae where identified and counted in two different areas of the spheroid: the periphery (i.e. the 3-4 first layers close to the periphery of the spheroid) and a more central domain.

The collected results shown a significant decrease of caveolae number after 5 minutes of compression as compared to control but not any significant change in the other conditions. On the contrary, we could observe a decrease of the number of caveolae rosettes after 5 days of compression **(Figure 14 b)**. By focusing on the different pool of cells regarding their position within the spheroid, we can observe a decrease of caveolae number after 5 minutes specifically in cells that are closer to the exterior of the spheroid **(Figure 14 c)**. This observation is an agreement with the first description of spheroids with the hyperosmotic induced compression system introduced by Cappello's team. At that time, they showed an increasing anisotropic cellular organization from the periphery towards the core with a drop in the core itself. This correlates with an ascending pressure profile towards the core of the spheroid (Dolega et al., 2017) **(Figure 6 b and c).** Thus, it is expected that cells on the periphery tend to rearrange more and have their caveolae flattened because they

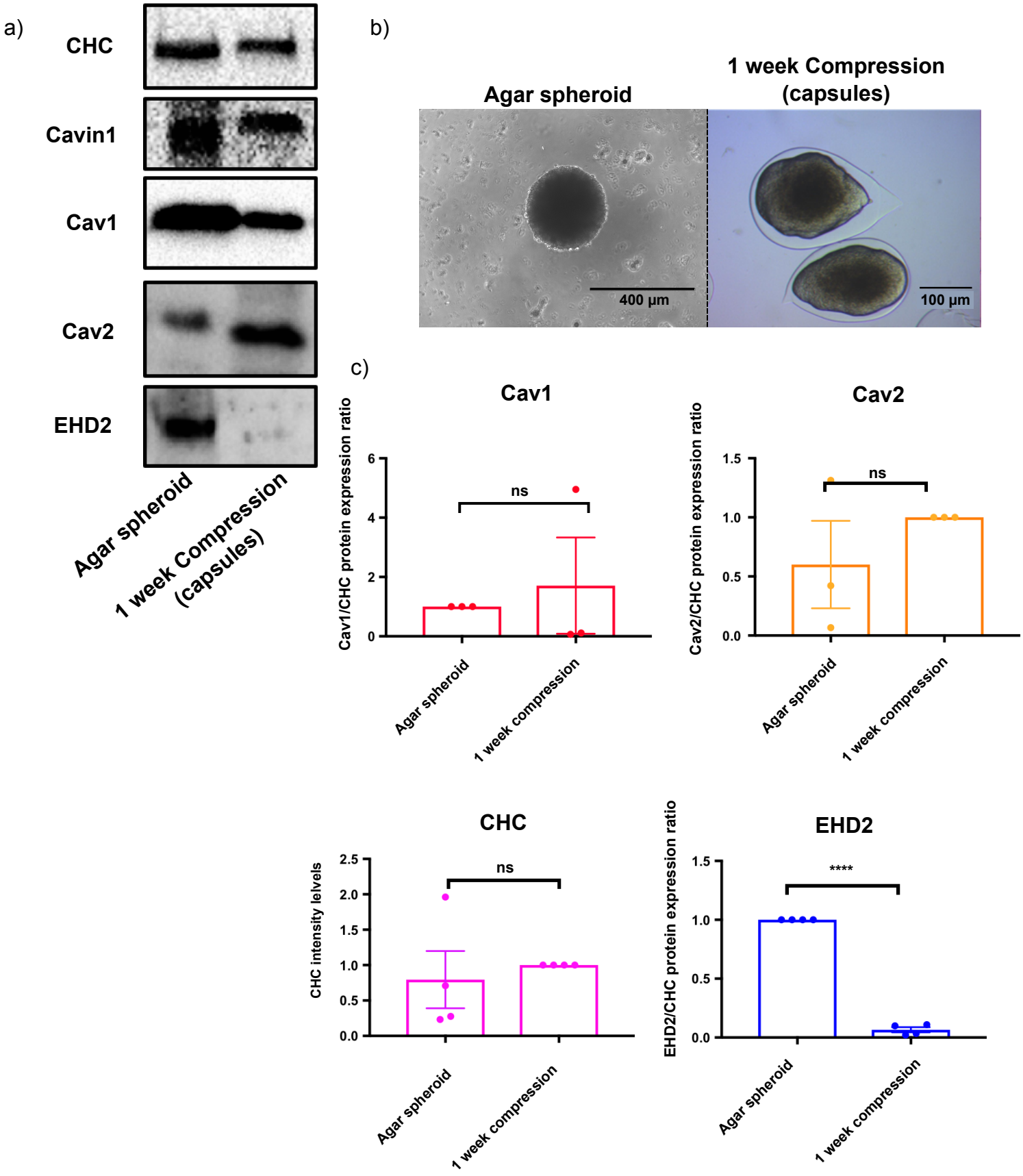

Figure 13. Compressive stress in alginate capsules reduces EHD2 protein levels.

(a) Representative immunoblot of caveolar components in Hs578t cells after one week of compression in alginate capsules (1-week compression) or in uncompressed spheroids grown over an agar cushion (Agar spheroid). **(b)** Representative pictures of Hs578t cells after one week of compression in alginate capsules or as uncompressed spheroids. Bar is 400 µm and 200 µm. **(c)** Expression level of caveolar components normalized to total protein levels in n=3 independent experiments (n=4 for EDH2). Data are mean values ± SEM. Statistical analysis with a two-tailed unpaired t test **** $P \leq 0.0001$.

probably face more membrane tension increase upon the compression of the whole spheroid.

Regulation of the JAK-STAT signaling pathway by compressive stress

The reduction of caveolae invaginations after short term compression suggested that caveolae could react as a compressive reactive mechano-switch, similar to what was reported by our team upon stretching. To test whether this could affect signaling, we monitored the activation status of STAT3 upon cytokine stimulation in spheroids under compression in agreement with previous results obtained in cells stretched (Dewulf et al., 2019; Tardif, 2018). Therefore, we analyzed how 5 minutes compression could modify the activation of STAT3 i.e. Tyr705 phosphorylation in spheroids after stimulation with interferon-α (IFN-α) for 15 minutes. Our data showed a significant decrease (70%) of STAT3 phosphorylation level in compressed spheroids as compared to control ones **(Figure 15 a)**. This result is consistent with those obtained after cell stretching (Tardif, 2018). We also tested the effect of compression on another effector of the JAK-STAT pathway, STAT1, that was reported not to behave like STAT3 (i.e. no modification by stretch) in our previous experiments. Surprisingly, in our compression system, mechanically challenged organoids also exhibited a decrease of STAT1 Tyr 701 phosphorylation upon IFN-α stimulation **(Figure 15 b)**. Curiously it had been reported how $Cav1^{-/-}$ mice do not show any change in STAT1 Tyr 701 phosphorylation, meanwhile $Cav2^{-/-}$ mice shown an increase on STAT1 Tyr 701 similar to the one found on STAT3 upon Cav1 depletion (Almeida et al., 2011). We should also consider that the depletion of Cav1 and Cav2 are co-transcriptionally regulated and no effect on STAT1 Ty 701 was shown when you deplete Cav1 as both Cav1 and Cav2 are affected.

Hyperosmotic induced compression and encapsulation show a differential expression pattern at the transcriptomic level

After showing the importance of compression in the regulation of cellular signaling with the 3D spheroid architecture, we wanted to broaden our analysis and identify new pathways that could be modified by this type of mechanical stimulations. Thus,

a)

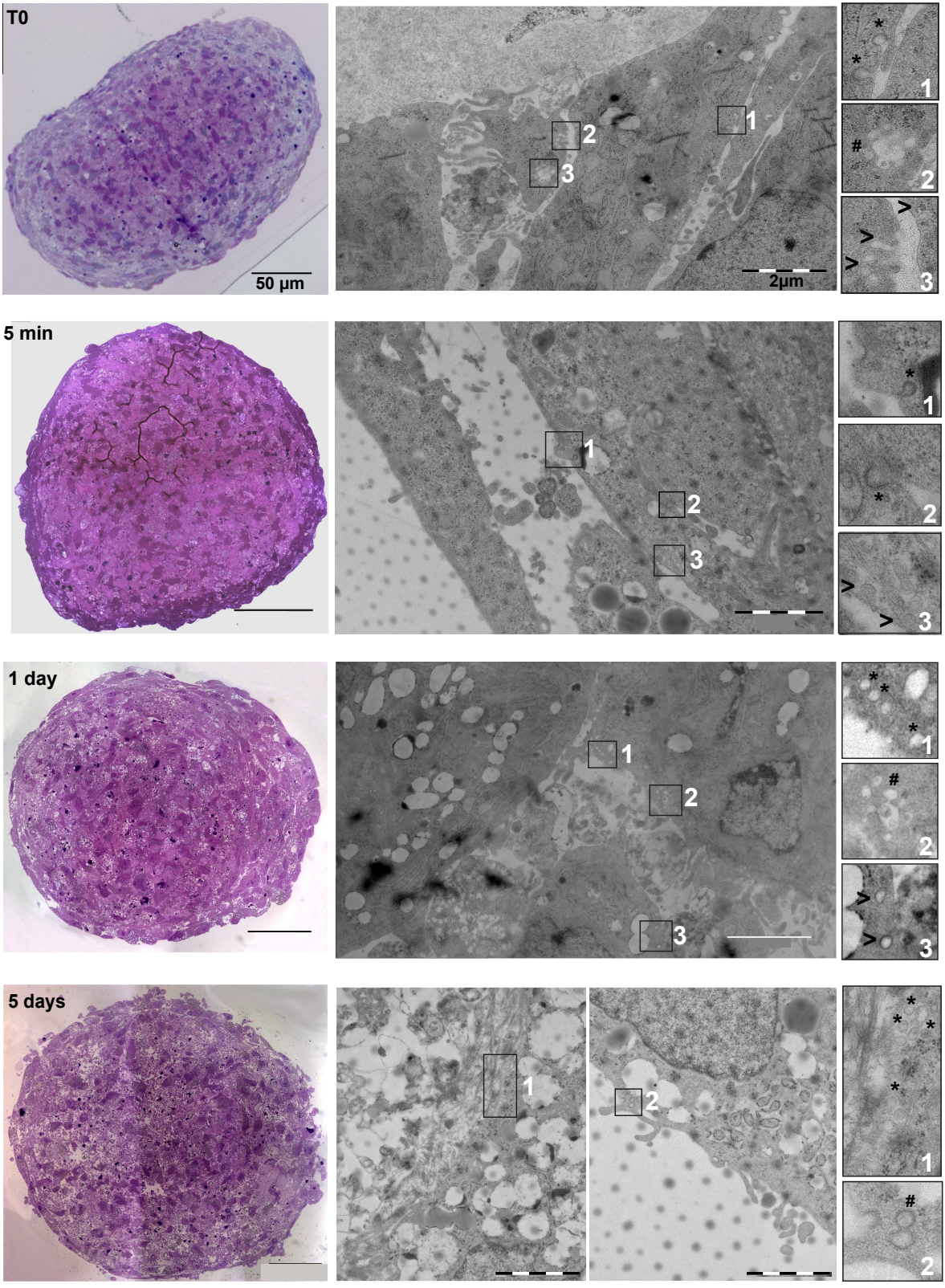

b)

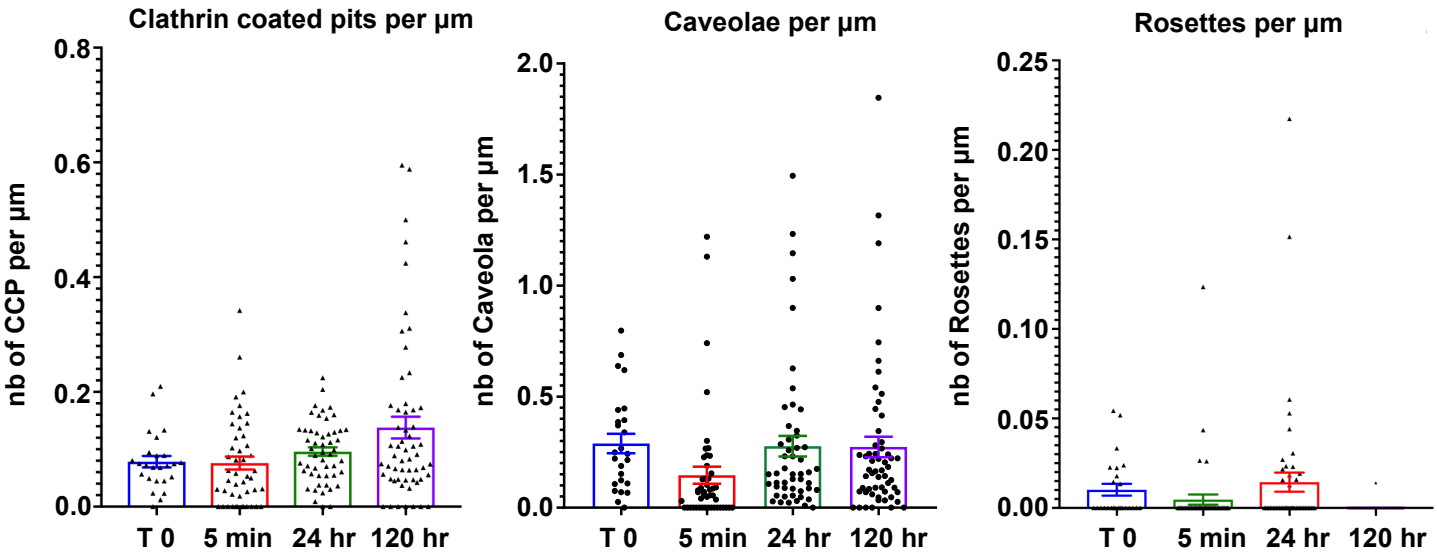

c)

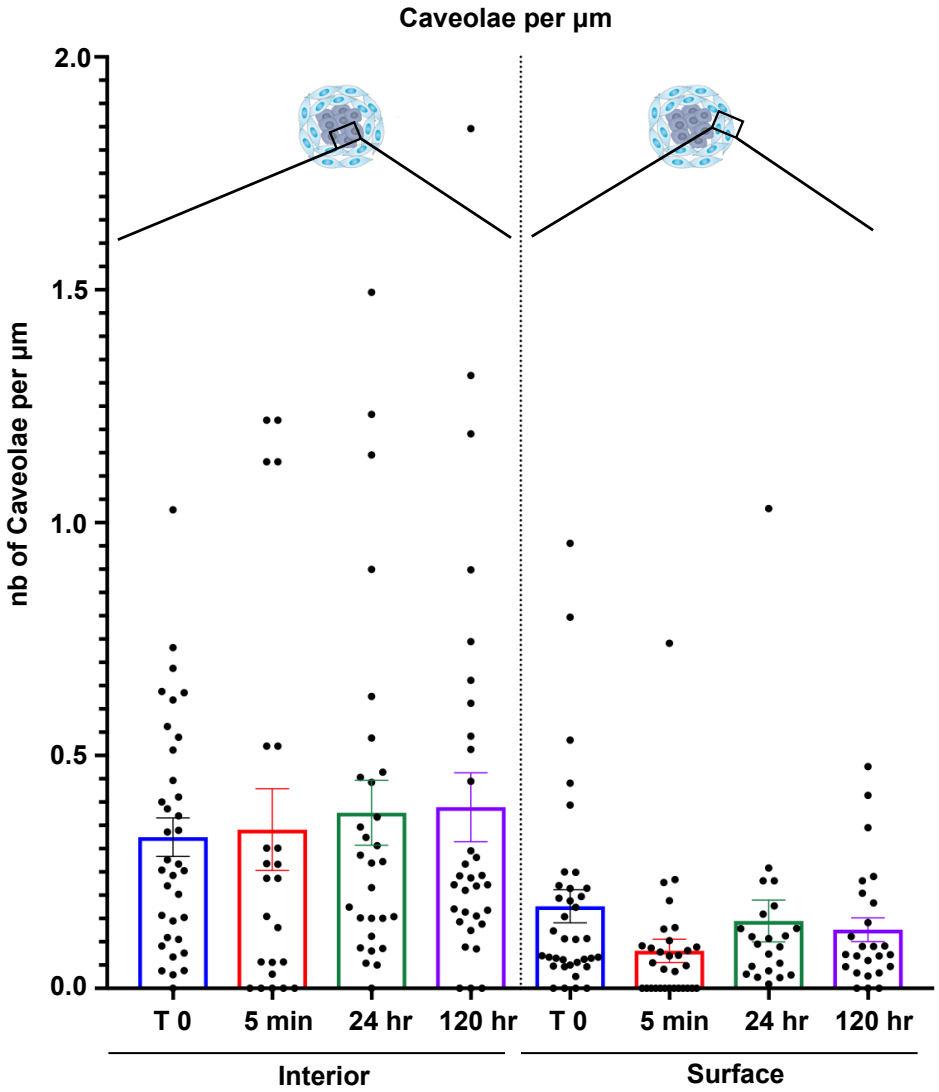

Figure 14. Hyperosmotic-induced compressive stress in spheroids reduce caveolae presence on short term and number of rosettes on long term.

(b) Semi thin sections (500 nm) of compressed spheroids for 5 min, 1 day or 5 days and uncompressed spheroids (T0) after cacodylate staining (left panel). Bar is 50 µm. Ultra thin sections (65 nm) of the corresponding spheroids imaged by electron microscopy. Magnified insets show membrane invaginations features, being labeled as follows: * for caveolae, # for caveolae rosettes and > for clathrin. Bar is 2 µm (b) Quantification of clathrin coated pits, caveolae, caveolar rosettes and caveolae numbers normalized by micrometer of PM analyzed at the surface of spheroids (first 4 rows of cells). **(c)** Number of caveolae per µm in cells inside (interior) the spheroid or at the edge (surface). Data are mean ± SEM.

we performed a high-throughput transcriptomics screening with Clariom^{TM} S assay (ThermoFischer). This microarray is a next generation transcriptome-wide gene-level expression profiling tool. For this exploratory assay, we compared uncompressed spheroids of TNBC Hs578t cells with compressed spheroids either after 5 days of hyperosmotic induced compression or encapsulated spheroids compressed for 5 days. After experiment completion, the array raw data were first processed by GenoSplice and this primary analysis gave us the principal component analysis (PCA). The PCA was a quality control of the differential expression between the samples, which decomposes high-dimensional dataset, by maximizing the variance between the expressed genes. The first component is the direction along which the samples show the largest variation, and the second is the direction uncorrelated to the first component which shows the largest variation (Ringnér, 2008). With this statistical analysis, we can observe how each condition of samples was grouped and shows different profiles. Only one sample (indicated by red arrow on the figure 16) from the dextran induced compressive system showed a more distant profile, likely because this sample was prepared on a different day to replace the original sample that did not give enough RNA when prepared. This sample was discarded for the final analysis **(Figure 16 a)**.

Then, we compared the difference of gene expression with the gene ontology terms (GO, a bioinformatics initiative that groups genes and gene products into functions) (Ashburner et al., 2000; “The Gene Ontology Resource,” 2019) which give us a comparison tool for the expression profile of gene groups involved in different pathways. Among the different categories, we found significant differences for several biological processes and cell domains (cellular and extracellular compartments, organelles) when comparing the 3 groups for gene expression.

In figure 16, we highlight some of the most relevant pathways that showed a differential expression between conditions. If we only consider the differences between capsules and uncompressed spheroids, we could find an increased expression for 118 pathways such as: response to hypoxia, protein ubiquitinylation, positive regulation of fat cell regulation, cell adhesion, exosomal components, cellular response to fluid shear stress, extracellular matrix, negative regulation of JUN kinase activity, response to mechanical stimulus and positive regulation of cell migration.

When we consider the comparison of hyperosmotic induced compression and uncompressed spheroid, we found the differential regulation of 133 GO terms, with

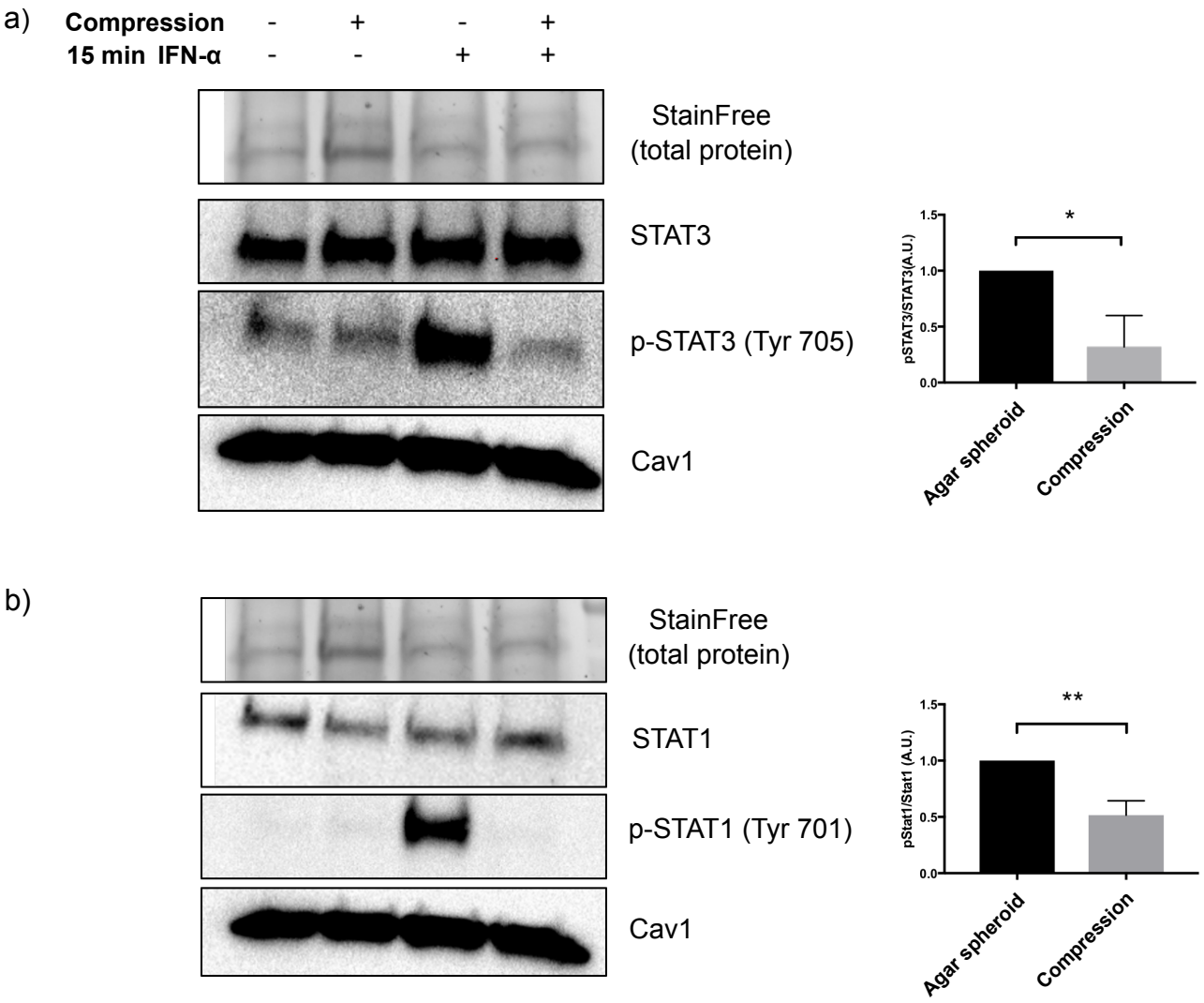

Figure 15. Compressive stress inhibits JAK-STAT signaling

(a,b) (Left) Representative western blot of STAT3 and pSTAT3 (Tyr 705) **(a)** or STAT1 and pSTAT1 (Tyr 701) **(b),** in Hs578t cells subjected or not to hyperosmotic-induced compression for 5 minutes followed by stimulation with IFN-α for 15 minutes. (Right) quantification of pSTAT3/STAT3 ratio. Data are mean ± SEM. Statistical analysis with two- tailed paired t test *P ≤ 0.05, **P ≤ 0.01.

an increase of expression for genes related to: cellular glucuronidation, negative regulation of fatty acid metabolic process **(Figure 16 b)**. On the contrary, we can observe a downregulation of the terms: mitochondrion, MAPK cascade, proteasome complex, JAK-STAT cascade, negative regulation of ERK1 and ERK2 cascade, cell-cell adherent junction, extracellular exosome, establishment of protein localization to plasma membrane, negative regulation of cell migration **(Figure 16 c)**.
Finally, the comparison of hyperosmotic induced compression and capsule compression revealed 215 GO terms differentially expressed such as the upregulation of negative regulation of glucuronosyltransferase activity, negative regulation of fatty acid metabolic process, keratin filament; but also the downregulation of nucleus related components, mitochondrion, cellular response to DNA damage stimulus, response to fatty acid, ubiquitin-protein transferase activity, positive regulation of cellular protein catabolic process, DNA replication initiation and apoptotic process **(Figure 16 c)**.

From these results, we can extract several interesting findings before we further analyze our data. First, we have observed that, even if both systems are exerting compressive stress, the confinement effect from capsules and the dextran addition have striking different effects on cells at the transcriptional level. It reveals a marked difference between these two compressive approaches. Here, we found an important variation of protein synthesis mechanisms between the two systems such as the G1/S transition of mitotic cell cycle, mRNA processing DNA replication initiation which are more expressed in capsules. This could reflect a possibly more active synthesis machinery in encapsulated cells after compression. We should consider that encapsulated cells grow from an initially smaller population and need to be cultured longer to reach comparable size and compression. Secondly, more genes are downregulated than upregulated in exosomal content when we check dextran-induced compression against control. On the contrary the situation is reversed in the condition capsules against control. When you check genes upregulated on both conditions for this term you can find some coincidences as is in the case of the gene CHI3L1.
Interestingly, the observed changes in exosomal components are consistent with previous literature in the field, linking caveolae dynamics to exosome release/uptake(Botos et al., 2008; Campos et al., 2018; Chen et al., 2011; Logozzi et

a)

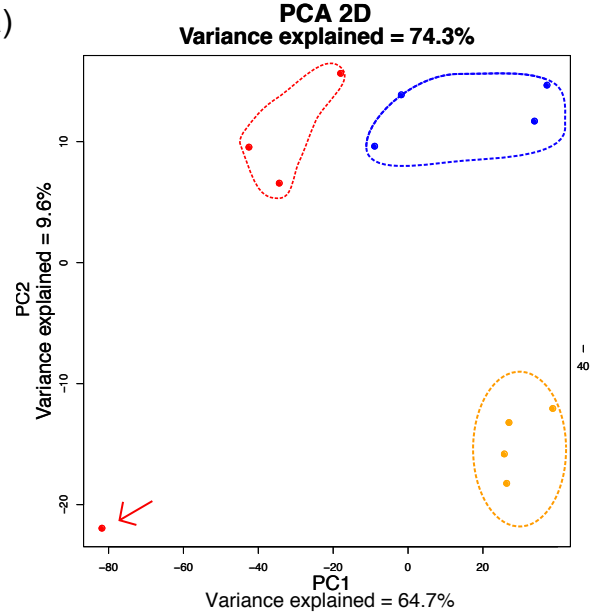
PCA 2D
Variance explained = 74.3%
PC2
Variance explained = 9.6%
PC1
Variance explained = 64.7%

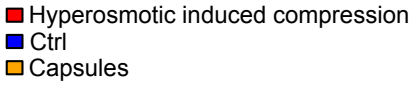
Hyperosmotic induced compression
Ctrl
Capsules

b)

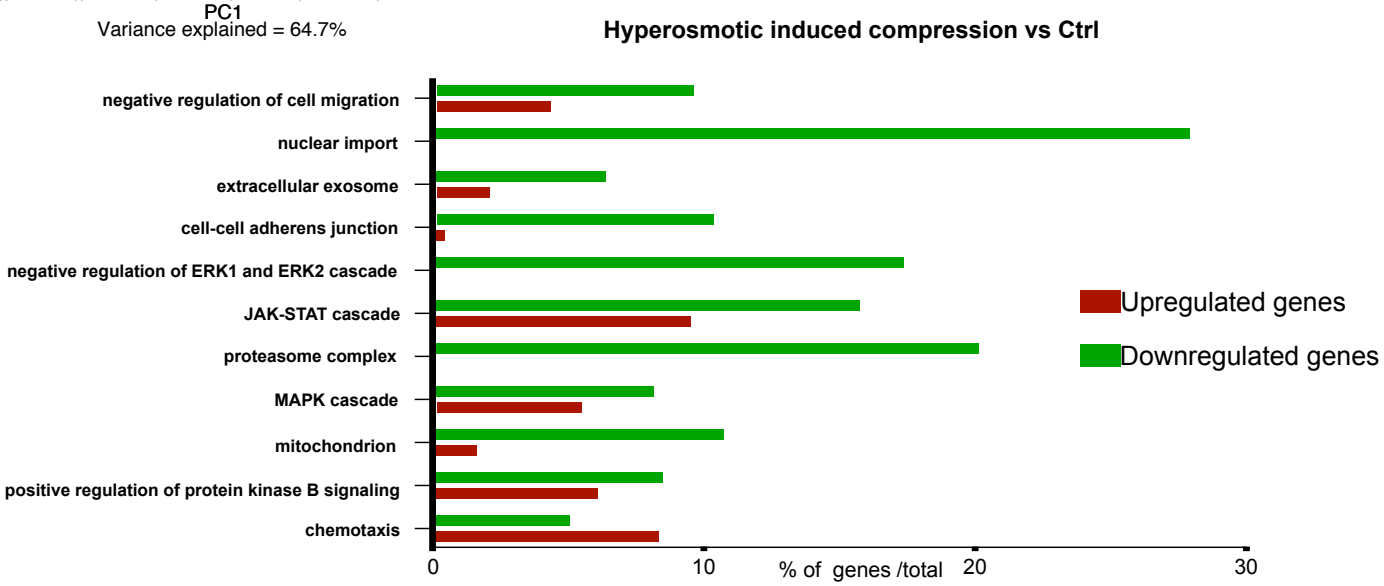
Hyperosmotic induced compression vs Ctrl
negative regulation of cell migration
nuclear import
extracellular exosome
cell-cell adherens junction
negative regulation of ERK1 and ERK2 cascade
JAK-STAT cascade
proteasome complex
MAPK cascade
mitochondrion
positive regulation of protein kinase B signaling
chemotaxis
Upregulated genes
Downregulated genes
% of genes /total

c)

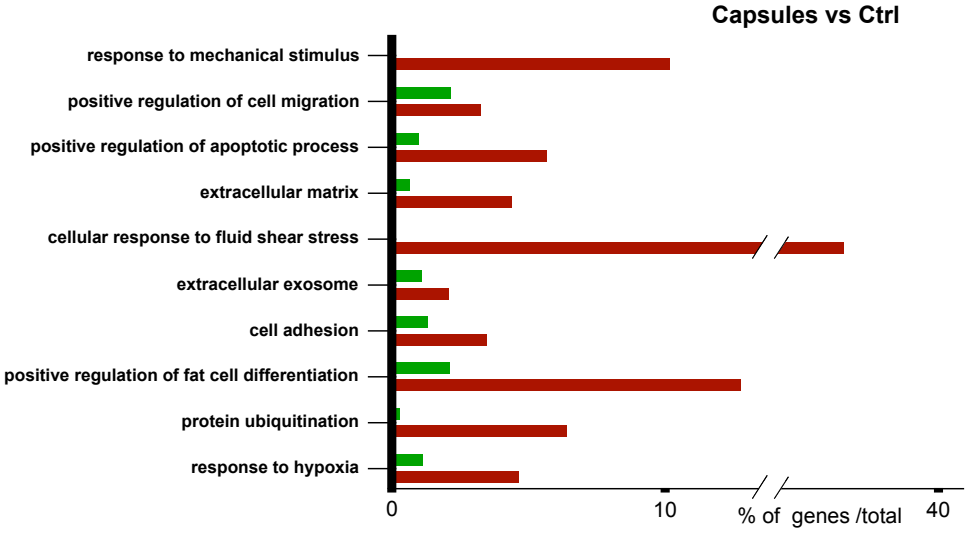
Capsules vs Ctrl
response to mechanical stimulus
positive regulation of cell migration
positive regulation of apoptotic process
extracellular matrix
cellular response to fluid shear stress
extracellular exosome
cell adhesion
positive regulation of fat cell differentiation
protein ubiquitination
response to hypoxia
% of genes /total

d)

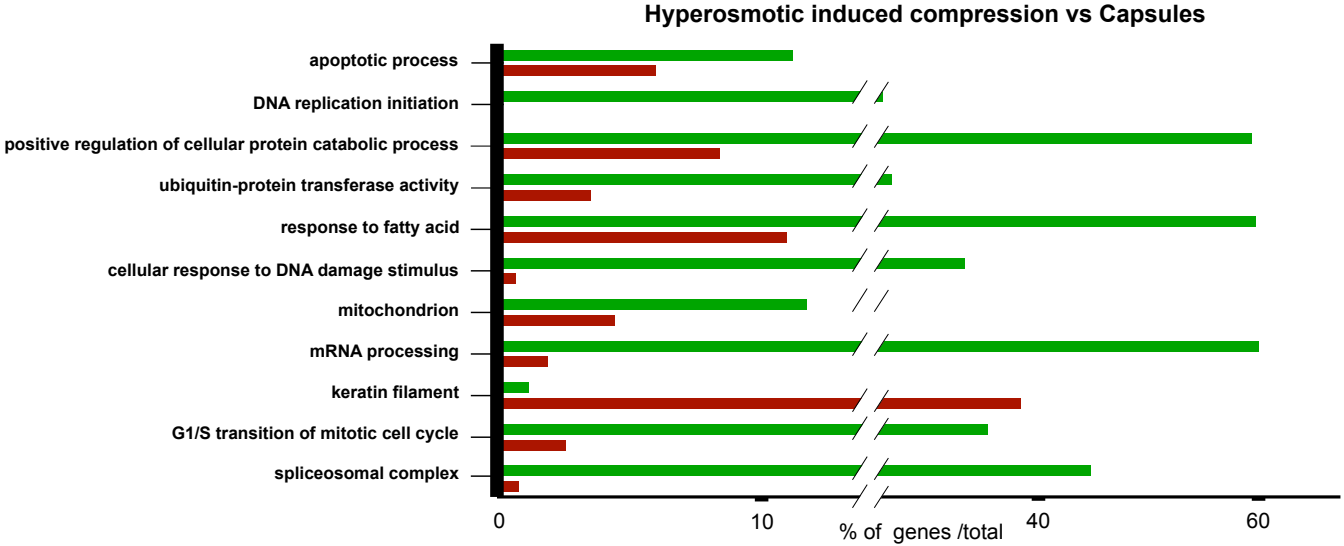
Hyperosmotic induced compression vs Capsules
apoptotic process
DNA replication initiation
positive regulation of cellular protein catabolic process
ubiquitin-protein transferase activity
response to fatty acid
cellular response to DNA damage stimulus
mitochondrion
mRNA processing
keratin filament
G1/S transition of mitotic cell cycle
spliceosomal complex
% of genes /total

Figure 16. Transcriptomics analysis of compressive stresses.

(a) Principal Component Analysis (PCA) of all the samples from the three experimental conditions: control (ctrl), hyperosmotic induced compression and capsules. Dashed colored lines delineate experiment groups. Red arrow indicates discarded samples. **(b,c,d)** Percentage of upregulated (red) or downregulated (green) genes for each differentially regulated Gene Ontology (GO) terms comparing hyperosmotic induced compression vs. ctrl **(a),** capsules vs. ctrl **(b)** and hyperosmotic induced compression vs. capsules conditions **(c)**.

a)

Hyperosmotic induced compression vs Ctrl

Gene Ontology (GO) term	Total genes in pathway	Genes regulated (up/down)	p-value	More than 2-fold change
negative regulation of cell migration	95	13 (4/9)	4,52E-02	EPPK1, STC1, TPM1
nuclear import	18	5 (0/5)	3,87E-02	SNRPD1
extracellular exosome	2811	231 (55/176)	4,07E-02	EFEMP1, PHGDH, KRT18, MEST, GPX1, PSAT1, UCHL3, PPA1, VPS36, RARRES1, ACTG2, GALNT3, SLC1A1, SYNGR2, CTSC, PSMB5, C5orf46, RAB23, HIST2H3D, C3, MGRN1, LILRA5, IL1RN, MAL2, CHI3L1, DEFA1B, DEFA3, DEFA1
cell-cell adherens junction	323	34 (1/33)	3,51E-02	LMO7, KRT18, TMPO
negative regulation of ERK1 and ERK2 cascade	58	10 (0/10)	2,47E-02	SPRY1
JAK-STAT cascade	32	8 (3/5)	7,51E-03	CCL2
proteasome complex	60	12 (0/12)	3,98E-03	PSMB5
MAPK cascade	262	35 (14/21)	8,58E-04	PSMB5, CCL2, CCR5
mitochondrion	1331	161 (20/141)	2,19E-10	MCUB, SLIT3, GPX1 ,TFB1M, ALDH1B1, NT5C3A, MRM2
positive regulation of protein kinase B signaling	84	12 (5/7)	4,31E-02	GPX1, CHI3L1, MYORG
chemotaxis	122	16 (10/6)	3,38E-02	CCL11, CCL2, CCR5, DEFA1, DEFA1B

b)

Capsules vs Ctrl

Gene Ontology (GO) term	Total genes in pathway	Genes regulated (up/down)	p-value	More than 2-fold change
response to hypoxia	172	10 (8/2)	3,11E-02	CITED2
protein ubiquitination	359	24 (23/1)	4,64E-05	MDM2, KBTBD8
positive regulation of fat cell differentiation	47	7 (6/1)	1,13E-03	ZFP36
cell adhesion	459	22 (16/6)	6,75E-03	IBSP, CD36, ABL2, AMTN
extracellular exosome	2811	90 (59/31)	6,27E-03	CHI3L1, COL14A1, SELENOP, C3, RBP4, DNAJB4, MME, COLEC12, SERPINI1, IL1RN, TTN, AOX1, IGFBP3
cellular response to fluid shear stress	12	4 (4/0)	2,98E-03	HAS2, PTGS2
extracellular matrix	296	15 (13/2)	1,52E-02	ADAMTSL1, CHI3L1, COL14A1, AMTN, ADAMTS1
positive regulation of apoptotic process	300	20 (17/3)	2,43E-04	BNIP3, BCL6, PTGS2, IGFBP3, FOSL1, FGD4, TXNIP
positive regulation of cell migration	184	10 (6/4)	4,48E-02	HAS2
response to mechanical stimulus	59	6 (6/0)	1,65E-02	CITED2, FOSL1, CHI3L1, TXNIP

c)

Hyperosmotic induced compression vs Capsules

Gene Ontology (GO) term	Total genes in pathway	Genes regulated (up/down)	p-value	More than 2-fold change
apoptotic process	567	129 (37/92)	1,02E-02	USP17L1, TNFRSF25, RASSF7, DCC, FGFR2, PHLDA2, MAL, PLAGL1, IL19, LY86, TP53AIP1, MECOM, TGFBR1, PAWR, TNFAIP8, SIAH1, PPP1R15A, TIGAR, ,NFKBIA, SH3RF1, AKTIP, IGFBP3, IFT57, BNIP3,BIRC3, MAP3K8, SGK1
DNA replication initiation	32	13 (0/13)	9,76E-03	CCNE2, MCM6, MCM7
positive regulation of cellular protein catabolic pr	11	7 (1/6)	8,26E-03	HMGB2
ubiquitin-protein transferase activity	329	84 (13/71)	1,75E-03	KLHL15, WSB1, RCHY1, SMURF2, SIAH1, BARD1, IPP, FBXL3, BIRC3, MDM2, KBTBD8, PRKN, ASB18, MGRN1
response to fatty acid	17	9 (2/7)	7,15E-03	CTGF, INSIG2, PTGS2
cellular response to DNA damage stimulus	208	55 (2/53)	5,72E-03	MCM7
mitochondrion	1331	291 (65/226)	1,44E-03	P4HA1, KYAT3 // RBMXL1, AGPS, NIT2, PARP1, OXCT1, MTFR2, FAM72A, FEZ1, PNPT1, ALDH1L2, PPP1R15A, KRAS, CLU, MRM2, NT5DC3, RPP14 // HTD2, BCAT1, MYC, BNIP3, FDX1, TFB2M, DDAH1, FAM162A, RGS2, MTHFD1L, PDK1, NT5C3A, MCUB, SGK1, PRODH2, PRKN, CYP24A1, TP53AIP1, CAMK2A
mRNA processing	179	57 (4/53)	3,24E-05	KYAT3 // RBMXL1, SON, RBM26, ZNF326, ESRP1
keratin filament	100	30 (28/2)	7,67E-03	KRTAP4-8, KRTAP4-11, KRTAP9-8, KRTAP5-10, KRTAP10-10, KRTAP10-1, EPPK1
G1/S transition of mitotic cell cycle	102	40 (3/37)	2,90E-06	RPA3, CCNH, CDKN3, FBXO5, MCM7, MCM6, INHBA, CCNE2, CDKN1A, BCAT1, CAMK2A
spliceosomal complex	94	41 (1/40)	7,16E-08	IVNS1ABP, SNRPA1, ZNF326, TXNL4B

Figure 17. Selection of genes highly regulated after compressive stresses in Hs578t cells.

(a,b,c) Number of upregulated (red) or downregulated (green) genes within GO terms (upregulated in red, downregulated in green) comparing hyperosmotic induced compression vs ctrl **(a)**, capsules vs ctrl **(b)** and hyperosmotic induced compression vs capsules conditions (c). The names of genes with more than 2-fold change are listed (right).

al., 2009). In addition, stretching has been described to promote exosome release in cardiomyocytes (Bang et al., 2014). Considering this evidence and the modified expression of exosomes related genes in our transcriptomic data, we then tested the hypothesis that caveolae-dependent mechanosignaling could trigger exosome synthesis and release.

Mechanical stimulations increase exosome release in a caveolae dependent manner.

To study the impact of mechanical forces on exosome release, we chose Schwann cells as a model because of the known upregulation of Cav1 during axonal remyelinization that occurs after nerve damage (Mikol et al., 2002) and its depletion on schwannomas (Aarhus et al., 2010). These studies make another possible relation between mechanical damage and the presence of functional caveolae. These experiments were developed and performed with our collaborators, the team of Felipe Court (Center for Integrative Biology, Universidad Mayor. Santiago de Chile, Chile), who have recognized expertise in the biology of exosomes. First, we made a series of experiments, with hypo-osmotic shock (150 and 30 mOsm) for 5 minutes to increase membrane tension in primary rat Schwann cells by swelling, prior to media collection and released exosomes counting. In this experiment, we observed an increase by 97,5% of the number of particles released in the exosome size ranges (50-150 nm) after purification by ultracentrifugation **(Figure 18 a,b)**.

The second set of experiments used the hyperosmotic-induced compression of Schwann cells spheroids for 48h, the optimal time point for exosome release assay determined by our collaborators. Here, we observed the same significant increase of exosome release by 103,1% of the number of particules after compression of cell spheroid **(Figure 18 c,d)**.

The next step was to determine whether the increased exosome release under mechanical constrains was dependent on caveolae or not. We then optimized the viral infection of primary Schwann cells to obtain a correct CAV1 knockdown by shRNA. Finally, after three different treatments, we succeeded to reduce Cav1 expression by approximately 50% **(Figure 18 e)**. Interestingly, the release of exosomes after mechanical stress did not have a significant increase in shCav1 cells as compared to control cells **(Figure 18 f)**. This experiment demonstrates the

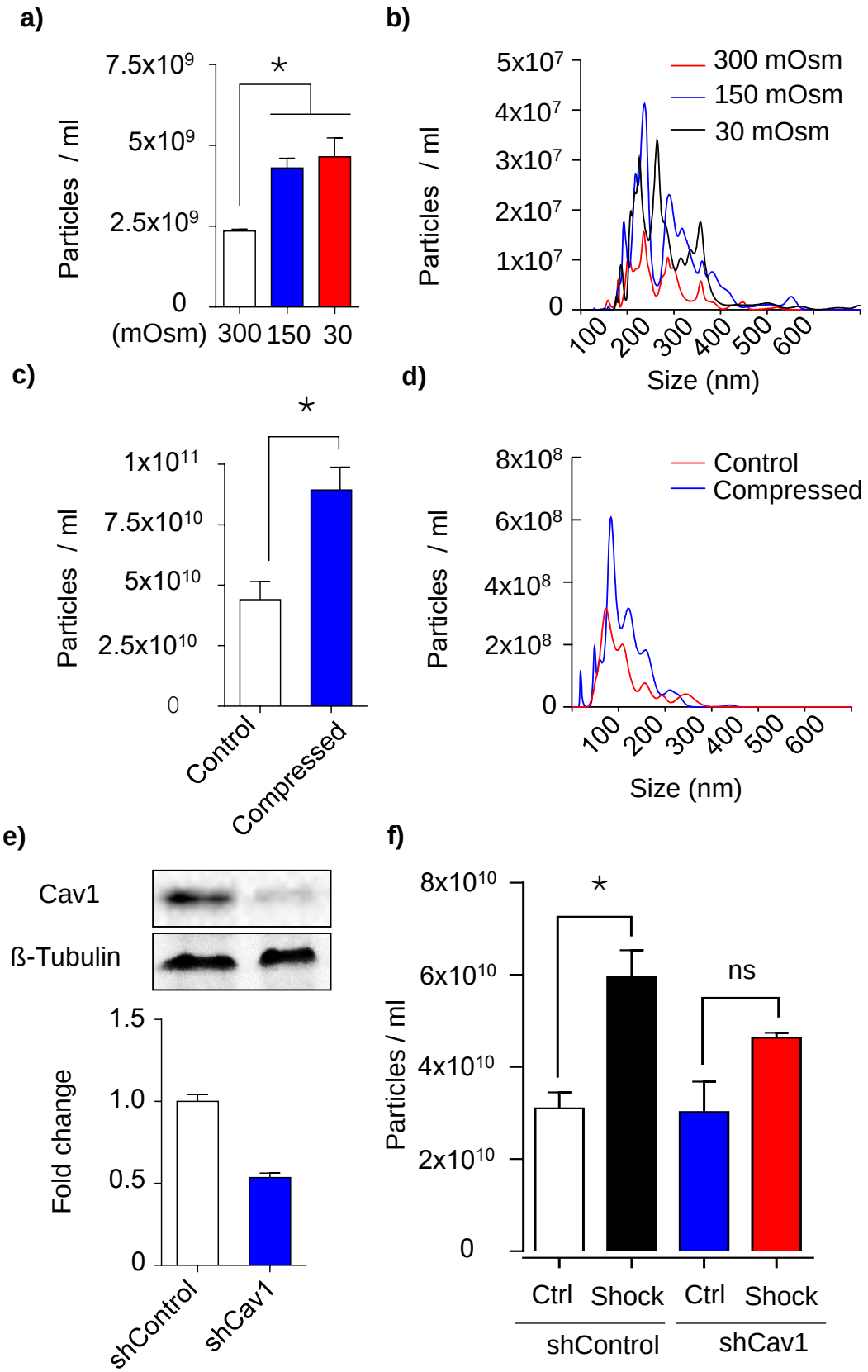
a)
7.5x10⁹
5x10⁹
2.5x10⁹
0
Particles / ml
*
(mOsm) 300 150 30
b)
5x10⁷
4x10⁷
3x10⁷
2x10⁷
1x10⁷
0
Particles / ml
300 mOsm
150 mOsm
30 mOsm
100 200 300 400 500 600
Size (nm)
c)
1x10¹¹
7.5x10¹⁰
5x10¹⁰
2.5x10¹⁰
0
Particles / ml
*
Control
Compressed
d)
8x10⁸
6x10⁸
4x10⁸
2x10⁸
0
Particles / ml
Control
Compressed
100 200 300 400 500 600
Size (nm)
e)
Cav1
ß-Tubulin
1.5
1.0
0.5
0
Fold change
shControl
shCav1
f)
8x10¹⁰
6x10¹⁰
4x10¹⁰
2x10¹⁰
0
Particles / ml
*
ns
Ctrl Shock Ctrl Shock
shControl
shCav1

Figure 18. Mechanical stress in Schwann cells increases the release of extracellular vesicles in a caveolae-dependent manner.

(a) Schwan cells (SCs) grown in 2D culture plates were subjected to mechanical stress by hypo-osmotic shock (150 and 30 mOsm) for 5 min. SCs were then incubated for 45 min in iso-osmotic medium (300 mOsm) and extracellular vesicles were purified by ultracentrifugation of the conditioned medium. (b) Representative size profile of the vesicles (particles) released after the osmotic shock. (c) SCs spheroids were compressed with dextran for 48 h and extracellular vesicles were purified by ultracentrifugation of the conditioned medium. (d) Representative size profile of the vesicles (particles) released after osmotic shock. (e) SCs grown in 2D were infected with control or Cav1 shRNA. Knock-down efficiency was evaluated by western blotting (~50% reduction). (f) Cav1 knocked-down SCs were subjected to mechanical stress by hypo-osmotic shock (150 mOsm) for 5 min. SCs were incubated for 45 min in iso-osmotic medium (300 mOsm) and extracellular vesicles were purified by ultracentrifugation of the conditioned medium. Data are mean ± SEM. Statistical analysis with one-way ANOVA (a,f) or two- tailed paired t test (c) *$P \leq 0.05$

caveolae dependency of mechanically increased release of exosomes in Schwann cells.

At last, to identify a possible role of caveolae in exosome uptake, we performed a proof-of-concept experiment comparing particles exchange between Schwann cells in spheroid, without compression or under 1h or 24h of hyperosmotic induced compression. Half of the cells forming spheroids were infected for the expression of either a cytosolic mCherry or a N-terminal palmitoylated GFP, a construct used for tracking extracellular vesicles (Lai et al., 2015). With this marker in half of the spheroid cells, we acquired z-section images and quantified the number of GFP positive particles colocalizing with the mCherry cytosolic mask. Our preliminary data suggest that mechanical stress inhibits the uptake of the released exosomes **(Figure 19 a,b)**. All together these results show an important role of caveolae in the sensing of mechanical forces and the resultant increase of exosomal release.

Figure 19

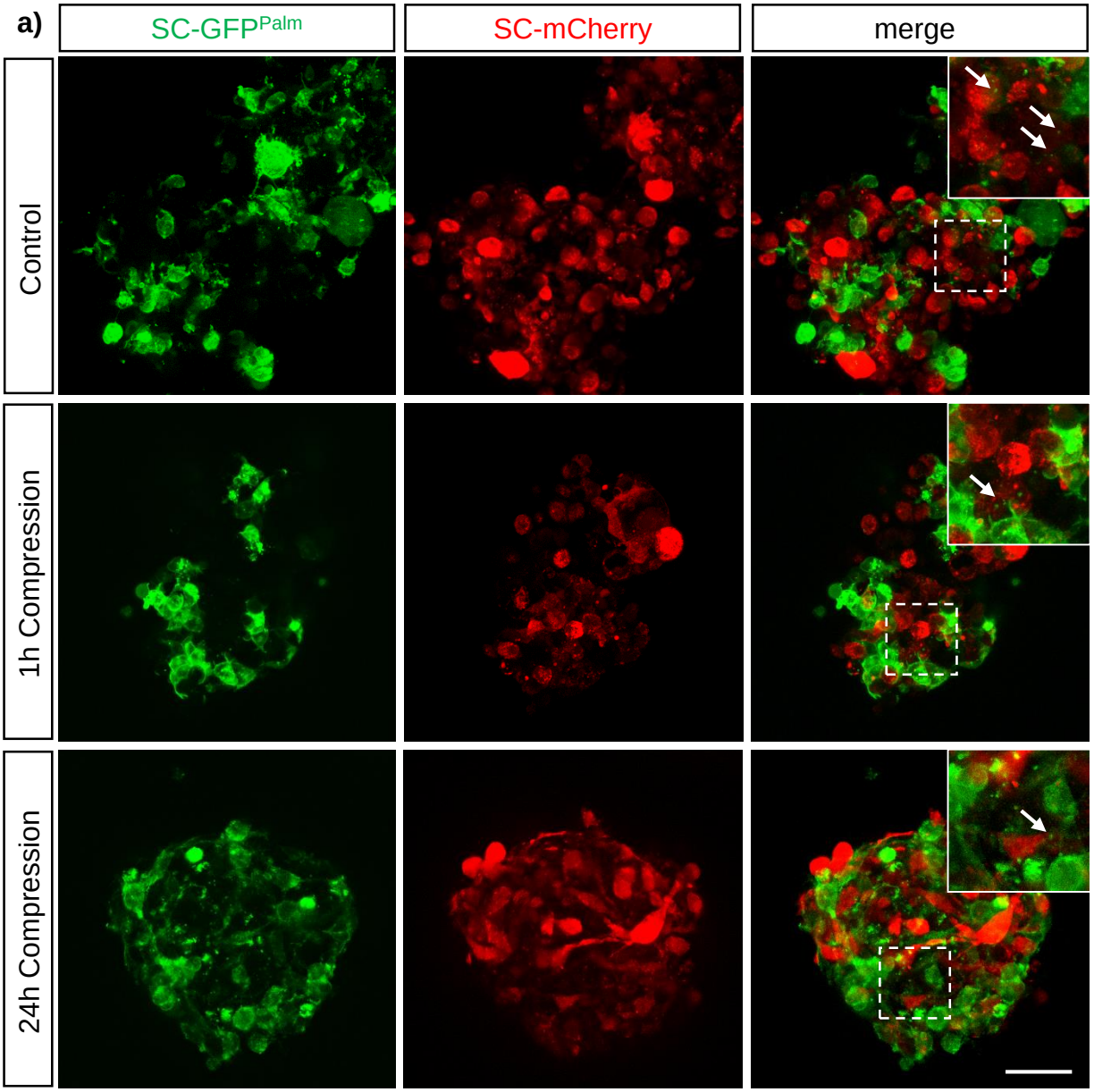
a)
SC-GFPPalm
SC-mCherry
merge
Control
1h Compression
24h Compression

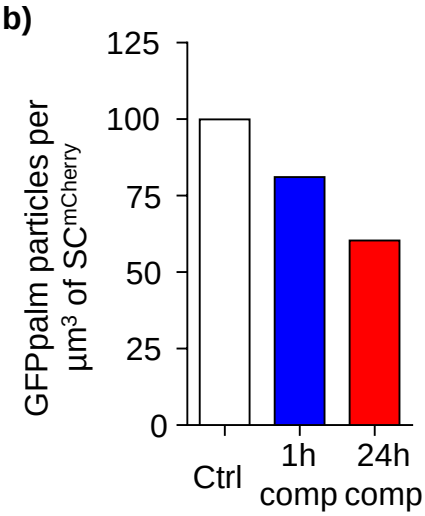
b)
GFPpalm particles per µm3 of SCmCherry
125
100
75
50
25
0
Ctrl
1h comp
24h comp

Figure 19. Hyperosmotic-induced compression inhibits EV transfer between SCs

(a) Two populations of SCs, each transfected with plasmids encoding either cytosolic mCherry or GFP-Palm, a membrane and EV marker, were co-cultured in spheroids and subjected or not to hyperosmotic-induced compression with dextran for 1 or 24 h. White arrows in insets indicate GFP-Palm positive EV. Bars are 50 µm. **(b)** Quantification of GFP-Palm positive spots density in mCherry positive SCs.

-DISCUSSION-

Cell type segregation induced by compression in capsules

The results of this project are partly discussed in the joined article in the results section. I will therefore briefly discuss the results on the interactions between fibroblast and colon cancer cells in a compressive 3D environment.

The results describe how fibroblasts can engulf cancer cells under 3D compression. This phenomenon could be explained by the differential adhesion hypothesis, described in the introduction **(Figure 8).** This hypothesis stipulates that homotypic cell-cell contacts are more stable than heterotypic ones. Based on our experimental set-up, we show that the interaction between colon cancer cell line Ht29 and fibroblast cell line NIH3T3 results in differetntial expression of N-cadherin for both cell types but with a differential expression of α5β1-integrins. To this, we should consider the repulsion generated by Eph-ephrin signaling (Solanas et al., 2011), which suppresses cadherin mediated adhesion, and promotes the retraction of adhesive contacts mediated by actomyosin contractility (Fagotto et al., 2013). In addition, the role of surface tension in the context of cell sorting, should be taken into account in the model, allowing to consider the spheroids as two separate fluids with different cohesive forces. Then, the reorganization of fibroblasts could be explained by a displacement of the equilibrium of surface tension of each spheroid. However, (Interestingly) when surface tension was measured we found that even though there was a displacement and increase of surface tension in the cancer cell population, it was not enough to explain by itself the change of behavior of fibroblasts, as the surface tension of cancer cells was still inferior to the one of fibroblasts.

In order to explain the change in fibroblasts behavior upon reaching of the compressive threshold, we hypothesized that changes in fibronectin deposition on the interphase between fibroblast spheroid and alginate could be formed. When we analyzed the images of fibroblast spreading, we found that fibronectin was localized onto the fibroblasts-alginate interphase where fibroblasts preferentially adhere onto the alginate wall. At this interface, fibronectin would promote surface wetting. In this situation, fibroblast segregation would be mainly regulated by the energy at the interphase of the tissue-ECM boundaries rather than by the hetero-homotypic contacts between both spheroids as proposed in a breast cancer model (Cerchiari et al., 2015). As this change of fibronectin distribution is likely to be due to the rearrangement of existing fibronectin or a new deposition, we inhibited fibronectin

interaction with αVβ3/αVβ5 integrins with using the RGD peptide antagonist Cilengitide. Under this condition, we observed that the spreading of fibroblasts over cancer cells was inhibited. This seems to confirm the hypothesis that spheroids need an active component (fibronectin pattern rearrangement) in order to fight the tendency of the spheroid with lower surface tension to spread over the one with higher surface tension. Further experiments will confirm this by analyzing spreading under knock down of fibronectin expression in fibroblasts. Moreover, it will be interesting to see if blocking the interaction with fibronectin will result also in changes of surface tension and displace the equilibrium to the point where spheroids will stop spreading over the others.

Caveolar response during tumor adaptation to compressive stress

The deregulation of the different caveolar components has been reported to influence cancer progression at several stages (Lamaze and Torrino, 2015b). First, the inhibitory role of Cav1 in proliferation and invasion has been described (Fiucci et al., 2002). Later, it was shown that EHD2 downregulation was promoting invasion and metastasis, and thus is a marker of poor prognosis in breast and prostate cancers (Yang et al., 2015). My host laboratory has demonstrated how caveolae respond to mechanical stresses by flattening out and protect cell membrane from bursting (Dewulf et al., 2019; Sinha et al., 2011b). Recently, my laboratory has also shown that EHD2 translocates to the nucleus in response to mechanical stress in triple negative breast cancer cell line Hs587t, establishing the first example of mechanotransduction by caveolae (Torrino et al., 2018). My laboratory also found that EHD2 is required to maintain the caveolae reservoir at the plasma membrane since breast cancer MDA-MB-436 cells, which do not express EHD2 revealed a complete absence of caveolae. Finally, preliminary results from my laboratory revealed a control of signaling by caveolae mechanics with the finding that the interaction of Cav1 with the tyrosine kinase was favored upon stretching or swelling of the cell membrane resulting in JAK1 negative regulation (Tardif, 2018). This process is likely to explain the lack of mechanosignaling regulation of the IL6/JAK2/STAT3 pathway that my laboratory recently reported in muscle cells isolated from patients with Cav3-associated muscle dystrophies (Dewulf et al., 2019)

In the present work, we found that the expression of the caveolar ATPase EHD2 was significantly reduced after long-term compressive stimuli **(Figure 12 and 13)**. Since EHD2 has been involved in the stability of caveolae at the plasma membrane (Stoeber et al., 2012; Torrino et al., 2018) through the control of their detachment from the cell surface (Matthaeus et al., 2019), we were expecting that adaptation to compressive stress may lead to changes in caveolae numbers. Interestingly, even after several days of compression within spheroids and loss of EHD2, cells still exhibited intact caveolar structures **(Figure 14 a)**. The reduction of EHD2 expression without modification of the expression of the other caveolar components (i.e. Cav1, Cav2 and Cavin-1) occurred when multicellular breast cancer spheroids where compressed for a long time period.

Thanks to a whole transcriptome high throughput screening, we identified pathways that were differentially affected by compression induced either by hyperosmotic shock or by encapsulation. Our data show a strong transcriptional adaptation of cells subjected to mechanical stimuli in both conditions. Thus, many different pathways were up- or down-regulated, in particular for some that are related to tumor progression and invasion such as cell migration, exosomal content, response to mechanical stimulus, cell adhesion, regulation and signaling pathways (MAPK and JAK/STAT cascades) **(Figure 15)**. These changes in expression patterns could be key elements of the adaptation of transformed cells to the compressive stresses they can experience through cancer progression from the hyperplasic stages (Lu and Kang, 2019; Sato and Weaver, 2018; Thomas et al., 2015; Wagner and Nebreda, 2009). To get more insight into the molecular mechanisms involved, we plan to further explore the responses of different signaling pathways to 3D compressive stimuli. Therefore, we are currently starting a reverse phase protein assay (RPPA) screening on samples treated with the same experimental conditions than the transcriptomics analysis with an additional condition where EHD2 has been depleted by siRNA. The RPPA is a high throughput dot-blot based analysis technique available at the Curie Institute, which gives access to the protein expression levels and the activation status (phosphorylation) of signaling pathways. This powerful tool will help us to investigate the impact of compressive stress on the regulation of around 100 different effectors of cellular signaling pathways.

Interestingly, if our experiments have shown a loss or reduction of EHD2 at the protein level, this downregulation was not observed at the mRNA levels in our

transcriptomic data. This suggests that compressive stress could trigger the degradation of EDH2 via post-translational modification such as sumoylation and ubiquitinylation. Indeed, our laboratory has already reported that hypo-osmotic shock led to EHD2 SUMOylation by SUMO2/3, a small ubiquitin-related modifier capable of targeting specific proteins and promoting poly-ubiquitinylation which can led to proteasomal degradation (Fan et al., 2018, p. 1; Torrino et al., 2018, p. 2). It is therefore likely that proteasomal degradation rather than a reduction of transcriptional level may be responsible for the loss of EHD2 protein expression in our experiments. It will be important to confirm this possibility in future experiments.

Caveolae flattening during short term compression

We monitored by electronic microscopy the presence of caveolae structures in multicellular spheroids submitted to compression induced by hyperosmotic shock. Cells show a decrease of 50% in caveolae density after 5 minutes of compression as compared to cells in uncompressed spheroids **(Figure 14 a,b)**. The decrease of *bona fide* caveolae could be the consequence of caveolae flattening as found initially in 2D cell cultures (Sinha et al., 2011b). Interestingly, the decrease of caveolae number was no longer observable in cells submitted to constant compressive force for longer periods, starting after 1 day of induced compression. It may indicate that cells quickly adapt after the first stress generated by the compressive system and recover their initial number of caveolae. In this context, cells inside the spheroid seem to respond in an anisotropic way to an isotropic stress. Indeed, cells are losing circularity (cells being more speeded up on the outer layers) upon hyperosmotic-induced compression. These results confirm previous data in this model (Dolega et al., 2017), where outer cells show a higher degree of anisotropy and compressive stress tends to reduce the circularity of cells on the more external domains.

We next asked if short-term compression which triggers cell rearrangement and caveolae flattening could also promote changes on cell signaling in a caveolae dependent manner. To start answering this question, we compared the effects of hyperosmotic-induced compression with 2D systems (uni-axial stretching and hypo-osmotic shock) on JAK/STAT signaling. We previously reported a reduced phosphorylation of the transcription factor STAT3 upon interferon stimulation in a caveolae-dependent manner when cells were mechanically stressed (Tardif, 2018). In cells submitted to 5 minutes of compressive stress, we also found a reduction of

STAT3 phosphorylation. In addition, we also observed a decrease of STAT1 phosphorylation in contrast to 2D conditions, which suggests that there is difference in the way cells respond to 2D vs. 3D mechanical stimuli in. These experiments need to be further confirmed, in particular with the depletion of Cav1 and/or Cav2. Finally, it is worth noting that $Cav1^{-/-}$ mice do not show any change in STAT1 Tyr 701 phosphorylation, whereas $Cav2^{-/-}$ mice show an increase of STAT1 Tyr 701 levels similar to the increase we found for STAT3 phosphorylation upon Cav1 depletion (Almeida et al., 2011). We should also consider that Cav1 and Cav2 are co-transcriptionally regulated, even though no effect on STAT1 Tyr 701 phosphorylation was found when Cav1 was depleted in our lab. Expression changes in the ratio between Cav1/Cav2, could alter the expression of Cav2 when we switch to 3D geometries. We could hypothesize that differences in STAT1 Tyr 701 phosphorylation after mechanical stress conditions in 2D and in 3D could be due to lesser expression of Cav2. Finally, an interesting feature that will be worth investigating is that in contrast to Cav1, Cav2 does not present a caveolin scaffolding domain (CSD), a domain proposed to mediate Cav1 binding with signaling effector, a difference that may explain distinct effects between Cav1 and Cav2 on interacting partners (Couet et al., 1997).

Besides the effects we report here on JAK-STAT signaling, we aim to identify whether caveolae dependent mechanosignaling may be implied in the regulation of additional signaling pathways. As mentioned above, we will test this possibility by using RPPA analysis in which we will monitor activation level of different signaling pathways after short-term or long-term responses in cells depleted or not for EHD2. It should allow us to uncover differentially activated pathways in the context of mechanical compression and illustrate how the loss of EHD2 can be linked to cell mechanosignaling.

Caveolae vs caveolin-1 impact on tumor and mechanosignaling

Previously, my host laboratory has established the role of caveolae in response to mechanical stress demonstrating that caveolae flattening was essential for buffering membrane tension increase (Sinha et al., 2011b). More recently, my laboratory showed the role of caveolae in mechanotransduction and mechanosignaling (Dewulf et al., 2019; Tardif, 2018; Torrino et al., 2018). By the present work, we aimed at

translating these discoveries in two different 3D cellular system that could be submitted to mechanical compression. This work has opened several questions that will be unanswered in future experiments. We need to distinguish the role of caveolae as an assembled plasma membrane invagination from the role of Cav1 protein itself on the signaling response to mechanical stress. Cav1 is the main component of caveolae and unpublished results from my laboratory show that under mechanical constraint conditions, caveolae flattening leads to the release of Cav1 oligomers that can diffuse at the PM to interact with proteins such as the JAK1 tyrosine kinase (Tardif, 2018). In my laboratory, we have shown that EHD2 depletion by RNA silencing impairs the recovery of caveolae at the PM after stretch, but not the initial membrane tension buffering capacity (Torrino et al., 2018). In this context, it would be important to address how the loss of EHD2, that we observed in compressed spheroids, could affect the amount of Cav1 oligomers diffusing at the PM. Is the downregulation of EHD2 affecting the behavior of cancer cells and more particularly their signaling pathways? In the present study, we have detected many changes in gene expression related to different pathways concomitantly to EHD2 protein expression decrease under long-term compression. Repeating these experiments under EHD2 depletion is however required to correlate these changes with the loss of EHD2. Moreover, in a previous work from my laboratory, differences in expression levels of caveolar components was also evidenced in various breast cancer cell lines. For example, in triple negative breast cancer cell lines, the most aggressive breast cancer subtype, there is often a reduction of EHD2 protein and mRNA levels but not on Cav1. On the other hand, HER2+ and ER+ breast cancer cell lines shows lower levels of Cav1 when EHD2 is expressed. Can the compression-induced reduction of EHD2 protein levels, knowing EHD2 contribution to caveolae stability in the plasma membrane, change the diffusion of Cav1 oligomers? Or the quantity of internalized caveolae regulated by the constant compressive stress?

Caveolae impact on exosome release

Finally, an additional interesting result of the present work is the role of caveolae in exosome release. Several studies have previously shown a link between mechanical stress and the induction of exosome release both in cell culture systems, such as

stretching (Wang et al., 2019) or in vivo, during cardiac pressure overload in mice (Pironti et al., 2015), and axon damage in rats (Mikol et al., 2002). During my thesis, we confirmed this link, first in 2D culture with hypo-osmotic shock and then in 3D culture with spheroids submitted to compressive stimuli. Our transcriptomics data show changes in the regulation of genes for exosome components using the two different compressive systems. Moreover, we have shown that the increase of exosome release found under both 3D compressive stresses and hypo-osmotic shock, was dependent on the presence of Cav1.

In the present work, we found a significant reduction in exosome uptake during hyperosmotic-induced compression in Schwann cells. These results are nonetheless not conclusive and will require additional experiments including other types of mechanical stress such as stretching. Moreover, recent unpublished data from our collaborators shows an increase on exosome uptake in mouse lung endothelial cells devoid of caveolin and therefore of caveolae ($MLEC^{Cav1-/-}$). It will be therefore interesting to elucidate if the effect on exosome uptake is due to an increase in the amount of Cav1 oligomers at the plasma membrane or to a decrease in membrane tension buffering due to the loss of caveolae.

The next question is to discover the precise mechanism that links exosome release to Cav1 and caveolae, and how compressive stress could affect exosome uptake. The relation between Cav1 and exosomes has already been reported. For instance, Cav1 enriched exosomes can promote malignancy (Campos et al., 2018) and Cav1 was enriched in multivesicular bodies (MSV) upon albumin-induced caveolae endocytosis (Botos et al., 2008). Later, other studies provided evidence for ubiquitin-mediated endosomal sorting and degradation of Cav1 in MVBs (Hayer et al., 2010b). Moreover, the membrane of exosomes is enriched in cholesterol and sphingolipids, the lipid species that are typically found in caveolae (Staubach et al., 2009; Wubbolts et al., 2003). Indeed, the depletion of Cav1 or cholesterol both reduce the amount of lipid nanodomain-associated proteins in exosomes showing a link between exosome composition and caveolae integrity (Chen et al., 2011). How mechanical constrains by affecting caveolae integrity could trigger exosome formation and/or release still remains poorly understood. One hypothesis is that Cav1 oligomers that are released upon caveolae flattening will be endocytosed to reach multivesicular bodies, where it would promote exosome formation by the clustering of specific lipids. We can propose also that the caveolae response to mechanical stress could have molecular

consequences at the cytoskeleton level and/or on the lipid composition of the PM. These events could favor signaling effectors that would enhance exosome release, such as Rab family proteins. Indeed, our transcriptomic analysis revealed that RAB27, reported to play an important role in exosome biogenesis and release (Hessvik and Llorente, 2018), is differentially expressed in the two compressive models as compared to the control condition.

Differences between hyperosmotic-induced compression and encapsulation

Both hyperosmotic-induced compression and encapsulation of cells, when applied to the CT26 colon cancer cell line were shown to have similar macroscopic phenotypes with the formation of a necrotic core, the same range of pressure exerted, and a reduction of Ki-67 pathway activation, associated with cell proliferation, in the regions close to the core of the spheroid (K. Alessandri et al., 2013; Montel et al., 2012). Interestingly, even though we observe almost identical phenotypes in the two compressive methodologies, the results of the transcriptomic expression analysis revealed major differences in the pattern of RNA expression between the two systems. Based on the GO terms selected, we found that nuclear related components, mitochondrion, response to DNA damage, and catabolic processes were upregulated in hyperosmotic-induced compression as compared to capsules. This indicates that the synthesis machinery is more active in the spheroids treated with hyperosmotic-induced compression, this could be due to growth conditions that differ between the two systems (calcium bath for synthesis, dextran hyperosmotic environment, and probably more shear stress present in capsules). In addition, one should consider two factors that could impact on the capsule response. First, the growth from an initially smaller cell population and therefore a higher number of division cycles to reach the compressive threshold. Second, a possible founder effect in the population of cells since, having a few cells with heterogeneous mutations will may promote a clonal selection of the cells that are more prone to grow in adherent independent growth. Moreover, differences between capsules and hyperosmotic-induced compression expression profiles could be explained by how spheroids accumulated growth-stress, which would depend more on spheroid age than size (Guillaume et al., 2019).

Nonetheless both systems have their own perks and give precious information on the effects of compression on cellular spheroid from the short time resolution in hyperosmotic-induced compression to the more physiological but passive induction of compression in confined capsules.

To conclude, in my doctoral work, I have used two different assays that allow to apply compressive stresses in a 3D environment and have compared the impact on some known caveolae functions that were previously analyzed in 2D. It includes the short-term disappearance of caveolae from the plasma membrane and the differential response on the JAK/STAT signaling pathway, to the long-term adaptation, which mimics the pattern on EHD2 expression during cancer progression. These data show that the translation from 2D to 3D is complex and needs to take into consideration all the changes in the mechanical and biochemical contexts. By combining transcriptomics with cell biology data, I also found possible links between the mechanical response of caveolae and the release and uptake of exosomes. Further challenges should identify the cellular reaction to mechanical stress in the complex context of a 3D system so as to elucidate the exact role of caveolae in every step when facing these stresses. For instance, the loss of EHD2 after long-term compression could affect the surface tension of the spheroid, and thus making it more or less deformable, promoting thereby the invasion of fragments of the tumor. It would be interesting to monitor the reaction of caveolae when compression leads to EHD2 loss. Overall, this work represents the first attempt to investigate the mechanical function of caveolae with the use of tools that allow to apply mechanical cues in an environment closer to the pathophysiological context, and to analyze the difference with our previous findings obtained in 2D models. Our data open new questions and challenges to further investigate the close relation of caveolae with cancer progression, and understand how the caveolae mechano-signaling response can promote or reduce cancer progression.

In this work, I used two new systems to attempt to reproduce the 3D mechanical environment that cancer cells may experience in vivo. The development of 3D systems for cell biology has been thriving for the last decade and should allow to better understand how mechanics affect cell behavior. We can find in the currently flourishing field of organoids, several powerful tools that are able to mimic precisely

the structural and functional features of tissues with precise details (Lancaster et al., 2014). These new tools allow to investigate micro-scale versions of tissues for their response to mechanical inputs, and to understand the role of changing biophysical parameters in the integrity of the tissue (Bayir et al., 2019). In parallel, organ on a chip approaches have also been developed, relying on precise tuning of physical parameters to mimic the mechanical environment of organ tissues. Examples include the reconstitution of lungs in a dish with air-liquid interphase, constant shear stress and ability to contract (Huh et al., 2010), to the architecture-based reconstitution of gut tissues with peristaltic induced motion, having the ability to permeate nutrients (Kim and Ingber, 2013). These chips increase the physiological and pathological relevance of the reconstructed environments, allowing to mimic almost the exact differentiation and architecture of tissues with highly tunable physical environments (Brassard and Lutolf, 2019). Altogether, the application of the current technologies in parallel with the compressive systems described in this thesis will allow us to further understand the response of cells to physical cues and in particular the role of caveolae.

Figure 20

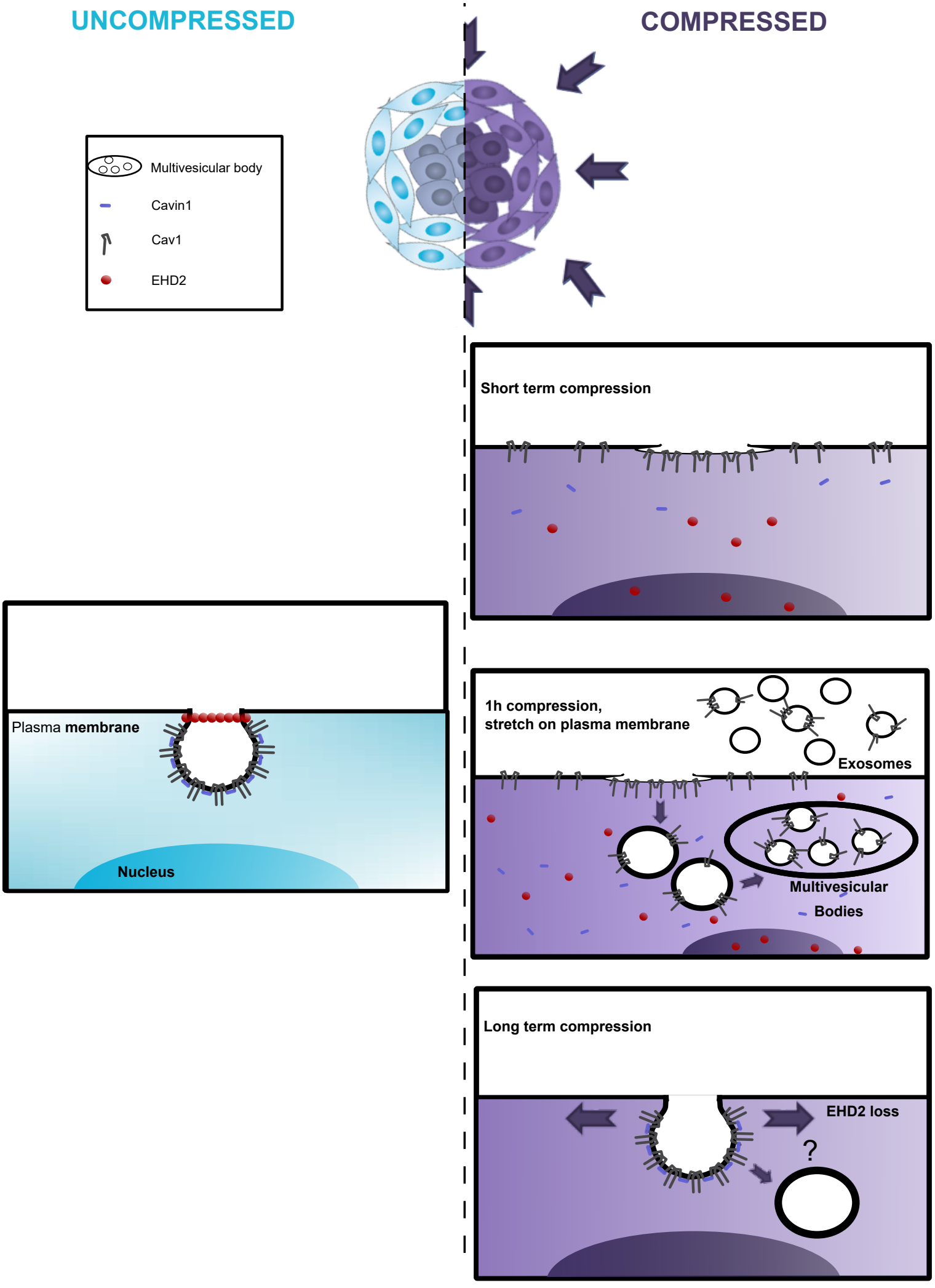
UNCOMPRESSED
COMPRESSED
Multivesicular body
Cavin1
Cav1
EHD2
Short term compression
Plasma membrane
Nucleus
1h compression,
stretch on plasma membrane
Exosomes
Multivesicular
Bodies
Long term compression
EHD2 loss
?

Figure 20. Molecular model of caveolae-mediated cellular adaptation to compressive stresses.

At steady state, when cells are not compressed (left panel), caveolae are invaginated. Cav1 oligomers are assembled with Cavin-1 into a coat covering the budded caveolae which is stabilized at the plasma membrane through the EHD2 ATPase located at the neck of the caveolae invagination. Upon 3D compression (right panel), we can propose 3 possible outcomes. First, as represented on the upper panel, upon short term compression (~5 min) caveolae flatten and release both Cav1 oligomers at the plasma membrane and other cytosolic caveolae components like EHD2 and Cavin-1. EHD2 is then able to freely diffuse in the cytoplasm to translocate to the nucleus and further regulates transcription. Second, in the middle panel, caveolae, upon flattening, would trigger Cav1 oligomers endocytosis and increase Cav1 presence in multivesicular bodies (MVB), promoting the release of Cav1 enriched exosomes. Finally, the lower panel represents the long term adaptation of caveolae with the loss of EHD2 that is likely to change caveolae dynamics at the plasma membrane.

-MATERIALS AND METHODS-

Materials and methods

Encapsulation protocol

Solution preparation.

The outermost phase (alginate) was prepared by dissolving 2.5% w/v sodium alginate (Protanal LF200S; FMC) in water and adding 0.5 mM SDS surfactant (VWR International). The solution was filtered at 1 µm using glass filter (Pall Life Science) and stored at 4 °C. The intermediate phase was prepared with sorbitol (Merck) at 300mM in water.

Cells preparation.

For the encapsulation of cells in alginate hollow spheres, we used cells around 70% of confluency. The innermost phase (cell solution) was obtained by harvesting cells with TrypLE (Stable Trypsin replacement enzyme, Gibco) from the culture flask. After being washed with the complete culture media, cells were spun down (300 g, 3 min, 20°C), and resuspended in 300 mM sorbitol solution at the concentration of 3.10^6 cells per ml.

Capsules preparation.

The three fluid phases (cell suspension, intermediate solution, and alginate) were loaded into syringes (10MDR-LL-GT SGE; Analytical Science) with needles fitted to Teflon tubes (0.5-mm inner diameter; Bohlender). The intermediate solution serves as a diffusion barrier to prevent the mixing and calcium released from the cell solution that could crosslink the alginate. The opposite ends of the tubing were inserted into the appropriate inlets of the co-extrusion device, which is clamped vertically to a post inside a laminar flow hood. The syringes were mounted on syringe pumps (Low Pressure Syringe Pump neMESYS) controlling fluid injection at the desired flow rates. In the current work, we mostly used one set of flow rates Cell solution = 20 $mL \cdot h^{-1}$, Sorbitol solution = 20 $mL \cdot h^{-1}$, and Alginate = 30 $mL \cdot h^{-1}$ to make capsules, typically with an average shell width of 30 µm for a radius between 100-200 µm. Upon jetting a stream with the 3 co-extrusion channels, the compound microdroplets were dropped unto a bath, containing 100 mM calcium chloride (VWR International) and traces of the surfactant Tween 20 (Sigma), placed at approximately at 0.5 m below the outlet of the device. Quick operation for few seconds was sufficient to produce several thousands of capsules, which were

immediately filtered and transferred to the appropriate culture media. After use, the microfluidic device was cleaned with disinfectant (Biocidal ZF; Biovalley) and deionized water. Before next use, the chip was rinsed with sorbitol solution.

Encapsulated cells culture.

Encapsulated multicellular spheroids were grown in incubator (37°C, 5% CO_2) with the same media as normally used for the corresponding cell line.

Electron microscopy.

Epon embedding was used to preserve the integrity of cell structures for electron microscopy (EM). Spheroids were fixed sequentially for 1 h at room temperature with 1.25% glutaraldehyde in 0.1 M Cacodylate and then overnight at 4 °C. Cells were washed extensively with 0.1 M Cacodylate, pH 7.2. Post-fixation was performed for 1 h at room temperature with 1% OsO4 in 0.1 M Cacodylate, pH 7.2. Spheroids were dehydrated through a graded-concentration series of ethanol (50, 70, 90, then 100%, each for 10 min at RT). Embedding was finally performed in LX112 resin. Cells were infiltrated with an increasing ratio of LX112:ethanol solution (1:2, 1:1 and 2:1) and finally with pure LX112. Samples in resin were polymerized overnight at 60°C.

Semithin 500 nm sections were sliced using a Leica UCT ultramicrotome and mounted onto microscopic glass slides and dried on a hot plate. Semithin sections were stained for 30 sec on a hot plate with a mix of Azure B and basic fuchsin in sodium tetraborate (Morikawa et al., 2018). Sections were then mounted in DPX Mountant for microscopy and covered with coverslips. Micrographs were acquired on an Upright Widefield Leica DM6000b Microscope equipped with a color CoolSNAP HQ2 camera.

Ultrathin 65 nm sections were sliced using a Leica UCT ultramicrotome and mounted on nickel formvar/carbon-coated grids for observations. Contrast was obtained by incubation of the sections for 10 min in 4% uranyl acetate followed by 1 min in lead citrate. Electron micrographs were acquired on a Tecnai Spirit electron microscope (FEI, Eindhoven, The Netherlands) equipped with a 4k CCD camera (EMSIS GmbH, Münster, Germany). Caveolae, rosettes and clathrin-coated pits were identified based on their ultrastructural features. The length of plasma membranes observed were measured using ImageJ software and the number of the structures observed was reported to µm of membrane.

RNA Microarray.

RNA was obtained by lysing an average of 100 spheroids per condition and suspended in 700 µl of qiazol lysis reagent (Qiagen). A starting quantity of 100 ng of RNA per sample underwent reverse transcription. SscDNA was purified using magnetic beads and fragmented using UDG. Fragmented samples were hybridized to Affymetrix Clariom S human arrays. Analysis of the data obtained was performed by GenoSplice

Short hairpin RNA mediated silencing.

Small hairpin RNA targeting sequence (AAG ATG TGA TTG CAG AAC CAG) corresponding to nucleotides 206 to 226 of canine Cav1 coding sequence. Annealed oligonucleotides (Cav1-KD-sense: 5'-GAT CCC CGA TGT GAT TGC AGA ACC AGT TCA AGA GAC TGG TTC TGC AAT CAC ATC TTT TTG GAA A-3' ; Cav1-KD antisense: 5'-AGC TTT TCC AAA AAG ATG TGA TTG CAG AAC CAG TCT CTT GAA CTG GTT CTG CAA TCA CAT CGG G-3' ; Sigma Genosys) Obtained from Simons laboratory (Manninen et al., 2005). Viral vectors were harvested on HEK293 and SC were infected two times with a 48 h gap.

Antibodies and reagents.

The following commercially available antibodies were used for Western blotting: mouse monoclonal antibodies against clathrin heavy chain (CHC; BD Biosciences; 610500), EHD2 (Santa Cruz Biotechnology; sc-100724), Cav1 (BD Biosciences; 610059), Cav2 (BD Biosciences; 610085) and Cavin1 (Sigma; AV36965); HRP-conjugated antibodies (Beckman Coulter and Invitrogen) were used as secondary antibodies.

Cell lines.

Hs578T cells were grown at 37 °C under 5% CO_2 in Dulbecco's Modified Eagle Medium (DMEM) GlutaMAX (Gibco, Life Technologies) supplemented with 10% FCS (Gibco, Life Technologies), 5 mM pyruvate (Gibco, Life Technologies), and 1% penicillin-streptomycin (Gibco, Life Technologies).

Hypo-osmotic shock.

Hypo-osmotic shock was performed by diluting growth medium with deionized water

(1:9 dilution for 30-mOsm hypo-osmotic shock).

Lysate preparation and immunoblot.

Cells were lysed with sample buffer containing 2% SDS, 10% glycerol, 4 mM DTT, and Tris, pH 6.8. Lysates were analyzed by SDS-PAGE electrophoresis and immunoblotted with the indicated primary antibodies and HRP-conjugated secondary antibodies. Chemiluminescence signal was revealed using SuperSignal West Dura (Thermo Fisher Scientific Life Technologies). Acquisition and quantification were performed on a ChemiDoc MP Imaging System (Bio-Rad).

Spheroid formation.

Hs578t cell line spheroids were prepared following the classical agarose cushion protocol. First, 50 µl of agarose 1,5% w/v in PBS (ultrapure agarose, Invitrogen) and 50 µl per well were dispensed in 96-well plate and incubate for 10-15 min for polymerization at room temperature. Then, cells were seeded on agarose cushion at 10^5 cells per well. Spheroid formation takes usually between 24 and 48 h.

Application of compressive stress on spheroids (Hyperosmotic induced compression).

To induce compression of agarose multicellular spheroids, we used hyperosmotic stress as described by Cappello's team (Dolega et al., 2017). Shortly, we prepared hyperosmotic media by adding of high molecular weight dextran to reach final concentration of 160 g/ml (2X solution). Here, we used a 2 MDa dextran (Sigma Aldrich, 95771) to avoid the penetration of the polymer in the cellular spheroid. Dextran containing media was added on spheroid at 80 g/ml final concentration. For long-term compression experiments, dextran containing culture medium is renewed after 3 days..

Schwann Cell Primary Culture.

Schwann Cell (SC) primary cultures were obtained from newborn Sprague Dawley (SD) rat sciatic nerves as previously described (Wilby et al., 1999; De Gregorio et al., 2018). Briefly, the perineurium was removed and the nerve was dissociated in 0.05% trypsin/1% collagenase type I solution. Cells were plated on laminin (40 ng/mL; Millipore) treated flasks in DMEM (Invitrogen) supplemented with 10% fetal bovine

serum (FBS, Invitrogen) and 10% penicillin-streptomycin (Invitrogen). The following day, cells were treated with 10 mM cytosine arabinoside (Sigma). After 1 week in culture, contaminant fibroblasts were eliminated by complement-mediated cell lysis using anti-CD90 antibody (Invitrogen) and rabbit complement (Sigma). SC were maintained in DMEM-10%, FBS-1%, penicillin–streptomycin supplemented with 2 µM forskolin (Millipore) and 20 mg/mL bovine pituitary extract (Invitrogen).

Exosome Purification and Analysis.

After treatments with different mechanical stimulations (Hypo osmotic shock or hyperosmotic induced compression) culture supernatant was collected and was subjected to serial centrifugations (2000 g for 10 min, 11,000 g for 30 min at 4°C), followed by ultracentrifugation at 100,000 g for 60 min at 4°C (T865 rotor, OTD Combi Sorvall ultracentrifuge, Dupont). The pellet containing exosomes was washed in cold 0.1 M phosphate buffer saline, pH 7.4 (PBS) and ultracentrifuged again at 100,000 g for 60 min at 4°C. Each exosome preparation was stored at -20°C for later use. For the analysis of exosomes, the pellets were resuspended in 1 mL PBS and the concentration and particle size distribution were analyzed under a Nanosight NS3000 (Malvern).

-BIBLIOGRAPHY-

Aarhus, M., Bruland, O., Sætran, H.A., Mork, S.J., Lund-Johansen, M., Knappskog, P.M., 2010. Global Gene Expression Profiling and Tissue Microarray Reveal Novel Candidate Genes and Down-Regulation of the Tumor Suppressor Gene CAV1 in Sporadic Vestibular Schwannomas. Neurosurgery 67, 998–1019. https://doi.org/10.1227/NEU.0b013e3181ec7b71

Aboulaich, N., Vainonen, J.P., Strålfors, P., Vener, A.V., 2004. Vectorial proteomics reveal targeting, phosphorylation and specific fragmentation of polymerase I and transcript release factor (PTRF) at the surface of caveolae in human adipocytes. Biochem. J. 383, 237–248. https://doi.org/10.1042/BJ20040647

Alessandri, K., Feyeux, M., Gurchenkov, B., Delgado, C., Trushko, A., Krause, K.-H., Vignjević, D., Nassoy, P., Roux, A., 2016. A 3D printed microfluidic device for production of functionalized hydrogel microcapsules for culture and differentiation of human Neuronal Stem Cells (hNSC). Lab. Chip 16, 1593–604. https://doi.org/10.1039/c6lc00133e

Alessandri, Kévin, Sarangi, B.R., Gurchenkov, V.V., Sinha, B., Kie\s sling, T.R., Fetler, L., Rico, F., Scheuring, S., Lamaze, C., Simon, A., Geraldo, S., Vignjevic, D., Doméjean, H., Rolland, L., Funfak, A., Bibette, J., Bremond, N., Nassoy, P., 2013. Cellular capsules as a tool for multicellular spheroid production and for investigating the mechanics of tumor progression in vitro. Proc. Natl. Acad. Sci. U. S. A. 110, 14843–8. https://doi.org/10.1073/pnas.1309482110

Alessandri, K., Sarangi, B.R., Gurchenkov, V.V., Sinha, B., Kiessling, T.R., Fetler, L., Rico, F., Scheuring, S., Lamaze, C., Simon, A., Geraldo, S., Vignjevic, D., Domejean, H., Rolland, L., Funfak, A., Bibette, J., Bremond, N., Nassoy, P., 2013. Cellular capsules as a tool for multicellular spheroid production and for investigating the mechanics of tumor progression in vitro. Proc. Natl. Acad. Sci. 110, 14843–14848. https://doi.org/10.1073/pnas.1309482110

Almeida, C.J. de, Witkiewicz, A.K., Jasmin, J.-F., Tanowitz, H.B., Sotgia, F., Frank, P.G., Lisanti, M.P., 2011. Caveolin-2-deficient mice show increased sensitivity to endotoxemia. Cell Cycle 10, 2151–2161. https://doi.org/10.4161/cc.10.13.16234

Altintas, D.M., Allioli, N., Decaussin, M., de Bernard, S., Ruffion, A., Samarut, J., Vlaeminck-Guillem, V., 2013. Differentially expressed androgen-regulated genes in androgen-sensitive tissues reveal potential biomarkers of early prostate cancer. PloS One 8, e66278. https://doi.org/10.1371/journal.pone.0066278

Anderson, H.A., Chen, Y., Norkin, L.C., 1996. Bound simian virus 40 translocates to caveolin-enriched membrane domains, and its entry is inhibited by drugs that selectively disrupt caveolae. Mol. Biol. Cell 7, 1825–1834. https://doi.org/10.1091/mbc.7.11.1825

Ariotti, N., Fernández-Rojo, M.A., Zhou, Y., Hill, M.M., Rodkey, T.L., Inder, K.L., Tanner, L.B., Wenk, M.R., Hancock, J.F., Parton, R.G., 2014. Caveolae regulate the nanoscale organization of the plasma membrane to remotely control Ras signaling. J. Cell Biol. 204, 777–792. https://doi.org/10.1083/jcb.201307055

Ashburner, M., Ball, C.A., Blake, J.A., Botstein, D., Butler, H., Cherry, J.M., Davis, A.P., Dolinski, K., Dwight, S.S., Eppig, J.T., Harris, M.A., Hill, D.P., Issel-Tarver, L., Kasarskis, A., Lewis, S., Matese, J.C., Richardson, J.E., Ringwald, M., Rubin, G.M., Sherlock, G., 2000. Gene Ontology: tool for the unification of biology. Nat. Genet. 25, 25–29. https://doi.org/10.1038/75556

Baker, B.M., Chen, C.S., 2012. Deconstructing the third dimension – how 3D culture microenvironments alter cellular cues. J. Cell Sci. 125, 3015–3024. https://doi.org/10.1242/jcs.079509

Bang, C., Batkai, S., Dangwal, S., Gupta, S.K., Foinquinos, A., Holzmann, A., Just, A., Remke, J., Zimmer, K., Zeug, A., Ponimaskin, E., Schmiedl, A., Yin, X., Mayr, M., Halder, R., Fischer, A., Engelhardt, S., Wei, Y., Schober, A., Fiedler, J., Thum, T., 2014. Cardiac fibroblast-derived microRNA passenger strand-enriched exosomes mediate cardiomyocyte hypertrophy. J. Clin. Invest. 124, 2136–2146. https://doi.org/10.1172/JCI70577

Bastiani, M., Liu, L., Hill, M.M., Jedrychowski, M.P., Nixon, S.J., Lo, H.P., Abankwa, D., Luetterforst, R., Fernandez-Rojo, M., Breen, M.R., Gygi, S.P., Vinten, J., Walser, P.J., North, K.N., Hancock, J.F., Pilch, P.F., Parton, R.G., 2009. MURC/Cavin-4 and cavin family members form tissue-specific caveolar complexes. J. Cell Biol. 185, 1259–1273. https://doi.org/10.1083/jcb.200903053

Bayir, E., Sendemir, A., Missirlis, Y.F., 2019. Mechanobiology of cells and cell systems, such as organoids. Biophys. Rev. 11, 721–728. https://doi.org/10.1007/s12551-019-00590-7

Beningo, K.A., Dembo, M., Wang, Y., 2004. Responses of fibroblasts to anchorage of dorsal extracellular matrix receptors. Proc. Natl. Acad. Sci. 101, 18024–18029. https://doi.org/10.1073/pnas.0405747102

Biro, M., Maître, J.-L., 2015. Chapter 14 - Dual pipette aspiration: A unique tool for studying intercellular adhesion, in: Paluch, E.K. (Ed.), Methods in Cell Biology, Biophysical Methods in Cell Biology. Academic Press, pp. 255–267. https://doi.org/10.1016/bs.mcb.2014.10.007

Botos, E., Klumperman, J., Oorschot, V., Ígyártó, B., Magyar, A., Oláh, M., Kiss, A.L., 2008. Caveolin-1 is transported to multi-vesicular bodies after albumin-induced endocytosis of caveolae in HepG2 cells. J. Cell. Mol. Med. 12, 1632–1639. https://doi.org/10.1111/j.1582-4934.2007.00167.x

Brassard, J.A., Lutolf, M.P., 2019. Engineering Stem Cell Self-organization to Build Better Organoids. Cell Stem Cell 24, 860–876. https://doi.org/10.1016/j.stem.2019.05.005

Brauchle, E., Kasper, J., Daum, R., Schierbaum, N., Falch, C., Kirschniak, A., Schäffer, T.E., Schenke-Layland, K., 2018. Biomechanical and biomolecular characterization of extracellular matrix structures in human colon carcinomas. Matrix Biol., SI : Fibrosis – Mechanisms and Translational Aspects 68–69, 180–193. https://doi.org/10.1016/j.matbio.2018.03.016

Butcher, D.T., Alliston, T., Weaver, V.M., 2009. A tense situation: forcing tumour progression. Nat. Rev. Cancer 9, 108–22. https://doi.org/10.1038/nrc2544

Campos, A., Salomon, C., Bustos, R., Díaz, J., Martínez, S., Silva, V., Reyes, C., Díaz-Valdivia, N., Varas-Godoy, M., Lobos-González, L., Quest, A.F., 2018. Caveolin-1-containing extracellular vesicles transport adhesion proteins and promote malignancy in breast cancer cell lines. Nanomed. 13, 2597–2609. https://doi.org/10.2217/nnm-2018-0094

Cerchiari, A.E., Garbe, J.C., Jee, N.Y., Todhunter, M.E., Broaders, K.E., Peehl, D.M., Desai, T.A., LaBarge, M.A., Thomson, M., Gartner, Z.J., 2015. A strategy for tissue self-organization that is robust to cellular heterogeneity and plasticity. Proc. Natl. Acad. Sci. 112, 2287–2292. https://doi.org/10.1073/pnas.1410776112

Chen, C.S., Ingber, D.E., 1999. Tensegrity and mechanoregulation: from skeleton to cytoskeleton. Osteoarthritis Cartilage 7, 81–94. https://doi.org/10.1053/joca.1998.0164
Chen, C.S., Mrksich, M., Huang, S., Whitesides, G.M., Ingber, D.E., 1997. Geometric Control of Cell Life and Death. Science 276, 1425–1428. https://doi.org/10.1126/science.276.5317.1425
Chen, T., Guo, J., Yang, M., Zhu, X., Cao, X., 2011. Chemokine-containing exosomes are released from heat-stressed tumor cells via lipid raft-dependent pathway and act as efficient tumor vaccine. J. Immunol. Baltim. Md 1950 186, 2219–2228. https://doi.org/10.4049/jimmunol.1002991
Cheng, J.P.X., Mendoza-Topaz, C., Howard, G., Chadwick, J., Shvets, E., Cowburn, A.S., Dunmore, B.J., Crosby, A., Morrell, N.W., Nichols, B.J., 2015. Caveolae protect endothelial cells from membrane rupture during increased cardiac output. J. Cell Biol. 211, 53–61. https://doi.org/10.1083/jcb.201504042
Collins, B.M., Davis, M.J., Hancock, J.F., Parton, R.G., 2012. Structure-based reassessment of the caveolin signaling model: do caveolae regulate signaling through caveolin-protein interactions? Dev. Cell 23, 11–20. https://doi.org/10.1016/j.devcel.2012.06.012
Coste, B., Mathur, J., Schmidt, M., Earley, T.J., Ranade, S., Petrus, M.J., Dubin, A.E., Patapoutian, A., 2010. Piezo1 and Piezo2 are essential components of distinct mechanically activated cation channels. Science 330, 55–60. https://doi.org/10.1126/science.1193270
Couet, J., Li, S., Okamoto, T., Ikezu, T., Lisanti, M.P., 1997. Identification of peptide and protein ligands for the caveolin-scaffolding domain. Implications for the interaction of caveolin with caveolae-associated proteins. J. Biol. Chem. 272, 6525–33.
Cukierman, E., Pankov, R., Stevens, D.R., Yamada, K.M., 2001. Taking Cell-Matrix Adhesions to the Third Dimension. Science 294, 1708–1712. https://doi.org/10.1126/science.1064829
Cushman, S.W., 1970. Structure-function relationships in the adipose cell. I. Ultrastructure of the isolated adipose cell. J. Cell Biol. 46, 326–341. https://doi.org/10.1083/jcb.46.2.326
Czarny, M., Fiucci, G., Lavie, Y., Banno, Y., Nozawa, Y., Liscovitch, M., 2000. Phospholipase D2: functional interaction with caveolin in low-density membrane microdomains. FEBS Lett. 467, 326–332. https://doi.org/10.1016/s0014-5793(00)01174-1
del Rio, A., Perez-Jimenez, R., Liu, R., Roca-Cusachs, P., Fernandez, J.M., Sheetz, M.P., 2009. Stretching single talin rod molecules activates vinculin binding. Science 323, 638–641. https://doi.org/10.1126/science.1162912
Delarue, M., Montel, F., Vignjevic, D., Prost, J., Joanny, J.-F., Cappello, G., 2014. Compressive stress inhibits proliferation in tumor spheroids through a volume limitation. Biophys. J. 107, 1821–8. https://doi.org/10.1016/j.bpj.2014.08.031
Dent, R., Trudeau, M., Pritchard, K.I., Hanna, W.M., Kahn, H.K., Sawka, C.A., Lickley, L.A., Rawlinson, E., Sun, P., Narod, S.A., 2007. Triple-Negative Breast Cancer: Clinical Features and Patterns of Recurrence. Clin. Cancer Res. 13, 4429–4434. https://doi.org/10.1158/1078-0432.CCR-06-3045
Dewulf, M., Köster, D.V., Sinha, B., Viaris de Lesegno, C., Chambon, V., Bigot, A., Bensalah, M., Negroni, E., Tardif, N., Podkalicka, J., Johannes, L., Nassoy, P., Butler-Browne, G., Lamaze, C., Blouin, C.M., 2019. Dystrophy-associated caveolin-3 mutations reveal that caveolae couple IL6/STAT3 signaling with

mechanosensing in human muscle cells. Nat. Commun. 10, 1974. https://doi.org/10.1038/s41467-019-09405-5
Díaz, J., Mendoza, P., Ortiz, R., Díaz, N., Leyton, L., Stupack, D., Quest, A.F.G., Torres, V.A., 2014. Rab5 is required in metastatic cancer cells for Caveolin-1-enhanced Rac1 activation, migration and invasion. J. Cell Sci. 127, 2401–6. https://doi.org/10.1242/jcs.141689
Dolega, M.E., Delarue, M., Ingremeau, F., Prost, J., Delon, A., Cappello, G., 2017. Cell-like pressure sensors reveal increase of mechanical stress towards the core of multicellular spheroids under compression. Nat. Commun. 8. https://doi.org/10.1038/ncomms14056
Dulhunty, A.F., Franzini-Armstrong, C., 1975. The relative contributions of the folds and caveolae to the surface membrane of frog skeletal muscle fibres at different sarcomere lengths. J. Physiol. 250, 513–539. https://doi.org/10.1113/jphysiol.1975.sp011068
Elosegui-Artola, A., Bazellières, E., Allen, M.D., Andreu, I., Oria, R., Sunyer, R., Gomm, J.J., Marshall, J.F., Jones, J.L., Trepat, X., Roca-Cusachs, P., 2014. Rigidity sensing and adaptation through regulation of integrin types. Nat. Mater. 13, 631–7. https://doi.org/10.1038/nmat3960
Emerman, J.T., Pitelka, D.R., 1977. Maintenance and induction of morphological differentiation in dissociated mammary epithelium on floating collagen membranes. In Vitro 13, 316–328. https://doi.org/10.1007/BF02616178
Engelman, J.A., Wykoff, C.C., Yasuhara, S., Song, K.S., Okamoto, T., Lisanti, M.P., 1997. Recombinant expression of caveolin-1 in oncogenically transformed cells abrogates anchorage-independent growth. J. Biol. Chem. 272, 16374–81.
Engler, A.J., Sen, S., Sweeney, H.L., Discher, D.E., 2006. Matrix elasticity directs stem cell lineage specification. Cell 126, 677–89. https://doi.org/10.1016/j.cell.2006.06.044
Evans, E., Yeung, A., 1989. Apparent viscosity and cortical tension of blood granulocytes determined by micropipet aspiration. Biophys. J. 56, 151–160. https://doi.org/10.1016/S0006-3495(89)82660-8
Fagotto, F., Rohani, N., Touret, A.-S., Li, R., 2013. A molecular base for cell sorting at embryonic boundaries: contact inhibition of cadherin adhesion by ephrin/Eph-dependent contractility. Dev. Cell 27, 72–87. https://doi.org/10.1016/j.devcel.2013.09.004
Fan, F., Zhao, J., Liu, Y., Zhao, H., Weng, L., Li, Q., Chen, G., Xu, Y., 2018. Identifying the SUMO1 modification of FAM122A leading to the degradation of PP2A-Cα by ubiquitin-proteasome system. Biochem. Biophys. Res. Commun. 500, 676–681. https://doi.org/10.1016/j.bbrc.2018.04.135
Fecchi, K., Volonte, D., Hezel, M.P., Schmeck, K., Galbiati, F., 2006. Spatial and temporal regulation of GLUT4 translocation by flotillin-1 and caveolin-3 in skeletal muscle cells. FASEB J. Off. Publ. Fed. Am. Soc. Exp. Biol. 20, 705–707. https://doi.org/10.1096/fj.05-4661fje
Fernández-Sánchez, M.E., Barbier, S., Whitehead, J., Béalle, G., Michel, A., Latorre-Ossa, H., Rey, C., Fouassier, L., Claperon, A., Brullé, L., Girard, E., Servant, N., Rio-Frio, T., Marie, H., Lesieur, S., Housset, C., Gennisson, J.-L., Tanter, M., Ménager, C., Fre, S., Robine, S., Farge, E., 2015. Mechanical induction of the tumorigenic β-catenin pathway by tumour growth pressure. Nature 523, 92–95. https://doi.org/10.1038/nature14329

Fiucci, G., Ravid, D., Reich, R., Liscovitch, M., 2002. Caveolin-1 inhibits anchorage-independent growth, anoikis and invasiveness in MCF-7 human breast cancer cells. Oncogene 21, 2365–75. https://doi.org/10.1038/sj.onc.1205300

Follain, G., Osmani, N., Azevedo, A.S., Allio, G., Mercier, L., Karreman, M.A., Solecki, G., Garcia Leòn, M.J., Lefebvre, O., Fekonja, N., Hille, C., Chabannes, V., Dollé, G., Metivet, T., Hovsepian, F.D., Prudhomme, C., Pichot, A., Paul, N., Carapito, R., Bahram, S., Ruthensteiner, B., Kemmling, A., Siemonsen, S., Schneider, T., Fiehler, J., Glatzel, M., Winkler, F., Schwab, Y., Pantel, K., Harlepp, S., Goetz, J.G., 2018. Hemodynamic Forces Tune the Arrest, Adhesion, and Extravasation of Circulating Tumor Cells. Dev. Cell 45, 33-52.e12. https://doi.org/10.1016/j.devcel.2018.02.015

Foty, null, Forgacs, null, Pfleger, null, Steinberg, null, 1994. Liquid properties of embryonic tissues: Measurement of interfacial tensions. Phys. Rev. Lett. 72, 2298–2301. https://doi.org/10.1103/PhysRevLett.72.2298

Foty, R.A., Steinberg, M.S., 2005. The differential adhesion hypothesis: a direct evaluation. Dev. Biol. 278, 255–263. https://doi.org/10.1016/j.ydbio.2004.11.012

Fujimoto, T., 1993. Calcium pump of the plasma membrane is localized in caveolae. J. Cell Biol. 120, 1147–1157. https://doi.org/10.1083/jcb.120.5.1147

Galbiati, F., Volonte, D., Engelman, J.A., Watanabe, G., Burk, R., Pestell, R.G., Lisanti, M.P., 1998. Targeted downregulation of caveolin-1 is sufficient to drive cell transformation and hyperactivate the p42/44 MAP kinase cascade. EMBO J. 17, 6633–6648. https://doi.org/10.1093/emboj/17.22.6633

Gambin, Y., Ariotti, N., McMahon, K.-A., Bastiani, M., Sierecki, E., Kovtun, O., Polinkovsky, M.E., Magenau, A., Jung, W., Okano, S., Zhou, Y., Leneva, N., Mureev, S., Johnston, W., Gaus, K., Hancock, J.F., Collins, B.M., Alexandrov, K., Parton, R.G., 2013. Single-molecule analysis reveals self assembly and nanoscale segregation of two distinct cavin subcomplexes on caveolae. eLife 3, e01434. https://doi.org/10.7554/eLife.01434

Garcia, J., Bagwell, J., Njaine, B., Norman, J., Levic, D.S., Wopat, S., Miller, S.E., Liu, X., Locasale, J.W., Stainier, D.Y.R., Bagnat, M., 2017. Sheath Cell Invasion and Trans-differentiation Repair Mechanical Damage Caused by Loss of Caveolae in the Zebrafish Notochord. Curr. Biol. CB 27, 1982–1989.e3. https://doi.org/10.1016/j.cub.2017.05.035

García-Cardeña, G., Martasek, P., Masters, B.S., Skidd, P.M., Couet, J., Li, S., Lisanti, M.P., Sessa, W.C., 1997. Dissecting the interaction between nitric oxide synthase (NOS) and caveolin. Functional significance of the nos caveolin binding domain in vivo. J. Biol. Chem. 272, 25437–25440. https://doi.org/10.1074/jbc.272.41.25437

Gervásio, O.L., Phillips, W.D., Cole, L., Allen, D.G., 2011. Caveolae respond to cell stretch and contribute to stretch-induced signaling. J. Cell Sci. 124, 3581–90. https://doi.org/10.1242/jcs.084376

Goetz, J.G., Joshi, B., Lajoie, P., Strugnell, S.S., Scudamore, T., Kojic, L.D., Nabi, I.R., 2008. Concerted regulation of focal adhesion dynamics by galectin-3 and tyrosine-phosphorylated caveolin-1. J. Cell Biol. 180, 1261–75. https://doi.org/10.1083/jcb.200709019

Goetz, J.G., Minguet, S., Navarro-Lérida, I., Lazcano, J.J., Samaniego, R., Calvo, E., Tello, M., Osteso-Ibáñez, T., Pellinen, T., Echarri, A., Cerezo, A., Klein-Szanto, A.J.P., Garcia, R., Keely, P.J., Sánchez-Mateos, P., Cukierman, E., Del Pozo, M.A., 2011. Biomechanical Remodeling of the Microenvironment by

Stromal Caveolin-1 Favors Tumor Invasion and Metastasis. Cell 146, 148–163. https://doi.org/10.1016/j.cell.2011.05.040
Gould, M.L., Williams, G., Nicholson, H.D., 2010. Changes in caveolae, caveolin, and polymerase 1 and transcript release factor (PTRF) expression in prostate cancer progression. The Prostate 70, 1609–1621. https://doi.org/10.1002/pros.21195
Gratton, J.P., Fontana, J., O'Connor, D.S., Garcia-Cardena, G., McCabe, T.J., Sessa, W.C., 2000. Reconstitution of an endothelial nitric-oxide synthase (eNOS), hsp90, and caveolin-1 complex in vitro. Evidence that hsp90 facilitates calmodulin stimulated displacement of eNOS from caveolin-1. J. Biol. Chem. 275, 22268–22272. https://doi.org/10.1074/jbc.M001644200
Griffith, L.G., Swartz, M.A., 2006. Capturing complex 3D tissue physiology in vitro. Nat. Rev. Mol. Cell Biol. 7, 211. https://doi.org/10.1038/nrm1858
Grimshaw, M.J., Cooper, L., Papazisis, K., Coleman, J.A., Bohnenkamp, H.R., Chiapero-Stanke, L., Taylor-Papadimitriou, J., Burchell, J.M., 2008. Mammosphere culture of metastatic breast cancer cells enriches for tumorigenic breast cancer cells. Breast Cancer Res. 10, R52. https://doi.org/10.1186/bcr2106
Guillaume, L., Rigal, L., Fehrenbach, J., Severac, C., Ducommun, B., Lobjois, V., 2019. Characterization of the physical properties of tumor-derived spheroids reveals critical insights for pre-clinical studies. Sci. Rep. 9, 6597. https://doi.org/10.1038/s41598-019-43090-0
Guo, Y., Golebiewska, U., Scarlata, S., 2011. Modulation of Ca^2+ activity in cardiomyocytes through caveolae-Gαq interactions. Biophys. J. 100, 1599–1607. https://doi.org/10.1016/j.bpj.2011.02.013
Guo, Y., Yang, L., Haught, K., Scarlata, S., 2015. Osmotic Stress Reduces Ca2+ Signals through Deformation of Caveolae. J. Biol. Chem. 290, 16698–16707. https://doi.org/10.1074/jbc.M115.655126
Hansen, C.G., Bright, N.A., Howard, G., Nichols, B.J., 2009. SDPR induces membrane curvature and functions in the formation of caveolae. Nat. Cell Biol. 11, 807–814. https://doi.org/10.1038/ncb1887
Hansen, C.G., Howard, G., Nichols, B.J., 2011. Pacsin 2 is recruited to caveolae and functions in caveolar biogenesis. J. Cell Sci. 124, 2777–2785. https://doi.org/10.1242/jcs.084319
Harris, A., Wild, P., Stopak, D., 1980. Silicone rubber substrata: a new wrinkle in the study of cell locomotion. Science 208, 177–179. https://doi.org/10.1126/science.6987736
Hayer, A., Stoeber, M., Bissig, C., Helenius, A., 2010a. Biogenesis of Caveolae: Stepwise Assembly of Large Caveolin and Cavin Complexes [WWW Document]. Traffic. https://doi.org/10.1111/j.1600-0854.2009.01023.x
Hayer, A., Stoeber, M., Ritz, D., Engel, S., Meyer, H.H., Helenius, A., 2010b. Caveolin-1 is ubiquitinated and targeted to intralumenal vesicles in endolysosomes for degradation. J. Cell Biol. 191, 615–629. https://doi.org/10.1083/jcb.201003086
Helmlinger, G., Netti, P.A., Lichtenbeld, H.C., Melder, R.J., Jain, R.K., 1997. Solid stress inhibits the growth of multicellular tumor spheroids. Nat. Biotechnol. 15, 778–783. https://doi.org/10.1038/nbt0897-778
Heo, S.-J., Nerurkar, N.L., Baker, B.M., Shin, J.-W., Elliott, D.M., Mauck, R.L., 2011. Fiber Stretch and Reorientation Modulates Mesenchymal Stem Cell Morphology and Fibrous Gene Expression on Oriented Nanofibrous

Microenvironments. Ann. Biomed. Eng. 39, 2780. https://doi.org/10.1007/s10439-011-0365-7
Hessvik, N.P., Llorente, A., 2018. Current knowledge on exosome biogenesis and release. Cell. Mol. Life Sci. 75, 193–208. https://doi.org/10.1007/s00018-017-2595-9
Hill, M.M., Bastiani, M., Luetterforst, R., Kirkham, M., Kirkham, A., Nixon, S.J., Walser, P., Abankwa, D., Oorschot, V.M.J., Martin, S., Hancock, J.F., Parton, R.G., 2008. PTRF-Cavin, a Conserved Cytoplasmic Protein Required for Caveola Formation and Function. Cell 132, 113–124. https://doi.org/10.1016/j.cell.2007.11.042
Hirama, T., Das, R., Yang, Y., Ferguson, C., Won, A., Yip, C.M., Kay, J.G., Grinstein, S., Parton, R.G., Fairn, G.D., 2017. Phosphatidylserine dictates the assembly and dynamics of caveolae in the plasma membrane. J. Biol. Chem. 292, 14292–14307. https://doi.org/10.1074/jbc.M117.791400
Hirschhaeuser, F., Menne, H., Dittfeld, C., West, J., Mueller-Klieser, W., Kunz-Schughart, L.A., 2010. Multicellular tumor spheroids: An underestimated tool is catching up again. J. Biotechnol., Organotypic Tissue Culture for Substance Testing 148, 3–15. https://doi.org/10.1016/j.jbiotec.2010.01.012
Huebsch, N., Arany, P.R., Mao, A.S., Shvartsman, D., Ali, O.A., Bencherif, S.A., Rivera-Feliciano, J., Mooney, D.J., 2010. Harnessing traction-mediated manipulation of the cell/matrix interface to control stem-cell fate. Nat. Mater. 9, 518–526. https://doi.org/10.1038/nmat2732
Huh, D., Matthews, B.D., Mammoto, A., Montoya-Zavala, M., Hsin, H.Y., Ingber, D.E., 2010. Reconstituting organ-level lung functions on a chip. Science 328, 1662–8. https://doi.org/10.1126/science.1188302
Inder, K.L., Zheng, Y.Z., Davis, M.J., Moon, H., Loo, D., Nguyen, H., Clements, J.A., Parton, R.G., Foster, L.J., Hill, M.M., 2012. Expression of PTRF in PC-3 Cells modulates cholesterol dynamics and the actin cytoskeleton impacting secretion pathways. Mol. Cell. Proteomics MCP 11, M111.012245. https://doi.org/10.1074/mcp.M111.012245
Ingber, D.E., Wang, N., Stamenovic, D., 2014. Tensegrity, cellular biophysics, and the mechanics of living systems. Rep. Prog. Phys. Phys. Soc. G. B. 77, 046603. https://doi.org/10.1088/0034-4885/77/4/046603
Iskratsch, T., Wolfenson, H., Sheetz, M.P., 2014. Appreciating force and shape — the rise of mechanotransduction in cell biology. Nat. Rev. Mol. Cell Biol. 15, 825–833. https://doi.org/10.1038/nrm3903
Izumi, Y., Hirai, S. i, Tamai, Y., Fujise-Matsuoka, A., Nishimura, Y., Ohno, S., 1997. A protein kinase Cdelta-binding protein SRBC whose expression is induced by serum starvation. J. Biol. Chem. 272, 7381–7389. https://doi.org/10.1074/jbc.272.11.7381
Jain, R.K., Martin, J.D., Stylianopoulos, T., 2014. The role of mechanical forces in tumor growth and therapy. Annu. Rev. Biomed. Eng. 16, 321–346. https://doi.org/10.1146/annurev-bioeng-071813-105259
Joshi, B., Strugnell, S.S., Goetz, J.G., Kojic, L.D., Cox, M.E., Griffith, O.L., Chan, S.K., Jones, S.J., Leung, S.-P., Masoudi, H., Leung, S., Wiseman, S.M., Nabi, I.R., 2008. Phosphorylated caveolin-1 regulates Rho/ROCK-dependent focal adhesion dynamics and tumor cell migration and invasion. Cancer Res. 68, 8210–8220. https://doi.org/10.1158/0008-5472.CAN-08-0343
Joyce, M.H., Lu, C., James, E.R., Hegab, R., Allen, S.C., Suggs, L.J., Brock, A., 2018. Phenotypic Basis for Matrix Stiffness-Dependent Chemoresistance of

Breast Cancer Cells to Doxorubicin. Front. Oncol. 8. https://doi.org/10.3389/fonc.2018.00337
Ju, H., Zou, R., Venema, V.J., Venema, R.C., 1997. Direct interaction of endothelial nitric-oxide synthase and caveolin-1 inhibits synthase activity. J. Biol. Chem. 272, 18522–18525. https://doi.org/10.1074/jbc.272.30.18522
Jung, W., Sierecki, E., Bastiani, M., O'Carroll, A., Alexandrov, K., Rae, J., Johnston, W., Hunter, D.J.B., Ferguson, C., Gambin, Y., Ariotti, N., Parton, R.G., 2018. Cell-free formation and interactome analysis of caveolae. J. Cell Biol. 217, 2141–2165. https://doi.org/10.1083/jcb.201707004
Kai, F., Laklai, H., Weaver, V.M., 2016. Force Matters: Biomechanical Regulation of Cell Invasion and Migration in Disease. Trends Cell Biol., Special Issue: 25 Years of Trends in Cell Biology 26, 486–497. https://doi.org/10.1016/j.tcb.2016.03.007
Kechagia, J.Z., Ivaska, J., Roca-Cusachs, P., 2019. Integrins as biomechanical sensors of the microenvironment. Nat. Rev. Mol. Cell Biol. https://doi.org/10.1038/s41580-019-0134-2
Khetan, S., Burdick, J.A., 2010. Patterning network structure to spatially control cellular remodeling and stem cell fate within 3-dimensional hydrogels. Biomaterials 31, 8228–8234. https://doi.org/10.1016/j.biomaterials.2010.07.035
Kim, H.J., Ingber, D.E., 2013. Gut-on-a-Chip microenvironment induces human intestinal cells to undergo villus differentiation. Integr. Biol. Quant. Biosci. Nano Macro 5, 1130–1140. https://doi.org/10.1039/c3ib40126j
Kim, Y., Kim, M.-H., Jeon, S., Kim, J., Kim, C., Bae, J.S., Jung, C.K., 2017. Prognostic implication of histological features associated with EHD2 expression in papillary thyroid carcinoma. PloS One 12, e0174737. https://doi.org/10.1371/journal.pone.0174737
Kovtun, O., Tillu, V.A., Ariotti, N., Parton, R.G., Collins, B.M., 2015. Cavin family proteins and the assembly of caveolae. J. Cell Sci. 128, 1269–1278. https://doi.org/10.1242/jcs.167866
Kovtun, O., Tillu, V.A., Jung, W., Leneva, N., Ariotti, N., Chaudhary, N., Mandyam, R.A., Ferguson, C., Morgan, G.P., Johnston, W.A., Harrop, S.J., Alexandrov, K., Parton, R.G., Collins, B.M., 2014. Structural insights into the organization of the cavin membrane coat complex. Dev. Cell 31, 405–19. https://doi.org/10.1016/j.devcel.2014.10.002
Krieg, M., Arboleda-Estudillo, Y., Puech, P.-H., Käfer, J., Graner, F., Müller, D.J., Heisenberg, C.-P., 2008. Tensile forces govern germ-layer organization in zebrafish. Nat. Cell Biol. 10, 429–436. https://doi.org/10.1038/ncb1705
Kumar, S., Weaver, V.M., 2009. Mechanics, malignancy, and metastasis: The force journey of a tumor cell. Cancer Metastasis Rev. 28, 113–127. https://doi.org/10.1007/s10555-008-9173-4
Kurpinski, K., Chu, J., Hashi, C., Li, S., 2006. Anisotropic mechanosensing by mesenchymal stem cells. Proc. Natl. Acad. Sci. 103, 16095–16100. https://doi.org/10.1073/pnas.0604182103
Kurzchalia, T.V., Dupree, P., Parton, R.G., Kellner, R., Virta, H., Lehnert, M., Simons, K., 1992. VIP21, a 21-kD membrane protein is an integral component of trans-Golgi-network-derived transport vesicles. J. Cell Biol. 118, 1003–1014. https://doi.org/10.1083/jcb.118.5.1003
Lai, C.P., Kim, E.Y., Badr, C.E., Weissleder, R., Mempel, T.R., Tannous, B.A., Breakefield, X.O., 2015. Visualization and tracking of tumour extracellular

vesicle delivery and RNA translation using multiplexed reporters. Nat. Commun. 6, 1–12. https://doi.org/10.1038/ncomms8029
Lamaze, C., Tardif, N., Dewulf, M., Vassilopoulos, S., Blouin, C.M., 2017. The caveolae dress code: structure and signaling. Curr. Opin. Cell Biol. 47, 117–125. https://doi.org/10.1016/j.ceb.2017.02.014
Lamaze, C., Torrino, S., 2015a. Caveolae and cancer: A new mechanical perspective. Biomed. J. 38, 367. https://doi.org/10.4103/2319-4170.164229
Lamaze, C., Torrino, S., 2015b. Caveolae and cancer: A new mechanical perspective. Biomed. J. 38, 367–379. https://doi.org/10.4103/2319-4170.164229
Lancaster, Madeline A, Knoblich, Juergen A, Hachitanda, Y., Tsuneyoshi, M., Zimmermann, B., Xinaris, C., Benedetti, V., Rizzo, P., Abbate, M., Corna, D., Azzollini, N., Conti, S., Unbekandt, M., Davies, J.A., Morigi, M., Benigni, A., Remuzzi, G., Armstrong, P.B., Dahmann, C., Oates, A.C., Brand, M., Kiecker, C., Lumsden, A., Weiss, P., Taylor, A.C., Moscona, A., Foty, R.A., Pfleger, C.M., Forgacs, G., Steinberg, M.S., Fujimori, T., Miyatani, S., Takeichi, M., Detrick, R.J., Dickey, D., Kintner, C.R., Agathocleous, M., Harris, W.A., Žigman, M., Cayouette, M., Charalambous, C., Schleiffer, A., Hoeller, O., Dunican, D., McCudden, C.R., Firnberg, N., Barres, B.A., Siderovski, D.P., Knoblich, J. A., Layer, P.G., Robitzki, A., Rothermel, A., Willbold, E., Vollmer, G., Layer, P.G., Rothermel, A., Willbold, E., Degrip, W.J., Layer, P.G., Sergi, C., Ehemann, V., Beedgen, B., Linderkamp, O., Otto, H.F., Kuno, N., Kadomatsu, K., Nakamura, M., Miwa-Fukuchi, T., Hirabayashi, N., Ishizuka, T., Evans, M., Weitzer, G., Montesano, R., Schaller, G., Orci, L., Hagios, C., Lochter, A., Bissell, M.J., Li, M.L., Aggeler, J., Farson, D.A., Hatier, C., Hassell, J., Bissell, M.J., Lancaster, M. A., Renner, M., Martin, C.A., Wenzel, D., Bicknell, L.S., Hurles, M.E., Homfray, T., Penninger, J.M., Jackson, A.P., Knoblich, J. A., Taguchi, A., Kaku, Y., Ohmori, T., Sharmin, S., Ogawa, M., Sasaki, H., Nishinakamura, R., Heath, J.K., Dessimoz, J., Opoka, R., Kordich, J.J., Grapin-Botton, A., Wells, J.M., McLin, V.A., Rankin, S.A., Zorn, A.M., Spence, J.R., Mayhew, C.N., Rankin, S.A., Kuhar, M.F., Vallance, J.E., Tolle, K., Hoskins, E.E., Kalinichenko, V.V., Wells, S.I., Zorn, A.M., Shroyer, N.F., Wells, J.M., Sato, T., Vries, R.G., Snippert, H.J., van de Wetering, M., Barker, N., Stange, D.E., van Es, J.H., Abo, A., Kujala, P., Peters, P.J., Clevers, H., Yui, S., Nakamura, T., Sato, T., Nemoto, Y., Mizutani, T., Zheng, X., Ichinose, S., Nagaishi, T., Okamoto, R., Tsuchiya, K., Clevers, H., Watanabe, M., Barker, N., Huch, M., Kujala, P., van de Wetering, M., Snippert, H.J., van Es, J.H., Sato, T., Stange, D.E., Begthel, H., van den Born, M., Danenberg, E., van den Brink, S., Korving, J., Abo, A., Peters, P.J., Wright, N., Poulsom, R., Clevers, H., Stange, D.E., Koo, B.K., Huch, M., Sibbel, G., Basak, O., Lyubimova, A., Kujala, P., Bartfeld, S., Koster, J., Geahlen, J.H., Peters, P.J., van Es, J.H., van de Wetering, M., Mills, J.C., Clevers, H., Hisha, H., Tanaka, T., Kanno, S., Tokuyama, Y., Komai, Y., Ohe, S., Yanai, H., Omachi, T., Ueno, H., Zaret, K.S., Huch, M., Dorrell, C., Boj, S.F., van Es, J.H., Li, V.S., van de Wetering, M., Sato, T., Hamer, K., Sasaki, N., Finegold, M.J., Haft, A., Vries, R.G., Grompe, M., Clevers, H., Takebe, T., Sekine, K., Enomura, M., Koike, H., Kimura, M., Ogaeri, T., Zhang, R.R., Ueno, Y., Zheng, Y.W., Koike, N., Aoyama, S., Adachi, Y., Taniguchi, H., Petros, T.J., Tyson, J.A., Anderson, S.A., Lehtinen, M.K., Walsh, C.A., Lancaster, M. A., Knoblich, J. A., Ishii, K., Conti, L., Cattaneo, E., Reynolds, B.A., Weiss, S., Elkabetz, Y., Panagiotakos,

G., Shamy, G.A., Socci, N.D., Tabar, V., Studer, L., Zhang, S.C., Wernig, M., Duncan, I.D., Brüstle, O., Thomson, J.A., Gaspard, N., Bouschet, T., Hourez, R., Dimidschstein, J., Naeije, G., van den Ameele, J., Espuny-Camacho, I., Herpoel, A., Passante, L., Schiffmann, S.N., Gaillard, A., Vanderhaeghen, P., Cyranoski, D., Watanabe, K., Kamiya, D., Nishiyama, A., Katayama, T., Nozaki, S., Kawasaki, H., Watanabe, Y., Mizuseki, K., Sasai, Y., Watanabe, K., Ueno, M., Kamiya, D., Nishiyama, A., Matsumura, M., Wataya, T., Takahashi, J.B., Nishikawa, S., Nishikawa, S., Muguruma, K., Sasai, Y., Eiraku, M., Watanabe, K., Matsuo-Takasaki, M., Kawada, M., Yonemura, S., Matsumura, M., Wataya, T., Nishiyama, A., Muguruma, K., Sasai, Y., Kadoshima, T., Sakaguchi, H., Nakano, T., Soen, M., Ando, S., Eiraku, M., Sasai, Y., Danjo, T., Eiraku, M., Muguruma, K., Watanabe, K., Kawada, M., Yanagawa, Y., Rubenstein, J.L., Sasai, Y., Su, H.-L., Muguruma, K., Matsuo-Takasaki, M., Kengaku, M., Watanabe, K., Sasai, Y., Muguruma, K., Nishiyama, A., Ono, Y., Miyawaki, H., Mizuhara, E., Hori, S., Kakizuka, A., Obata, K., Yanagawa, Y., Hirano, T., Sasai, Y., Wataya, T., Ando, S., Muguruma, K., Ikeda, H., Watanabe, K., Eiraku, M., Kawada, M., Takahashi, J., Hashimoto, N., Sasai, Y., Heavner, W., Pevny, L., Stefanelli, A., Zacchei, A.M., Ceccherini, V., Moscona, A.A., Nakagawa, S., Takada, S., Takada, R., Takeichi, M., Eiraku, M., Takata, N., Ishibashi, H., Kawada, M., Sakakura, E., Okuda, S., Sekiguchi, K., Adachi, T., Sasai, Y., Nakano, T., Ando, S., Takata, N., Kawada, M., Muguruma, K., Sekiguchi, K., Saito, K., Yonemura, S., Eiraku, M., Sasai, Y., Little, M.H., McMahon, A.P., Humphreys, B.D., Xia, Y., Nivet, E., Sancho-Martinez, I., Gallegos, T., Suzuki, K., Okamura, D., Wu, M.Z., Dubova, I., Esteban, C.R., Montserrat, N., Campistol, J.M., Belmonte, J.C.I., Takasato, M., Er, P.X., Becroft, M., Vanslambrouck, J.M., Stanley, E.G., Elefanty, A.G., Little, M.H., Antonica, F., Kasprzyk, D.F., Opitz, R., Iacovino, M., Liao, X.H., Dumitrescu, A.M., Refetoff, S., Peremans, K., Manto, M., Kyba, M., Costagliola, S., Lee, J.-H., Bhang, D.H., Beede, A., Huang, T.L., Stripp, B.R., Bloch, K.D., Wagers, A.J., Tseng, Y.H., Ryeom, S., Kim, C.F., Greggio, C., Franceschi, F.D., Figueiredo-Larsen, M., Gobaa, S., Ranga, A., Semb, H., Lutolf, M., Grapin-Botton, A., Suga, H., Kadoshima, T., Minaguchi, M., Ohgushi, M., Soen, M., Nakano, T., Takata, N., Wataya, T., Muguruma, K., Miyoshi, H., Yonemura, S., Oiso, Y., Sasai, Y., Koehler, K.R., Mikosz, A.M., Molosh, A.I., Patel, D., Hashino, E., Konigsberg, I.R., Moscona, A., Moscona, H., Lévy, E., Delvin, E., Ménard, D., Beaulieu, J.-F., Sato, T., van Es, J.H., Snippert, H.J., Stange, D.E., Vries, R.G., van den Born, M., Barker, N., Shroyer, N.F., van de Wetering, M., Clevers, H., Durand, A., Donahue, B., Peignon, G., Letourneur, F., Cagnard, N., Slomianny, C., Perret, C., Shroyer, N.F., Romagnolo, B., Finkbeiner, S.R., Zeng, X.L., Utama, B., Atmar, R.L., Shroyer, N.F., Estes, M.K., Castellanos-Gonzalez, A., Cabada, M.M., Nichols, J., Gomez, G., White, A.C., Yeung, T.M., Gandhi, S.C., Wilding, J.L., Muschel, R., Bodmer, W.F., Onuma, K., Ochiai, M., Orihashi, K., Takahashi, M., Imai, T., Nakagama, H., Hippo, Y., Bigorgne, A.E., Farin, H.F., Lemoine, R., Mahlaoui, N., Lambert, N., Gil, M., Schulz, A., Philippet, P., Schlesser, P., Abrahamsen, T.G., Oymar, K., Davies, E.G., Ellingsen, C.L., Leteurtre, E., Moreau-Massart, B., Berrebi, D., Bole-Feysot, C., Nischke, P., Brousse, N., Fischer, A., Clevers, H., Basile, G. de S., Dekkers, J.F., Wiegerinck, C.L., de Jonge, H.R., Bronsveld, I., Janssens, H.M., Groot, K.M. de W., Brandsma, A.M., de Jong, N.W., Bijvelds, M.J., Scholte, B.J., Nieuwenhuis, E.E., van den

Brink, S., Clevers, H., van der Ent, C.K., Middendorp, S., Beekman, J.M., Luni, C., Serena, E., Elvassore, N., Ramsden, C.M., Powner, M.B., Carr, A.J., Smart, M.J., da Cruz, L., Coffey, P.J., Fordham, R.P., Yui, S., Hannan, N.R., Soendergaard, C., Madgwick, A., Schweiger, P.J., Nielsen, O.H., Vallier, L., Pedersen, R.A., Nakamura, T., Watanabe, M., Jensen, K.B., Hilfer, S.R., Iszard, L.B., Hilfer, E.K., Mallette, J.M., Anthony, A., Longmire, T.A., Ikonomou, L., Hawkins, F., Christodoulou, C., Cao, Y., Jean, J.C., Kwok, L.W., Mou, H., Rajagopal, J., Shen, S.S., Dowton, A.A., Serra, M., Weiss, D.J., Green, M.D., Snoeck, H.W., Ramirez, M.I., Kotton, D.N., Grover, J.W., Mou, H., Zhao, R., Sherwood, R., Ahfeldt, T., Lapey, A., Wain, J., Sicilian, L., Izvolsky, K., Lau, F.H., Musunuru, K., Cowan, C., Rajagopal, J., Bernfield, M.R., Fell, P.E., Lumelsky, N., Blondel, O., Laeng, P., Velasco, I., Ravin, R., McKay, R., D'Amour, K.A., Bang, A.G., Eliazer, S., Kelly, O.G., Agulnick, A.D., Smart, N.G., Moorman, M.A., Kroon, E., Carpenter, M.K., Baetge, E.E., Shirahashi, H., Wu, J., Yamamoto, N., Catana, A., Wege, H., Wager, B., Okita, K., Zern, M.A., Urase, K., Yasugi, S., Montgomery, R.K., Zinman, H.M., Smith, B.T., Cao, L., Gibson, J.D., Miyamoto, S., Sail, V., Verma, R., Rosenberg, D.W., Nelson, C.E., Giardina, C., Halbert, S.P., Bruderer, R., Lin, T.M., Boheler, K.R., Czyz, J., Tweedie, D., Yang, H.T., Anisimov, S.V., Wobus, A.M., Stevens, K.R., Kreutziger, K.L., Dupras, S.K., Korte, F.S., Regnier, M., Muskheli, V., Nourse, M.B., Bendixen, K., Reinecke, H., Murry, C.E., Tedesco, F.S., Gerli, M.F., Perani, L., Benedetti, S., Ungaro, F., Cassano, M., Antonini, S., Tagliafico, E., Artusi, V., Longa, E., Tonlorenzi, R., Ragazzi, M., Calderazzi, G., Hoshiya, H., Cappellari, O., Mora, M., Schoser, B., Schneiderat, P., Oshimura, M., Bottinelli, R., Sampaolesi, M., Torrente, Y., Broccoli, V., Cossu, G., van der Schaft, D.W.J., van Spreeuwel, A.C., Boonen, K.J., Langelaan, M.L., Bouten, C.V., Baaijens, F.P., Buttery, L.D., Bourne, S., Xynos, J.D., Wood, H., Hughes, F.J., Hughes, S.P., Episkopou, V., Polak, J.M., Bielby, R.C., Boccaccini, A.R., Polak, J.M., Buttery, L.D.K., Kale, S., Biermann, S., Edwards, C., Tarnowski, C., Morris, M., Long, M.W., Nishikawa, M., Yanagawa, N., Kojima, N., Yuri, S., Hauser, P.V., Jo, O.D., Yanagawa, N., Mae, S., Shono, A., Shiota, F., Yasuno, T., Kajiwara, M., Gotoda-Nishimura, N., Arai, S., Sato-Otubo, A., Toyoda, T., Takahashi, K., Nakayama, N., Cowan, C.A., Aoi, T., Ogawa, S., McMahon, A.P., Yamanaka, S., Osafune, K., Ikeda, H., Osakada, F., Watanabe, K., Mizuseki, K., Haraguchi, T., Miyoshi, H., Kamiya, D., Honda, Y., Sasai, N., Yoshimura, N., Takahashi, M., Sasai, Y., Lamba, D.A., Karl, M.O., Ware, C.B., Reh, T.A., Sobel, H., Lee, G.Y., Kenny, P.A., Lee, E.H., Bissell, M.J., Orr, M.F., Li, H., Roblin, G., Liu, H., Heller, S., Coraux, C., Hilmi, C., Rouleau, M., Spadafora, A., Hinnrasky, J., Ortonne, J.P., Dani, C., Aberdam, D., Wilson, H.V., Holtfreter, J., Pierce, G.B., Verney, E.L., Evans, M., Martin, G.R., Shannon, J.M., Mason, R.J., Jennings, S.D., Thomson, J.A., Itskovitz-Eldor, J., Shapiro, S.S., Waknitz, M.A., Swiergiel, J.J., Marshall, V.S., Jones, J.M., 2014. Organogenesis in a dish: modeling development and disease using organoid technologies. Science 345, 1247125. https://doi.org/10.1126/science.1247125

Langevin, H.M., Bouffard, N.A., Badger, G.J., Iatridis, J.C., Howe, A.K., 2005. Dynamic fibroblast cytoskeletal response to subcutaneous tissue stretch ex vivo and in vivo. Am. J. Physiol.-Cell Physiol. 288, C747–C756. https://doi.org/10.1152/ajpcell.00420.2004

Lanzafame, A.A., Turnbull, L., Amiramahdi, F., Arthur, J.F., Huynh, H., Woodcock, E.A., 2006. Inositol phospholipids localized to caveolae in rat heart are regulated by α1-adrenergic receptors and by ischemia-reperfusion. Am. J. Physiol.-Heart Circ. Physiol. 290, H2059–H2065. https://doi.org/10.1152/ajpheart.01210.2005

Le Lay, S., Hajduch, E., Lindsay, M.R., Le Lièpvre, X., Thiele, C., Ferré, P., Parton, R.G., Kurzchalia, T., Simons, K., Dugail, I., 2006. Cholesterol-induced caveolin targeting to lipid droplets in adipocytes: a role for caveolar endocytosis. Traffic Cph. Den. 7, 549–561. https://doi.org/10.1111/j.1600-0854.2006.00406.x

Le Lay, S., Kurzchalia, T.V., 2005. Getting rid of caveolins: phenotypes of caveolin-deficient animals. Biochim. Biophys. Acta 1746, 322–333. https://doi.org/10.1016/j.bbamcr.2005.06.001

Levental, K.R., Yu, H., Kass, L., Lakins, J.N., Egeblad, M., Erler, J.T., Fong, S.F.T., Csiszar, K., Giaccia, A., Weninger, W., Yamauchi, M., Gasser, D.L., Weaver, V.M., 2009. Matrix Crosslinking Forces Tumor Progression by Enhancing Integrin Signaling. Cell 139, 891–906. https://doi.org/10.1016/j.cell.2009.10.027

Li, M., Yang, X., Zhang, J., Shi, H., Hang, Q., Huang, X., Liu, G., Zhu, J., He, S., Wang, H., 2013. Effects of EHD2 interference on migration of esophageal squamous cell carcinoma. Med. Oncol. 30, 396. https://doi.org/10.1007/s12032-012-0396-4

Li, T., Sotgia, F., Vuolo, M.A., Li, M., Yang, W.C., Pestell, R.G., Sparano, J.A., Lisanti, M.P., 2006. Caveolin-1 mutations in human breast cancer: functional association with estrogen receptor alpha-positive status. Am. J. Pathol. 168, 1998–2013. https://doi.org/10.2353/ajpath.2006.051089

Li, X., Jia, Z., Shen, Y., Ichikawa, H., Jarvik, J., Nagele, R.G., Goldberg, G.S., 2008. Coordinate suppression of Sdpr and Fhl1 expression in tumors of the breast, kidney, and prostate. Cancer Sci. 99, 1326–1333. https://doi.org/10.1111/j.1349-7006.2008.00816.x

Lim, Y.-W., Lo, H.P., Ferguson, C., Martel, N., Giacomotto, J., Gomez, G.A., Yap, A.S., Hall, T.E., Parton, R.G., 2017. Caveolae Protect Notochord Cells against Catastrophic Mechanical Failure during Development. Curr. Biol. 27, 1968–1981.e7. https://doi.org/10.1016/j.cub.2017.05.067

Lisanti, M.P., Scherer, P.E., Tang, Z., Sargiacomo, M., 1994. Caveolae, caveolin and caveolin-rich membrane domains: a signalling hypothesis. Trends Cell Biol. 4, 231–235.

Liu, J., Ni, W., Qu, L., Cui, X., Lin, Z., Liu, Q., Zhou, H., Ni, R., 2016. Decreased Expression of EHD2 Promotes Tumor Metastasis and Indicates Poor Prognosis in Hepatocellular Carcinoma. Dig. Dis. Sci. 61, 2554–2567. https://doi.org/10.1007/s10620-016-4202-6

Liu, L., Brown, D., McKee, M., LeBrasseur, N.K., Yang, D., Albrecht, K.H., Ravid, K., Pilch, P.F., 2008. Deletion of Cavin/PTRF Causes Global Loss of Caveolae, Dyslipidemia, and Glucose Intolerance. Cell Metab. 8, 310–317. https://doi.org/10.1016/j.cmet.2008.07.008

Lo, H.P., Nixon, S.J., Hall, T.E., Cowling, B.S., Ferguson, C., Morgan, G.P., Schieber, N.L., Fernandez-Rojo, M.A., Bastiani, M., Floetenmeyer, M., Martel, N., Laporte, J., Pilch, P.F., Parton, R.G., 2015. The caveolin-cavin system plays a conserved and critical role in mechanoprotection of skeletal muscle. J. Cell Biol. 210, 833–849. https://doi.org/10.1083/jcb.201501046

Logozzi, M., De Milito, A., Lugini, L., Borghi, M., Calabrò, L., Spada, M., Perdicchio, M., Marino, M.L., Federici, C., Iessi, E., Brambilla, D., Venturi, G., Lozupone, F., Santinami, M., Huber, V., Maio, M., Rivoltini, L., Fais, S., 2009. High levels of exosomes expressing CD63 and caveolin-1 in plasma of melanoma patients. PloS One 4, e5219. https://doi.org/10.1371/journal.pone.0005219

Lu, W., Kang, Y., 2019. Epithelial-Mesenchymal Plasticity in Cancer Progression and Metastasis. Dev. Cell 49, 361–374. https://doi.org/10.1016/j.devcel.2019.04.010

Ludwig, A., Howard, G., Mendoza-Topaz, C., Deerinck, T., Mackey, M., Sandin, S., Ellisman, M.H., Nichols, B.J., 2013. Molecular composition and ultrastructure of the caveolar coat complex. PLoS Biol. 11, e1001640. https://doi.org/10.1371/journal.pbio.1001640

Ma, S., Fu, A., Chiew, G.G.Y., Luo, K.Q., 2017. Hemodynamic shear stress stimulates migration and extravasation of tumor cells by elevating cellular oxidative level. Cancer Lett. 388, 239–248. https://doi.org/10.1016/j.canlet.2016.12.001

Mahoney, L., Csima, A., 1982. Efficiency of palpation in clinical detection of breast cancer. Can. Med. Assoc. J. 127, 729–730.

Maître, J.-L., Niwayama, R., Turlier, H., Nédélec, F., Hiiragi, T., 2015. Pulsatile cell-autonomous contractility drives compaction in the mouse embryo. Nat. Cell Biol. 17, 849–855. https://doi.org/10.1038/ncb3185

Majkut, S., Idema, T., Swift, J., Krieger, C., Liu, A., Discher, D.E., 2013. Heart-Specific Stiffening in Early Embryos Parallels Matrix and Myosin Expression to Optimize Beating. Curr. Biol. 23, 2434–2439. https://doi.org/10.1016/j.cub.2013.10.057

Manninen, A., Verkade, P., Le Lay, S., Torkko, J., Kasper, M., Füllekrug, J., Simons, K., 2005. Caveolin-1 is not essential for biosynthetic apical membrane transport. Mol. Cell. Biol. 25, 10087–10096. https://doi.org/10.1128/MCB.25.22.10087-10096.2005

Manning, M.L., Foty, R.A., Steinberg, M.S., Schoetz, E.-M., 2010. Coaction of intercellular adhesion and cortical tension specifies tissue surface tension. Proc. Natl. Acad. Sci. U. S. A. 107, 12517–12522. https://doi.org/10.1073/pnas.1003743107

Mark, K.V.D., Gauss, V., Mark, H.V.D., Müller, P., 1977. Relationship between cell shape and type of collagen synthesised as chondrocytes lose their cartilage phenotype in culture. Nature 267, 531. https://doi.org/10.1038/267531a0

Mascheroni, P., Boso, D., Preziosi, L., Schrefler, B.A., 2017. Evaluating the influence of mechanical stress on anticancer treatments through a multiphase porous media model. J. Theor. Biol. 421, 179–188. https://doi.org/10.1016/j.jtbi.2017.03.027

Matthaeus, C., Lian, X., Kunz, S., Lehmann, M., Zhong, C., Bernert, C., Lahmann, I., Müller, D.N., Gollasch, M., Daumke, O., 2019. eNOS-NO-induced small blood vessel relaxation requires EHD2-dependent caveolae stabilization. PLOS ONE 14, e0223620. https://doi.org/10.1371/journal.pone.0223620

McMahon, K.-A., Zajicek, H., Li, W.-P., Peyton, M.J., Minna, J.D., Hernandez, V.J., Luby-Phelps, K., Anderson, R.G.W., 2009. SRBC/cavin-3 is a caveolin adapter protein that regulates caveolae function. EMBO J. 28, 1001–1015. https://doi.org/10.1038/emboj.2009.46

Mikol, D.D., Scherer, S.S., Duckett, S.J., Hong, H.L., Feldman, E.L., 2002. Schwann cell caveolin-1 expression increases during myelination and decreases after axotomy. Glia 38, 191–199. https://doi.org/10.1002/glia.10063
Mineo, C., Ying, Y.-S., Chapline, C., Jaken, S., Anderson, R.G.W., 1998. Targeting of Protein Kinase Cα to Caveolae. J. Cell Biol. 141, 601–610.
Mitchell, M.J., Denais, C., Chan, M.F., Wang, Z., Lammerding, J., King, M.R., 2015. Lamin A/C deficiency reduces circulating tumor cell resistance to fluid shear stress. Am. J. Physiol. Cell Physiol. 309, C736-746. https://doi.org/10.1152/ajpcell.00050.2015
Mitchison, J.M., Swann, M., 2005. THE MECHANICAL PROPERTIES OF THE CELL SURFACE III. THE SEA-URCHIN EGG FROM FERTILIZATION TO CLEAVAGE.
Montel, F., Delarue, M., Elgeti, J., Malaquin, L., Basan, M., Risler, T., Cabane, B., Vignjevic, D., Prost, J., Cappello, G., Joanny, J.-F., 2011a. Stress Clamp Experiments on Multicellular Tumor Spheroids. Phys. Rev. Lett. 107, 188102. https://doi.org/10.1103/PhysRevLett.107.188102
Montel, F., Delarue, M., Elgeti, J., Malaquin, L., Basan, M., Risler, T., Cabane, B., Vignjevic, D., Prost, J., Cappello, G., Joanny, J.-F., 2011b. Stress Clamp Experiments on Multicellular Tumor Spheroids. Phys. Rev. Lett. 107, 188102. https://doi.org/10.1103/PhysRevLett.107.188102
Montel, F., Delarue, M., Elgeti, J., Vignjevic, D., Cappello, G., Prost, J., 2012. Isotropic stress reduces cell proliferation in tumor spheroids. New J. Phys. 14, 055008. https://doi.org/10.1088/1367-2630/14/5/055008
Morén, B., Hansson, B., Negoita, F., Fryklund, C., Lundmark, R., Göransson, O., Stenkula, K.G., 2019. EHD2 regulates adipocyte function and is enriched at cell surface-associated lipid droplets in primary human adipocytes. Mol. Biol. Cell 30, 1147–1159. https://doi.org/10.1091/mbc.E18-10-0680
Morén, B., Shah, C., Howes, M.T., Schieber, N.L., McMahon, H.T., Parton, R.G., Daumke, O., Lundmark, R., 2012. EHD2 regulates caveolar dynamics via ATP-driven targeting and oligomerization. Mol. Biol. Cell 23, 1316–29. https://doi.org/10.1091/mbc.E11-09-0787
Moutinho, C., Martinez-Cardús, A., Santos, C., Navarro-Pérez, V., Martínez-Balibrea, E., Musulen, E., Carmona, F.J., Sartore-Bianchi, A., Cassingena, A., Siena, S., Elez, E., Tabernero, J., Salazar, R., Abad, A., Esteller, M., 2014. Epigenetic inactivation of the BRCA1 interactor SRBC and resistance to oxaliplatin in colorectal cancer. J. Natl. Cancer Inst. 106, djt322. https://doi.org/10.1093/jnci/djt322
Mueller-Klieser, W., 1997. Three-dimensional cell cultures: from molecular mechanisms to clinical applications. Am. J. Physiol. 273, C1109-1123. https://doi.org/10.1152/ajpcell.1997.273.4.C1109
Murata, M., Peränen, J., Schreiner, R., Wieland, F., Kurzchalia, T.V., Simons, K., 1995. VIP21/caveolin is a cholesterol-binding protein. Proc. Natl. Acad. Sci. 92, 10339. https://doi.org/10.1073/pnas.92.22.10339
Muz, B., de la Puente, P., Azab, F., Azab, A.K., 2015. The role of hypoxia in cancer progression, angiogenesis, metastasis, and resistance to therapy. Hypoxia Auckl. NZ 3, 83–92. https://doi.org/10.2147/HP.S93413
Na, S., Collin, O., Chowdhury, F., Tay, B., Ouyang, M., Wang, Y., Wang, N., 2008. Rapid signal transduction in living cells is a unique feature of mechanotransduction. Proc. Natl. Acad. Sci. U. S. A. 105, 6626–6631. https://doi.org/10.1073/pnas.0711704105

Nassoy, P., Lamaze, C., 2012. Stressing caveolae new role in cell mechanics. Trends Cell Biol. 22, 381–9. https://doi.org/10.1016/j.tcb.2012.04.007
Navarro, A.P., Collins, M.A., Folker, E.S., 2016. The nucleus is a conserved mechanosensation and mechanoresponse organelle. Cytoskelet. Hoboken NJ 73, 59–67. https://doi.org/10.1002/cm.21277
Ogata, T., Ueyama, T., Isodono, K., Tagawa, M., Takehara, N., Kawashima, T., Harada, K., Takahashi, T., Shioi, T., Matsubara, H., Oh, H., 2008. MURC, a muscle-restricted coiled-coil protein that modulates the Rho/ROCK pathway, induces cardiac dysfunction and conduction disturbance. Mol. Cell. Biol. 28, 3424–3436. https://doi.org/10.1128/MCB.02186-07
Oh, P., McIntosh, D.P., Schnitzer, J.E., 1998. Dynamin at the Neck of Caveolae Mediates Their Budding to Form Transport Vesicles by GTP-driven Fission from the Plasma Membrane of Endothelium. J. Cell Biol. 141, 101–114. https://doi.org/10.1083/jcb.141.1.101
Örtegren, U., Karlsson, M., Blazic, N., Blomqvist, M., Nystrom, F.H., Gustavsson, J., Fredman, P., Strålfors, P., 2004. Lipids and glycosphingolipids in caveolae and surrounding plasma membrane of primary rat adipocytes. Eur. J. Biochem. 271, 2028–2036. https://doi.org/10.1111/j.1432-1033.2004.04117.x
Padera, T.P., Stoll, B.R., Tooredman, J.B., Capen, D., Tomaso, E. di, Jain, R.K., 2004. Cancer cells compress intratumour vessels. Nature 427, 695. https://doi.org/10.1038/427695a
Palade, G., 1953. The fine structure of blood capillaries. J Appl Phys 24, 1424.
Pang, H., Le, P.U., Nabi, I.R., 2004. Ganglioside GM1 levels are a determinant of the extent of caveolae/raft-dependent endocytosis of cholera toxin to the Golgi apparatus. J. Cell Sci. 117, 1421–1430. https://doi.org/10.1242/jcs.01009
Parton, R.G., Pozo, M.A., Vassilopoulos, S., Nabi, I.R., Le Lay, S., Lundmark, R., Kenworthy, A.K., Camus, A., Blouin, C.M., Sessa, W.C., Lamaze, C., 2019. Caveolae: The FAQs. Traffic tra.12689. https://doi.org/10.1111/tra.12689
Pathak, A., Kumar, S., 2011. Biophysical regulation of tumor cell invasion: moving beyond matrix stiffness. Integr. Biol. 3, 267. https://doi.org/10.1039/c0ib00095g
Pelham, R.J., Wang, Y. -l., 1997. Cell locomotion and focal adhesions are regulated by substrate flexibility. Proc. Natl. Acad. Sci. 94, 13661–13665. https://doi.org/10.1073/pnas.94.25.13661
Petersen, O.W., Rønnov-Jessen, L., Howlett, A.R., Bissell, M.J., 1992. Interaction with basement membrane serves to rapidly distinguish growth and differentiation pattern of normal and malignant human breast epithelial cells. Proc. Natl. Acad. Sci. 89, 9064–9068. https://doi.org/10.1073/pnas.89.19.9064
Pironti, G., Strachan, R.T., Abraham, D., Yu, S.M.-W., Chen, M., Chen, W., Hanada, K., Mao, L., Watson, L.J., Rockman, H.A., 2015. Circulating Exosomes Induced by Cardiac Pressure Overload Contain Functional Angiotensin II Type 1 Receptors. Circulation 131, 2120–2130. https://doi.org/10.1161/CIRCULATIONAHA.115.015687
Regmi, S., Fu, A., Luo, K.Q., 2017. High Shear Stresses under Exercise Condition Destroy Circulating Tumor Cells in a Microfluidic System. Sci. Rep. 7, 39975. https://doi.org/10.1038/srep39975
Rief, M., Gautel, M., Oesterhelt, F., Fernandez, J.M., Gaub, H.E., 1997. Reversible unfolding of individual titin immunoglobulin domains by AFM. Science 276, 1109–1112. https://doi.org/10.1126/science.276.5315.1109

Ringnér, M., 2008. What is principal component analysis? Nat. Biotechnol. 26, 303–304. https://doi.org/10.1038/nbt0308-303
Riwaldt, S., Bauer, J., Pietsch, J., Braun, M., Segerer, J., Schwarzwälder, A., Corydon, T.J., Infanger, M., Grimm, D., 2015. The Importance of Caveolin-1 as Key-Regulator of Three-Dimensional Growth in Thyroid Cancer Cells Cultured under Real and Simulated Microgravity Conditions. Int. J. Mol. Sci. 16, 28296–310. https://doi.org/10.3390/ijms161226108
Rothberg, K.G., Heuser, J.E., Donzell, W.C., Ying, Y.-S., Glenney, J.R., Anderson, R.G.W., 1992. Caveolin, a protein component of caveolae membrane coats. Cell 68, 673–682. https://doi.org/10.1016/0092-8674(92)90143-Z
Samani, A., Bishop, J., Luginbuhl, C., Plewes, D.B., 2003. Measuring the elastic modulus ofex vivosmall tissue samples. Phys. Med. Biol. 48, 2183–2198. https://doi.org/10.1088/0031-9155/48/14/310
Sato, S., Weaver, A.M., 2018. Extracellular vesicles: important collaborators in cancer progression. Essays Biochem. 62, 149–163. https://doi.org/10.1042/EBC20170080
Scherer, P.E., Okamotot, T., Chun, M., Nishimotot, I., Lodish, H.F., Lisanti, M.P., 1996. Identification, sequence, and expression of caveolin-2 defines a caveolin gene family. Cell Biol. 93, 131–135.
Senju, Y., Itoh, Y., Takano, K., Hamada, S., Suetsugu, S., 2011. Essential role of PACSIN2/syndapin-II in caveolae membrane sculpting. J. Cell Sci. 124, 2032. https://doi.org/10.1242/jcs.086264
Shajahan, A.N., Dobbin, Z.C., Hickman, F.E., Dakshanamurthy, S., Clarke, R., 2012. Tyrosine-phosphorylated caveolin-1 (Tyr-14) increases sensitivity to paclitaxel by inhibiting BCL2 and BCLxL proteins via c-Jun N-terminal kinase (JNK). J. Biol. Chem. 287, 17682–17692. https://doi.org/10.1074/jbc.M111.304022
Sharma, D.K., Choudhury, A., Singh, R.D., Wheatley, C.L., Marks, D.L., Pagano, R.E., 2003. Glycosphingolipids internalized via caveolar-related endocytosis rapidly merge with the clathrin pathway in early endosomes and form microdomains for recycling. J. Biol. Chem. 278, 7564–7572. https://doi.org/10.1074/jbc.M210457200
Shi, Y., Liu, X., Sun, Y., Wu, D., Qiu, A., Cheng, H., Wu, C., Wang, X., 2015. Decreased expression and prognostic role of EHD2 in human breast carcinoma: correlation with E-cadherin. J. Mol. Histol. 46, 221–231. https://doi.org/10.1007/s10735-015-9614-7
Shield, K., Ackland, M.L., Ahmed, N., Rice, G.E., 2009. Multicellular spheroids in ovarian cancer metastases: Biology and pathology. Gynecol. Oncol. 113, 143–148. https://doi.org/10.1016/j.ygyno.2008.11.032
Singh, R.D., Puri, V., Valiyaveettil, J.T., Marks, D.L., Bittman, R., Pagano, R.E., 2003. Selective caveolin-1-dependent endocytosis of glycosphingolipids. Mol. Biol. Cell 14, 3254–3265. https://doi.org/10.1091/mbc.e02-12-0809
Sinha, B., Köster, D., Ruez, R., Gonnord, P., Bastiani, M., Abankwa, D., Stan, R.V., Butler-Browne, G., Vedie, B., Johannes, L., Morone, N., Parton, R.G., Raposo, G., Sens, P., Lamaze, C., Nassoy, P., 2011a. Cells Respond to Mechanical Stress by Rapid Disassembly of Caveolae. Cell 144, 402–413. https://doi.org/10.1016/j.cell.2010.12.031
Sinha, B., Köster, D., Ruez, R., Gonnord, P., Bastiani, M., Abankwa, D., Stan, R.V., Butler-Browne, G., Vedie, B., Johannes, L., Morone, N., Parton, R.G., Raposo, G., Sens, P., Lamaze, C., Nassoy, P., 2011b. Cells respond to mechanical

stress by rapid disassembly of caveolae. Cell 144, 402–13. https://doi.org/10.1016/j.cell.2010.12.031
Solanas, G., Cortina, C., Sevillano, M., Batlle, E., 2011. Cleavage of E-cadherin by ADAM10 mediates epithelial cell sorting downstream of EphB signalling. Nat. Cell Biol. 13, 1100–1107. https://doi.org/10.1038/ncb2298
Sonnino, S., Prinetti, A., 2009. Sphingolipids and membrane environments for caveolin. FEBS Lett. 583, 597–606. https://doi.org/10.1016/j.febslet.2009.01.007
Staubach, S., Razawi, H., Hanisch, F.-G., 2009. Proteomics of MUC1-containing lipid rafts from plasma membranes and exosomes of human breast carcinoma cells MCF-7. Proteomics 9, 2820–2835. https://doi.org/10.1002/pmic.200800793
Steinberg, M.S., 1963. Reconstruction of Tissues by Dissociated Cells. Science 141, 401–408. https://doi.org/10.1126/science.141.3579.401
Stoeber, M., Schellenberger, P., Siebert, C.A., Leyrat, C., Helenius, A., Grünewald, K., 2016. Model for the architecture of caveolae based on a flexible, net-like assembly of Cavin1 and Caveolin discs. Proc. Natl. Acad. Sci. 113, E8069. https://doi.org/10.1073/pnas.1616838113
Stoeber, Miriam, Stoeck, I.K., Hänni, C., Bleck, C.K.E., Balistreri, G., Helenius, Ari, Aboulaich, N., Vainonen, JP., Stralfors, P., Vener, AV., Bastiani, M., Liu, L., Hill, MM., Jedrychowski, MP., Nixon, SJ., Lo, HP., Abankwa, D., Luetterforst, R., Fernandez□Rojo, M., Breen, MR., Schedl, A., Haller, H., Kurzchalia, TV., Benjamin, S., Weidberg, H., Rapaport, D., Pekar, O., Nudelman, M., Segal, D., Hirschberg, K., Katzav, S., Ehrlich, M., Horowitz, M., Blume, JJ., Halbach, A., Behrendt, D., Paulsson, M., Plomann, M., Botos, E., Klumperman, J., Oorschot, V., Igyarto, B., Magyar, A., Olah, M., Kiss, AL., Boucrot, E., Howes, MT., Kirchhausen, T., Parton, RG., Chinnapen, DJ., Chinnapen, H., Saslowsky, D., Lencer, WI., Daumke, O., Lundmark, R., Vallis, Y., Martens, S., Butler, PJ., McMahon, HT., Drab, M., Verkade, P., Elger, M., Kasper, M., Lohn, M., Lauterbach, B., Menne, J., Lindschau, C., Mende, F., Luft, FC., Schedl, A., Haller, H., Kurzchalia, TV., Foti, M., Porcheron, G., Fournier, M., Maeder, C., Carpentier, JL., Fra, AM., Williamson, E., Simons, K., Parton, RG., George, M., Ying, G., Rainey, MA., Solomon, A., Parikh, PT., Gao, Q., Band, V., Band, H., Guilherme, A., Soriano, NA., Bose, S., Holik, J., Bose, A., Pomerleau, DP., Furcinitti, P., Leszyk, J., Corvera, S., Czech, MP., Hansen, CG., Bright, NA., Howard, G., Nichols, BJ., Hansen, CG., Howard, G., Nichols, BJ., Hansen, CG., Nichols, BJ., Hayer, A., Stoeber, M., Bissig, C., Helenius, A., Hayer, A., Stoeber, M., Ritz, D., Engel, S., Meyer, HH., Helenius, A., Henley, JR., Krueger, EW., Oswald, BJ., McNiven, MA., Hill, MM., Bastiani, M., Luetterforst, R., Kirkham, M., Kirkham, A., Nixon, SJ., Walser, P., Abankwa, D., Oorschot, VM., Martin, S., Hancock, JF., Parton, RG., Jakobsson, J., Ackermann, F., Andersson, F., Larhammar, D., Low, P., Brodin, L., Kirkham, M., Fujita, A., Chadda, R., Nixon, SJ., Kurzchalia, TV., Sharma, DK., Pagano, RE., Hancock, JF., Mayor, S., Parton, RG., Kirkham, M., Parton, RG., Lajoie, P., Nabi, IR., Lee, DW., Zhao, X., Scarselletta, S., Schweinsberg, PJ., Eisenberg, E., Grant, BD., Greene, LE., Li, G., Zhang, XC., McMahon, KA., Zajicek, H., Li, WP., Peyton, MJ., Minna, JD., Hernandez, VJ., Luby□Phelps, K., Anderson, RG., Moren, B., Shah, C., Howes, MT., Schieber, NL., McMahon, HT., Parton, RG., Daumke, O., Lundmark, R., Mundy, DI., Machleidt, T., Ying, YS., Anderson, RG., Bloom, GS., Muriel, O., Echarri, A., Hellriegel, C., Pavon, DM., Beccari, L., Pozo, MA.D., Naslavsky,

N., Caplan, S., Oh, P., McIntosh, DP., Schnitzer, JE., Parton, RG., Parton, RG., Joggerst, B., Simons, K., Parton, RG., Simons, K., Pelkmans, L., Burli, T., Zerial, M., Helenius, A., Pelkmans, L., Fava, E., Grabner, H., Hannus, M., Habermann, B., Krausz, E., Zerial, M., Pelkmans, L., Helenius, A., Pelkmans, L., Puntener, D., Helenius, A., Pelkmans, L., Zerial, M., Pike, LJ., Han, X., Chung, KN., Gross, RW., Richter, T., Floetenmeyer, M., Ferguson, C., Galea, J., Goh, J., Lindsay, MR., Morgan, GP., Marsh, BJ., Parton, RG., Rothberg, KG., Heuser, JE., Donzell, WC., Ying, YS., Glenney, JR., Anderson, RG., Sargiacomo, M., Scherer, PE., Tang, Z., Kubler, E., Song, KS., Sanders, MC., Lisanti, MP., Schliwa, M., Euteneuer, U., Bulinski, JC., Izant, JG., Sharma, DK., Brown, JC., Cheng, Z., Holicky, EL., Marks, DL., Pagano, RE., Sharma, M., Naslavsky, N., Caplan, S., Singh, RD., Marks, DL., Holicky, EL., Wheatley, CL., Kaptzan, T., Sato, SB., Kobayashi, T., Ling, K., Pagano, RE., Sinha, B., Koster, D., Ruez, R., Gonnord, P., Bastiani, M., Abankwa, D., Stan, RV., Butler□Browne, G., Vedie, B., Johannes, L., Morone, N., Parton, RG., Raposo, G., Sens, P., Lamaze, C., Nassoy, P., Stahlhut, M., van Deurs, B., Sverdlov, M., Shajahan, AN., Minshall, RD., Sverdlov, M., Shinin, V., Place, AT., Castellon, M., Minshall, RD., Tagawa, A., Mezzacasa, A., Hayer, A., Longatti, A., Pelkmans, L., Helenius, A., Thomsen, P., Roepstorff, K., Stahlhut, M., van Deurs, B., Tokuyasu, KT., van Deurs, B., Roepstorff, K., Hommelgaard, AM., Sandvig, K., Wanaski, SP., Ng, BK., Glaser, M., 2012. Oligomers of the ATPase EHD2 confine caveolae to the plasma membrane through association with actin. EMBO J. 31, 2350–64. https://doi.org/10.1038/emboj.2012.98

Stylianopoulos, T., Martin, J.D., Snuderl, M., Mpekris, F., Jain, S.R., Jain, R.K., 2013. Coevolution of solid stress and interstitial fluid pressure in tumors during progression: implications for vascular collapse. Cancer Res. 73, 3833–3841. https://doi.org/10.1158/0008-5472.CAN-12-4521

Tang, Z., Scherer, P.E., Okamoto, T., Song, K., Chu, C., Kohtz, D.S., Nishimoto, I., Lodish, H.F., Lisanti, M.P., 1996. Molecular Cloning of Caveolin-3, a Novel Member of the Caveolin Gene Family Expressed Predominantly in Muscle. J. Biol. Chem. 271, 2255–2261. https://doi.org/10.1074/jbc.271.4.2255

Tardif, N., 2018. Mechanosignaling through Caveolae : A New Role for the Control of JAK-STAT Signaling (thesis). Paris Saclay.

The Gene Ontology Resource: 20 years and still GOing strong, 2019. . Nucleic Acids Res. 47, D330–D338. https://doi.org/10.1093/nar/gky1055

Théry, M., 2010. Micropatterning as a tool to decipher cell morphogenesis and functions. J. Cell Sci. 123, 4201–4213. https://doi.org/10.1242/jcs.075150

Thomas, S.J., Snowden, J.A., Zeidler, M.P., Danson, S.J., 2015. The role of JAK/STAT signalling in the pathogenesis, prognosis and treatment of solid tumours. Br. J. Cancer 113, 365–371. https://doi.org/10.1038/bjc.2015.233

Thompson, D.W., 1917. On Growth and Form. https://doi.org/10.1038/100021a0

Torrino, S., Shen, W.-W., Blouin, C.M., Mani, S.K., Viaris de Lesegno, C., Bost, P., Grassart, A., Köster, D., Valades-Cruz, C.A., Chambon, V., Johannes, L., Pierobon, P., Soumelis, V., Coirault, C., Vassilopoulos, S., Lamaze, C., 2018. EHD2 is a mechanotransducer connecting caveolae dynamics with gene transcription. J. Cell Biol. 217, 4092–4105. https://doi.org/10.1083/jcb.201801122

Tran, D., Carpentier, J.L., Sawano, F., Gorden, P., Orci, L., 1987. Ligands internalized through coated or noncoated invaginations follow a common

intracellular pathway. Proc. Natl. Acad. Sci. U. S. A. 84, 7957–7961. https://doi.org/10.1073/pnas.84.22.7957
Trimmer, C., Sotgia, F., Whitaker-Menezes, D., Balliet, R.M., Eaton, G., Martinez-Outschoorn, U.E., Pavlides, S., Howell, A., Iozzo, R.V., Pestell, R.G., Scherer, P.E., Capozza, F., Lisanti, M.P., 2011. Caveolin-1 and mitochondrial SOD2 (MnSOD) function as tumor suppressors in the stromal microenvironment: a new genetically tractable model for human cancer associated fibroblasts. Cancer Biol. Ther. 11, 383–394. https://doi.org/10.4161/cbt.11.4.14101
Upton, M.L., Gilchrist, C.L., Guilak, F., Setton, L.A., 2008. Transfer of Macroscale Tissue Strain to Microscale Cell Regions in the Deformed Meniscus. Biophys. J. 95, 2116–2124. https://doi.org/10.1529/biophysj.107.126938
Usukura, E., Narita, A., Yagi, A., Ito, S., Usukura, J., 2016. An Unroofing Method to Observe the Cytoskeleton Directly at Molecular Resolution Using Atomic Force Microscopy. Sci. Rep. 6, 27472. https://doi.org/10.1038/srep27472
Vinten, J., Johnsen, A.H., Roepstorff, P., Harpøth, J., Tranum-Jensen, J., 2005. Identification of a major protein on the cytosolic face of caveolae. Biochim. Biophys. Acta 1717, 34–40. https://doi.org/10.1016/j.bbamem.2005.09.013
Vinten, J., Voldstedlund, M., Clausen, H., Christiansen, K., Carlsen, J., Tranum-Jensen, J., 2001. A 60-kDa protein abundant in adipocyte caveolae. Cell Tissue Res. 305, 99–106. https://doi.org/10.1007/s004410100389
Volkers, L., Mechioukhi, Y., Coste, B., 2015. Piezo channels: from structure to function. Pflugers Arch. 467, 95–99. https://doi.org/10.1007/s00424-014-1578-z
Volonte, D., Galbiati, F., 2009. Inhibition of thioredoxin reductase 1 by caveolin 1 promotes stress-induced premature senescence. EMBO Rep. 10, 1334–1340. https://doi.org/10.1038/embor.2009.215
Voutouri, C., Mpekris, F., Papageorgis, P., Odysseos, A.D., Stylianopoulos, T., 2014. Role of Constitutive Behavior and Tumor-Host Mechanical Interactions in the State of Stress and Growth of Solid Tumors. PLoS ONE 9. https://doi.org/10.1371/journal.pone.0104717
Wagner, E.F., Nebreda, Á.R., 2009. Signal integration by JNK and p38 MAPK pathways in cancer development. Nat. Rev. Cancer 9, 537–549. https://doi.org/10.1038/nrc2694
Wang, N., Butler, J., Ingber, D., 1993. Mechanotransduction across the cell surface and through the cytoskeleton. Science 260, 1124–1127. https://doi.org/10.1126/science.7684161
Wang, Z., Maruyama, K., Sakisaka, Y., Suzuki, S., Tada, H., Suto, M., Saito, M., Yamada, S., Nemoto, E., 2019. Cyclic Stretch Force Induces Periodontal Ligament Cells to Secrete Exosomes That Suppress IL-1β Production Through the Inhibition of the NF-κB Signaling Pathway in Macrophages. Front. Immunol. 10. https://doi.org/10.3389/fimmu.2019.01310
Way, M., Parton, R.G., 1995. M-caveolin, a muscle-specific caveolin-related protein. FEBS Lett. 376, 108–112. https://doi.org/10.1016/0014-5793(95)01256-7
Welinder, C., Paw\lowski, K., Szasz, A.M., Yakovleva, M., Sugihara, Y., Malm, J., Jönsson, G., Ingvar, C., Lundgren, L., Baldetorp, B., Olsson, H. akan, Rezeli, M., Laurell, T., Wieslander, E., Marko-Varga, G., 2017. Correlation of histopathologic characteristics to protein expression and function in malignant melanoma. PloS One 12, e0176167. https://doi.org/10.1371/journal.pone.0176167

Wirtz, D., Konstantopoulos, K., Searson, P.C., 2011. The physics of cancer: the role of physical interactions and mechanical forces in metastasis. Nat. Rev. Cancer 11, 512.
Witkiewicz, A.K., Dasgupta, A., Sotgia, F., Mercier, I., Pestell, R.G., Sabel, M., Kleer, C.G., Brody, J.R., Lisanti, M.P., 2009. An Absence of Stromal Caveolin-1 Expression Predicts Early Tumor Recurrence and Poor Clinical Outcome in Human Breast Cancers. Am. J. Pathol. 174, 2023–2034. https://doi.org/10.2353/ajpath.2009.080873
Wolff, J., 1892. Das Gesetz der Transformation der Knochen. Hirshwald 1, 1–152.
Wubbolts, R., Leckie, R.S., Veenhuizen, P.T.M., Schwarzmann, G., Möbius, W., Hoernschemeyer, J., Slot, J.-W., Geuze, H.J., Stoorvogel, W., 2003. Proteomic and Biochemical Analyses of Human B Cell-derived Exosomes POTENTIAL IMPLICATIONS FOR THEIR FUNCTION AND MULTIVESICULAR BODY FORMATION. J. Biol. Chem. 278, 10963–10972. https://doi.org/10.1074/jbc.M207550200
Yamada, E., 1955. The Fine Structure of the Gall Bladder Epithelium of the Mouse. J. Cell Biol. 1, 445–458. https://doi.org/10.1083/jcb.1.5.445
Yang, G., Truong, L.D., Timme, T.L., Ren, C., Wheeler, T.M., Park, S.H., Nasu, Y., Bangma, C.H., Kattan, M.W., Scardino, P.T., Thompson, T.C., 1998. Elevated expression of caveolin is associated with prostate and breast cancer. Clin. Cancer Res. Off. J. Am. Assoc. Cancer Res. 4, 1873–1880.
Yang, X., Ren, H., Yao, L., Chen, X., He, A., 2015. Role of EHD2 in migration and invasion of human breast cancer cells. Tumor Biol. 36, 3717–3726. https://doi.org/10.1007/s13277-014-3011-9
Yeow, I., Howard, G., Chadwick, J., Mendoza-Topaz, C., Hansen, C.G., Nichols, B.J., Shvets, E., 2017. EHD Proteins Cooperate to Generate Caveolar Clusters and to Maintain Caveolae during Repeated Mechanical Stress. Curr. Biol. 27, 2951-2962.e5. https://doi.org/10.1016/j.cub.2017.07.047
Yeow, I.E.-T., 2018. The role of EHD proteins in caveolae, and the role of caveolae in adipocytes (Thesis). University of Cambridge. https://doi.org/10.17863/CAM.23168
Yu, H., Mouw, J.K., Weaver, V.M., 2011. Forcing form and function: biomechanical regulation of tumor evolution. Trends Cell Biol. 21, 47–56. https://doi.org/10.1016/j.tcb.2010.08.015

Etude de la mécanotransduction des cavéoles sous contraintes de compression 3D: Analyse comparative de deux modèles imitant les caractéristiques structurales et mécaniques des tumeurs.

Mots clés : Mechanosignalisation ; Mechanotransducsion ; Caveolae ; Culture ceullaire 3D

Résumé: La mécanique et le stress compressif jouent un rôle important dans la progression tumorale. Récemment, plusieurs approches ont été développées pour tester le stress en compression dans des modèles 3D in vitro (Alessandri, 2013; Montel et al., 2012). Dans le présent travail, nous montrons d'abord la pertinence de la compression dans l'organisation des fibroblastes associés au cancer (CAF), en enveloppant les cellules cancéreuses lors d'une compression isotrope 3D dans des capsules d'alginate creux. Dans ce système, les CAF couvrent les cellules cancéreuses en présence de compression selon un processus impliquant vraisemblablement une réorganisation du dépôt de fibronectine et non un réarrangement passif des deux sphéroïdes.
Dans la deuxième partie de ce travail, nous avons étudié la réaction des composants de la cavéole au stress en compression. Les cavéoles sont des invaginations de la membrane plasmique capables d'amortir la tension de la membrane, protégeant ainsi la cellule de son éclatement (Sinha et al., 2011). Nous montrons ici comment les cavéoles réduisent leur présence lors de la compression 3D à court terme et comment cette compression inhibe l'activation de STAT1 et STAT3 induite par l'interféron. De plus, les effets à long terme des contraintes de compression sur les sphéroïdes entraînent également la perte du composant cavéole EHD2, une ATPase centrale pour la stabilité des cavéoles sur la membrane. Enfin, nous avons trouvé différentes voies avec une transcription modifiée du gène après un stress compressif. Parmi eux, nous avons caractérisé l'effet de la perte de cavéoline-1 sur la libération d'exosomes sous compression 3D.

Study of caveolae mechanotransduction under 3D compressive stresses: Comparative analysis of two models mimicking structural and mechanical tumor characteristics.

Keywords : Mechanosignaling ; Mechanotransduction ; Caveolae ; 3D culture

Abstract: Mechanics and compressive stress play an important role in tumor progression. Recently, several approaches have been developed to test compressive stress in 3D *in vitro* models (Alessandri, 2013; Montel et al., 2012). In the present work, we first show the relevance of compression in the organization of cancer associated fibroblasts (CAFs), enwrapping cancer cells upon 3D isotropic compression in capsules of hollow alginate. In this system, CAFs cover cancer cells in the presence of compression by a process which most likely involves fibronectin deposition reorganization, and not a passive rearrangement of the two spheroids.

In the second part of this work, we investigated the response of caveolae components to compressive stress. Caveolae are plasma membrane invaginations which are able to buffer membrane tension, thus protecting the cell from bursting (Sinha et al., 2011). Here, we show how caveolae reduce their presence under 3D short term compression, and how this compression inhibits interferon induced STAT1 and STAT3 activation. Moreover, long term effects of compressive stress in spheroids result also in loss of the caveolae component EHD2, a central ATPase for caveolae stability on the membrane. Lastly, we found different pathways with altered gene transcription after compressive stress. Among them, we characterized the effect of caveolin-1 loss on the release of exosomes under 3D compression.